Contributions to the Analysis of Biochemical Reaction-Diffusion Networks

Stability, Analysis, and Numerical Solutions

Fernando López-Caamal

A dissertation submitted for
the degree of Doctor of Philosophy

Under the supervision of

Prof. Richard H. Middleton

and the cosupervision of

Dr. Míriam R. García

and

Dr. Heinrich J. Huber

Hamilton Institute
Directed by
Prof. Douglas Leith

National University of Ireland Maynooth
Ollscoil na hÉireann, Má Nuad

2012

Contents

Summary

In this thesis we address dynamic systems problems that arise from the study of biochemical networks. Here we prefer a rigorous treatment of the differential equations that govern their spatio-temporal dynamics, at the cost of studying simplified scenarios of the biological systems under study. Although these simplified scenarios do not model all aspects of the complex interplay in the biological system, they are derived to study the relationship between specific causes and effects. However, by abstracting the systems under study, we obtain the benefit of having models that represent a large variety of processes. For instance, a simple activation mechanism studied here may be used to model the autoactivation of the effector caspase in the apoptosis pathway, the activation of the Akt/mTOR complex implicated in muscular growth, and two-species population dynamics.

In particular, we derive analytical expressions for the equilibrium points of a circular protein activation mechanism with an arbitrary number of intermediate steps and characterise its local stability. Later we analyse the signalling progression due to a protein autoactivation in a long cell. Furthermore, we avail of a projection method for partial differential equations to obtain associated ordinary differential equations that will assist on the reduction of the computational load for the numerical solution of a class of reaction diffusion networks. This projection method will also be used to compute the time-integral of some species concentration in a class of reaction-diffusion networks.

Since we chose a theoretical approach, our results provide analytical expressions that link the kinetic parameters and topology of the reaction network with its dynamical behaviour. These formulas can be further studied to analyse the sensitivity of the systems characteristic with respect to variation of parameters as well as explicitly unveiling the main processes that affect

the features of interest. We believe that these theoretical approaches provide a deeper insight in selected biochemical pathways such as: the Akt/mTOR activation pathway, mediated by the IGF receptor; the core apoptosis pathway; and Ca^{2+} homeostasis in non-excitable cells.

Acknowledgements

Firstly, I would like to thank my family for its continuous and ever-present support. I dedicate this work to each and every one of you.

The contents, organisation, and presentation of this thesis are the result of the guidance of Prof. Richard H. Middleton, Dr. Míriam R. García, and Dr. Heinrich H. Huber. I thank you all for your constant help, efforts, advice, and infinite patience. Also I gratefully acknowledge the collaboration with Dr. Diego A. Oyarzún and Dr. Ben-Fillippo Krippendorff, from which the topics in Section 4.4 were derived. I would like to thank Prof. Peter Wellstead for giving me the opportunity of being part of the Hamilton Institute.

Most of the contents presented here were developed at the Hamilton Institute, directed by Prof. Douglas Leith, at the National University of Ireland, Maynooth in close collaboration with the Royal College of Surgeons in Ireland. This manuscript took its final form at the University of Newcastle. Thanks to all these institutions that provided the means and the appropriate work atmosphere. Also, I would like to thank the National Autonomous University of Mexico where interesting discussions took place, which helped to shape this thesis, and for providing me with the tools to pursue this degree. Especially, I thank Prof. Jaime A. Moreno for his support and advice during these years.

For the thorough revision of the manuscript, I would like to thank Dr. Jorge Gonçalves, Dr. Ken Duffy, and Ms. Sonja Stüdli. I sincerely appreciate your time and efforts to provide your insightful commentaries and suggestions. With your help this manuscript was highly enhanced.

Pursuing a PhD can be a difficult task which may become an almost frustrating experience. However, these last years are full of good memories and experiences with all the friends that I had the chance to make: Arieh Schlote, Andrés Peters Rivas, Míriam Rodríguez García, Sonja Stüdli,

Steffi, Florian, and Sophie Knorn, Esteban Hernández Vargas, Buket Benek Gursoy, Magdalena Zebrowska, Vahid Bokharaie, Hessan Feghhi, Alessandro Checco, Emanuele Crisostomi, Karl O'Dwyer, Febe Francis, Wynita Griggs, Paul Patras, Maximilian Würstle, Jasmin Schmid, and all the people in the Hamilton Institute, CCDSC, and RCSI. My warm thanks for your company, support and, foremost, for your friendship.

To the gang in the Centre for Complex Dynamic Systems and Control at Newcaslte University, I am very grateful for the warm welcome during this brief visit to Australia. Especially, I would like to thank the Knorn and Middleton families that often welcomed me in their houses. Also I would like to thank Octavio Díaz Hernández for his friendship and for keeping alive my link with Mexico.

It would certainly be ungrateful not to mention the fine organising skills of Rosemary Hunt, Kate Moriarty, Ruth Middleton, and Dianne Piefke. Many thanks for making our lives easier.

Lastly, but not least, I would like to thank the financial support provided by NBIP Ireland without which this work would have been impossible. [1]

[1]This work was supported by the National Biophotonics and Imaging Platform, Ireland, and funded by the Irish Government's Programme for Research in Third Level Institutions, Cycle 4, Ireland EU Structural Funds Programmes 2007-2013.

Chapter 1

Introduction

The study of biological systems by analytical approaches is not a new idea. In the middle of the 20th century, Erwin Schrödiger posed the question: 'Can the phenomena present in the living matter be explained with current physical knowledge? Or are they explained with a new physical law?' [1]

Since that time there have been many advances in the understanding of living systems. Several perspectives are now available to explain the different levels of interactions in biological systems. For example, Mathematical and Theoretical Biology provide an accurate description of complex biological processes by means of the study of the equations that describe them [2]. In contrast, when the joint work of large-scale signalling networks is of interest, Systems Biology links the behaviours of molecules to system functions [3, 4, 5]. Given the number of developments in this field, we have reached the possibility of theoretically design biological pathways with a prescribed behaviour. This engineering design approach is adopted by Synthetic Biology [6, 7], which, not forgetting the principal motivation of studying living systems, also intends to unveil the design principles that underpin the dynamical properties of these systems.

In addition to the common objective, these disciplines are also unified by the use of mathematical tools to provide a deeper insight into the process under study. Just as the biological phenomena vary over a wide range, the set of mathematical tools that describe them are also very diverse. In this work we apply several mathematical tools that are used in Control Engineering to study the differential equations that govern the dynamics of the states of the system. From this presentation, the mathematical approaches might appear as a pure service discipline towards the understanding of living systems. However, the analysis of such systems have posed

new theoretical problems that, in turn, enrich the mathematical machinery [8, 9].

In the biochemical context, we focus on reaction systems that can be idealised as isobaric, isochoric, isothermal processes. This allows us to determine the state of the reaction network by means of the concentrations of the species in the network. We focus on continuous time differential equations that describe the variation of the species concentrations in time. In general, these differential equations are nonlinear and their dynamical behaviour is as rich as the range of processes that they model. This includes, but is not limited to: oscillations which define rhythms in cellular and population systems [10, 11]; bistable behaviours [12], required to toggle the biological state of the reaction network in a plethora of processes, such as cell death [13]; and, among many others, relaxation-oscillation mechanisms that model the spiking voltage in neurons [14].

The temporal description of the species concentrations can be understood as an average of the effects among a population. However, a more detailed description of the process shows how the species progress in the spatial domain in which they are constrained. This progression can be described by differential equations that, in addition to the temporal variation, also depend on spatial coordinates. We consider that the spatial dynamics of the species is *only* driven by thermally induced random molecular vibrations in the spatial domain. This leads to reaction diffusion systems that are described by partial differential equations, which enhance the range of dynamics phenomena that the continuous time differential equations exhibit [15]. Foremost, partial differential equations are capable of describing the interaction of the species in the spatial domain with the surroundings, by means of the boundary conditions. Moreover, there are some effects that ordinary differential equations do not produce, such as gradient and pattern formation of species [16, 17, 2], which are of paramount importance in cell differentiation processes [18]. In addition, we can also model a sustained signal progression in the spatial domain in the form of travelling waves and fronts. Such waves can be used in epidemiology to describe the progression of an infectious disease [19] or to show signal progression within a cell [20], for instance.

This accurate description of biochemical processes come at the price of having nonlinear models that are often complex and difficult to tackle by analytical methods. Towards this end, in this work we have developed a set of mathematical tools, in a general framework, to analyse some dynamic characteristics of the continuous time and space differential equations that arise from the models of biochemical reaction networks. These results characterise the equilibrium set of a reaction-diffusion network, the stability analysis of two specific reaction networks, the

reduction of the computational time in a class of reaction diffusion system, and the computation of the time-integral of selected species.

The common objective of these results is to provide a quantitative, rather than qualitative, description of this set of characteristics. We support this quantitative approach by the derivation of analytical expressions that link the topology and parameters of the reaction networks with their dynamical behaviour. We believe this approach will enhance the understanding of the process under study. Moreover, by this perspective, we can distinguish if the phenomenon under consideration is a consequence of fine-tuned kinetic parameters or arise from structural properties of the reaction system's topology [21], assuming the caveats of the model are reasonable.

To present these ideas, we start by deriving the differential equations that describe the species concentrations in time and space of a reaction network. In addition, in Chapter 2 we also compute the equilibrium set for a general reaction network and, in particular, for a circular protein activation mechanism. Having characterised the equilibrium set, in Chapter 3 we quantify different performance indices for two mechanisms of positive feedback loops that represent protein activation. In turn, Chapter 4 avails of a projection method for partial differential equations to derive reduced order models, which we use to perform rapid simulations of a class of reaction diffusion systems. We also utilise this projection method to compute the time-integral of some species in a reaction-(diffusion) network. Finally, in Chapter 5 we exemplify the use of the theoretical results presented in the previous chapters to selected pathways such as: the Akt/mTOR pathway, the core of the apoptosis pathway, and calcium dynamics in non-excitable cells.

1.1 List of Contributions

The results derived in this thesis are the product of collaboration of specialists in diverse disciplines and are currently reported in peer-reviewed journals. Specifically, the study of a protein autoactivation mechanism in a unidimensional spatial domain has been reported in
F. López-Caamal, M. R. García, R. H. Middleton, and H. J. Huber. Positive feedback in the Akt/mTOR pathway and its implications for growth signal progression in skeletal muscle cells: An analytical study. Journal of Theoretical Biology*, 301(0):15–27, 2012.*
This analysis is motivated by the study of skeletal muscular growth, mediated by the PI3K/ Akt/ mTOR pathway. In this thesis, we present a simplified analysis of this study in Example 3.2 and highlight some of the conclusions in Section 5.1.

As a generalisation of the pathway studied above, we analyse a circular protein activation mechanism with an arbitrary number of intermediate steps of activation. We present these results in

F. López-Caamal, R.H. Middleton, and H.J. Huber. Equilibria and stability of a class of positive feedback loops: Mathematical analysis and its application to caspase-dependent apoptosis, ***To appear***. Journal of Mathematical Biology*, 2013,*

where we study the local stability of the two steady states that this network exhibit by means of the computation of the input-output gain of the subsystems that compose the pathway. In this thesis, we show the computation of the fixed points in Example 2.2, whereas the study of their stability is shown in Example 3.1. Some implications in the caspase-6-mediated apoptosis pathway are presented in Section 5.2.

Moreover, in Section 2.3.1, we show that the equilibrium points of a class of reaction network belongs to a lower dimensional space characterised by the orthogonal complement to the reaction vectors associated to the nonlinear reaction rates.

Availing of a projection method for partial differential equations, we identify a class of reaction-diffusion systems for which we can reduce the computational load to obtain their numerical solutions. This is a hybrid approach that uses the analytical solution for some species and a numerical solution of the reduced order model associated to the rest of the species. From this study arose

López-Caamal F., M. R. García, and R. H. Middleton. Reducing computational time via order reduction of a class of reaction-diffusion system. In Proceedings of the American Control Conference*, 2012.*

There, we also introduce a matrix notation to handle the reduced order models that result from the projection approach.

For a biochemical reaction network, we compute a characteristic of the cues that have been implicated in downstream signalisation: the integral of species concentration. The computation of the time-integral of a linear combination of species was reported in

F. López-Caamal, D. A. Oyarzún and, J. A. Moreno, and D. Kalamatianos. Control structure and limitations of biochemical networks. In Proceedings of the American Control Conference*,*

pages 6668–6673, 2010.

We present this theoretical derivation in Section 4.4.1.

In turn, the computation of some species in the reaction network, reported here in Section 4.4.2, has supported the identification of a linear characteristic for signal transduction in the epidermal growth factor receptor, in the paper currently under review a

D. A. Oyarzún, Jo L. Bramhall, F. López-Caamal, Duncan Jodrell, and Ben-Fillippo Krippendorff. Deconvolution of growth factor signalling demonstrates linear information transmission of the EGFR, ***Under review****. 2012,*

Finally, we present in Section 4.4.3 the computation of the time-integral of some species in a reaction-diffusion network. These results are reported in

F López-Caamal, M. R. García, D. A. Oyarzún, and R.H. Middleton. Analytic computation of the integrated response in nonlinear reaction-diffusion systems. In Proceedings of the 51st IEEE Conference on Decision and Control*, 2012,* and

D. A. Oyarzún, F. López-Caamal, Míriam R. García, and R. H. Middleton. Cumulative signal transmission in nonlinear reaction-diffusion networks, ***Under review****. 2013.*

Moreover, we are currently using these results to the study Ca^{2+} homeostasis in nonexcitable cells as outlined in Section 5.3.

1.2 Notation

To conclude this chapter, we present the notation used throughout the thesis. We denote the set of real numbers with $\mathbb{R}$ and the set of complex numbers with $\mathbb{C}$. Table 1.1, shows the notation used for scalar, vectors and matrices. Likewise Table 1.2 presents the notation for used to denote

Table 1.1: *Notation for vectors and matrices*

Element	Notation
Real or complex number	$a \in \mathbb{R}$ or $\in \mathbb{C}$
Column vector with n real elements	$\mathbf{v} \in \mathbb{R}^n$
Matrix with n rows and m columns	$\mathbf{N} \in \mathbb{R}^{n \times m}$

some characteristics of matrices, such as rank and nullity of a matrix. In turn, Table 1.3 shows the notation used for operation applied to vectors and matrices. We note that the operation of integration and differentiation of a matrix are applied element-wise.

Table 1.2: *Characteristics of a matrix*

Characteristic	Notation
Rank of $\mathbf{N} \in \mathbb{R}^{n \times m}$	$\mathrm{rank}\,(\mathbf{N}) \in \mathbb{R}$
Dimension of the column null space of $\mathbf{N} \in \mathbb{R}^{n \times m}$	$\mathrm{nullity}\,(\mathbf{N}) \in \mathbb{R}$
Maximum eigenvalue of $\mathbf{A} \in \mathbb{R}^{n \times n}$	$\bar{\lambda}\,(\mathbf{A})$

Table 1.3: *Notation for matrix operations*

Operation	Notation
Inverse of $\mathbf{A} \in \mathbb{R}^{n \times n}$	$\mathbf{A}^{-1} \in \mathbb{R}^{n \times n}$
Transpose of $\mathbf{P} \in \mathbb{R}^{n \times m}$	$\mathbf{P}^{T} \in \mathbb{R}^{m \times n}$
Left Pseudo Inverse of $\mathbf{N}$	$\mathbf{N}^{+}$
Orthogonal complement of $\mathbf{N}$'s column space	$\mathbf{N}^{\perp}$
Complex conjugate of $\mathbf{H} \in \mathbb{C}^{n \times m}$	$\mathbf{H}^{*} \in \mathbb{C}^{m \times n}$
Differentiation of a scalar function f w.r.t. a vector $\mathbf{c} \in \mathbb{R}^{n}$	$\frac{\mathrm{d}}{\mathrm{d}\mathbf{c}} f \in \mathbb{R}^{1 \times n}$
Differentiation of a vector $\mathbf{c} \in \mathbb{R}^{n}$ w.r.t. a scalar t	$\frac{\mathrm{d}}{\mathrm{d}t}\mathbf{c} \in \mathbb{R}^{n}$
Laplacian of $\mathbf{c} \in \mathbb{R}^{n}$	$\nabla^{2}\mathbf{c} \in \mathbb{R}^{n}$
Kronecker product of $\mathbf{N} \in \mathbb{R}^{n \times m}$ and $\mathbf{P} \in \mathbb{R}^{p \times q}$	$\mathbf{N} \otimes \mathbf{P} \in \mathbb{R}^{np \times mq}$
Vectorisation of $\mathbf{N} \in \mathbb{R}^{n \times m}$	$\mathrm{vec}\,(\mathbf{N}) \in \mathbb{R}^{nm}$
Inner product of $\mathbf{v}$ and $\mathbf{w}$	$\langle \mathbf{v}, \mathbf{w} \rangle$ *or* $\mathbf{v} \cdot \mathbf{w}$ *or* $\mathbf{v}^{T}\mathbf{w}$

Chapter 2

Models of Biochemical Reaction Networks

Contents

In this chapter we present a constructive approach to the formulation of the dynamical models which will be analysed in the remaining chapters of this thesis. Firstly, from biomolecular interactions we derive a set of continuous time ordinary differential equations (ODEs) that describes the variation in time of the species' concentration. Secondly, we account for the diffusion of the species in a given spatial domain in order to derive a set of partial differential equations (PDEs) that govern the dynamical behaviour in both time and space. We note that these two classes of differential equations are by no means exhaustive. There is a wide range of dynamical models available in the literature to study the behaviour of biochemical reaction networks.

However, we will limit our attention to ODE and PDE formulations. To conclude this chapter, we will comment on the equilibrium set of the reaction(-diffusion) networks. And finally, we exemplify the computation of the equilibrium set of a circular protein activation of variable length.

Once a qualitative understanding of a particular biochemical process has been achieved, a further quantitative characterisation of the systems properties helps to classify them as structural properties of the biochemical pathway or consequences of fine-tuned kinetic parameters. Thus, providing a clearer understanding of the process itself. A key tool to perform these quantitative analyses are the mathematical models of biochemical reaction networks. In addition these provide a means to systematically propose and test hypotheses on the dynamics of the biological process under study. The outcome of this analysis further illuminates the principles that underpin the biochemical processes under study.

Given this twofold advantage of using mathematical models, in the remaining of this work we present a set of analytical approaches that will assist in the study of such models. In this chapter we present generic mathematical expressions that describe the reaction rates of the species in a reaction network. Furthermore, from these reaction rates, we build-up models that describe the rate of change of the species concentrations in space and/or time. Later on we provide a general view of the equilibrium set of a reaction network and exemplify its calculation in protein autoactivation with an arbitrary number of intermediate activation steps. To finalise, we avail of a coordinate transformation to express the systems in the deviation coordinates from an equilibrium point of the system.

2.1 Reaction Mechanisms

When two affine chemical species meet their electro-chemical interaction leads to the formation of a third species. Although this simple conception of a reaction broadly describes chemical interaction among species, it does not indicate the rich spectrum of mechanisms by which a reaction can occur. Consequently, the mathematical laws that describe the rate at which the reactants become products similarly follows a rich spectrum. In the rest of this section we provide an overview of the mathematical expressions that model biochemical reaction rates.

Firstly, we note that molecular interactions behave as discrete stochastic events; that is to say, the concentration of one species in a future time $t + \mathrm{d}t$, depends on the concentration at time

t, and the probability for the reaction to occur [29]. The literature in this regard ranges from the reduction of the computational load required to approximate the moments of the probability density function of the concentrations in time [30], to the analytical treatment of the stochastic differential equation that allows the inference of the properties of the system itself, such as the identification of the systems parameters [31]. For instance, in the simple reaction

$$A \underset{k_b}{\overset{k_f}{\rightleftharpoons}} B, \tag{2.1}$$

the probability $P(A,t)$ of a molecule being in state A at time t is determined by

$$\frac{\mathrm{d}}{\mathrm{d}t}P(A,t) = k_b P(B,t) - k_f P(A,t).$$

The equation above governs the change of the probability of the reaction to happen in time. Although an analytical treatment is possible for simple cases, for more complex reactions it is necessary to perform a huge amount of simulations in order to determine the characteristic of the resulting time course of the probabilities of being in states A, B. Although the molecular interaction is driven by the random collision of reactants, when their concentration is large enough, we can idealise the reaction as a deterministic, continuous process. We adopt this approach in the following. Depending on the details of the chemical interaction of the reactants there are different mathematical models that reproduce the reaction rates behaviour.

A widely used principle that supports the mathematical model of a reaction rate under the presence of a large enough concentration of the reactants, is the Law of Mass Action. For a detailed treatment of this law we refer the reader to [32], where further implications about the positivity and stability of the dynamical systems that arise from the Law of Mass Action can be found. This law states that the rate at which the reacting substrates are transformed to products is proportional to the product of the concentrations raised to the power of their molecularity. In what follows we will denote the concentration of the species A by $[A] \in \mathbb{R}_+$. That is to say, the reaction rate v of the reaction

$$aA + bB \xrightarrow{k} C \tag{2.2}$$

is given by

$$v \propto [A]^a [B]^b.$$

The equality is achieved by the proportionality parameter k, defined as

$$k(T) = \mathcal{A} \exp\left(-\frac{E_a}{RT}\right).$$

Where

$\mathcal{A}$	Arrhenius constant	Reaction dependent
E_a	Activation energy	Reaction dependent $[\frac{kJ}{mol}]$
R	Universal Gas constant	$8.314 \times 10^{-3}\left[\frac{kJ}{molK}\right]$
T	Absolute temperature	$[K]$.

In what follows we will focus on biochemical reactions under a constant temperature environment. Consequently, we will consider the parameter k to be constant for each reaction.

Although widely used, the Law of Mass Action does not always give an accurate description of the reaction rate, especially when a reaction comprises several intermediate chemical interactions. For such a case, we can avail of a family of sigmoid curves that describe the reaction rate [4]. Consider the reaction in (2.2) where we have set $a, b = 1$. Let A be the substrate that saturates under the presence of the species B. Then the rate of this reaction may take the functional form

$$v = k\frac{[A]^m}{K^m + [A]^m}[B],$$

here $m \in \mathbb{R}_+$ is the Hill coefficient of the reaction and $K \in \mathbb{R}$ is a constant that determines the location inflexion point of the sigmoid characteristic.

A more general reaction rate model is the Power Law [33], which is used to fit experimental data for a broad kind of reaction. Consider again the reaction in (2.2). The reaction rate based on the Power Law is

$$v = k[A]^{g_1}[B]^{g_2}.$$

Here g_1 and g_2 are positive real numbers that represent the cooperativity of the species in the reaction. Although this functional form of the reaction rate v resembles that obtained with the Mass Action Law, the coefficients g do not represent any particular characteristic of the reaction, but combines several kinetic effects so as to reproduce the macroscopic behaviour of the reaction.

So far in this section, we considered some of the main laws that are used to model reaction rates. However, we just focused on a single reaction. In contrast, a reaction network comprises a

relatively large number of reactions. In the following section we present the dynamical models of reaction networks, which are widely available in the literature.

2.2 Reaction Networks

Once we have defined each of the reactions, a general way to express their interaction is via the following expression for the j^{th} reaction:

$$\sum_{i=1}^{n} a_{ij} S_i \overset{v_j}{\rightleftharpoons} \sum_{i=1}^{n} b_{ij} S_i. \tag{2.3}$$

Here S_i is the i^{th} reactant or product for the j^{th} reaction. In addition, $i \in [1, n]$ and $j \in [1, m]$. The real numbers a_{ij} and b_{ij} denote the yield or stoichiometric coefficients of the corresponding species. When a reaction can be approximated as irreversible, we will just use a forward arrow to describe the species interaction. Note that we will focus on biological systems that can be idealized as adiabatic and isothermal. This allows us to fully determine the state of the network exclusively from the species' concentration. An intuitive way to built these models up is to add or subtract the rates at which each species is being created or consumed, in order to obtain the differential equation that governs the concentration dynamics. That is to say

$$\frac{\mathrm{d}}{\mathrm{d}t}[S_i] = \sum_j (b_{ij} - a_{ij}) v_j. \tag{2.4}$$

Nevertheless, this intuitive approach might require a big effort when the number of species is large. One systematic approach to modelling the reaction network is to define a matrix $\mathbf{N}$ that links the reaction rates $\mathbf{v}(\mathbf{c})$ with the change rate of the species concentration gathered in $\mathbf{c}$. Accounting for external inputs, $\mathbf{u}$, a compact notation for this kind of system is given by

$$\frac{\mathrm{d}}{\mathrm{d}t}\mathbf{c} = \mathbf{N}\mathbf{v}(\mathbf{c}) + \mathbf{B}\mathbf{u}. \tag{2.5}$$

Here, $\mathbf{c}(t) : \mathbb{R}^n \to \mathbb{R}^n$ is a vector containing the species concentrations in (2.3). The rates at which the reactants are becoming products form the vector $\mathbf{v}(\mathbf{c}(t)) : \mathbb{R}_+ \to \mathbb{R}^m$. Apart from simple reactions such as synthesis and degradation, these reaction rates are nonlinear functions of the state $\mathbf{c}(t)$, which can be modelled by well-known principles such as the Mass Action Law, Power Law, and Hill kinetics, defined in Section 2.1. Further, $\mathbf{u}(t) : \mathbb{R}_+ \to \mathbb{R}^q$ accounts for the influx and efflux rates of the relevant species, resulting from the interaction of the reaction

network with its surroundings. Accordingly, $\mathbf{B} \in \mathbb{R}^{n\times q}$ shows how this interaction affects the change rate of the species. The link from reaction rates to the actual concentration change is the stoichiometric matrix $\mathbf{N} \in \mathbb{R}^{n\times m}$, whose ij^{th} element is defined as

$$N_{ij} = b_{ij} - a_{ij}.$$

From the definition above, we note that each column of the matrix $\mathbf{N}$ is obtained by subtracting a vector composed of the products yield coefficients minus those of the reactants. In the rest of this work we exploit the properties of the linear map $\mathbf{N}$, which has been well characterised in the literature. For instance, the analysis of the subspaces of the stoichiometric matrix has led to the characterisation of different influx and efflux subspaces, hence showing the role and effects of the network with its surroundings [34]. In a related line of work, the left null space of $\mathbf{N}$ has been implicated in the characterisation of achievable biological states of a network [35]. Also a further singular value decomposition of the stoichiometric matrix, has been used to correlate systemic properties of genome-scale reaction networks [36].

One important milestone in the analysis of the differential equations is the characterisation of the equilibrium set. Hence, in the following section we present the definitions of the equilibrium points and a generic approach to obtain them for the systems in (2.5).

2.3 Equilibrium Set

In this section, we characterise the manifold to which the equilibrium set of the reaction network in (2.5) belongs. Without loss of generality, we assume that the external influxes represented by $\mathbf{u}$ in (2.5) equal zero. The existence of equilibrium sets has been investigated by different approaches. The Chemical Reaction Network Theory (CRNT) of Feinberg, Horn, and Jackson calculates the number of equilibrium points of a chemical reaction network and investigates their local stability [37]. Likewise, in [38] the number of positive equilibrium points is studied by means of the degree theory for general complex reaction networks. However, both approaches fail to provide formulas to calculate equilibrium concentrations of the species, in terms of the kinetic parameters. The equilibrium points are closely related to the column null space of the stoichiometric matrix $\mathbf{N}$. We recall that all the fixed points (denoted as $\bar{\mathbf{c}} \in \mathbb{R}^n_+$) satisfy

$$\mathbf{N}\mathbf{v}\left(\bar{\mathbf{c}}\right) = \mathbf{0}. \tag{2.6}$$

Let the columns of $\mathbf{K} \in \mathbb{R}^{m\times r}$ form a basis for this null space. The Rank Nullity Theorem states that the dimension of the (right) null space of a matrix $\mathbf{X}$ (also denoted as $\mathrm{nullity}\,(\mathbf{X})$) is the difference of the number of the columns of $\mathbf{X}$ and the rank of $\mathbf{X}$ [39]. Hence, the number of columns of $\mathbf{K}$ is $r = \#\mathrm{col}(\mathbf{N}) - \mathrm{rank}\,(\mathbf{N})$. Since (2.6) implies that $\mathbf{v}\,(\bar{\mathbf{c}}) \in \mathrm{Null}(\mathbf{N})$, we can express any element of a vector space as a linear combination of its basis. Hence, there exists a vector $\mathbf{a} \in \mathbb{R}^r$ such that

$$\mathbf{K}\mathbf{a} = \mathbf{v}\,(\bar{\mathbf{c}}). \tag{2.7}$$

Although the solutions of the equation above for $\bar{\mathbf{c}}$ are the equilibrium points of the system, it is necessary to invert the nonlinear map $\mathbf{v}(\circ)$. This is a difficult task to address in a general framework. We, furthermore, note that if the null space of $\mathbf{N}$ is trivial, then the equilibrium point $\bar{\mathbf{c}}$ must comply with $\mathbf{v}(\bar{\mathbf{c}}) = \mathbf{0}$. In order to exemplify the use of the null space for the computation of the equilibrium set, let us consider a simple protein autoactivation mechanism.

Example 2.1. *For this example, all superindexes will be used to denote different variables, rather than an exponent. That is to say c_1^1 and c_1^2 refer to different variables. In turn, when required, the operation of exponentiation will be denoted with round brackets, for example: $c_j^i \times c_j^i = \left(c_j^i\right)^2$. The autoactivation mechanism is represented by the interaction of a protein P^1 with its activated version A^1 to produce two molecules of A^1. We also consider a turnover for P^1 and degradation for A^1. These effects can be described by the following reactions*

$$P^1 + A^1 \xrightarrow{k_1^1} 2A^1,$$
$$A^1 \xrightarrow{k_2^1} 0,$$
$$P^1 \underset{k_{3b}^1}{\overset{k_{3f}^1}{\rightleftharpoons}} 0.$$

By means of the vector order $\mathbf{c}^1 = ([P^1]\ [A^1])^T$ and assuming a mass-action reaction mecha-

nism, the stoichiometric matrix $\mathbf{N}^1$ *and the reaction vector* $\mathbf{v}^1(\mathbf{c}^1)$ *are*

$$\mathbf{N}^1 = \begin{pmatrix} -1 & 0 & -1 \\ 1 & -1 & 0 \end{pmatrix}, \tag{2.8}$$

$$\mathbf{v}^1(\mathbf{c}^1) = \begin{pmatrix} k_1^1 c_1^1 c_2^1 \\ k_2^1 c_2^1 \\ k_{3f}^1 c_1^1 - k_{3b}^1 \end{pmatrix}. \tag{2.9}$$

In particular for our case study, the dimension of the Null Space is $r = 3 - 2 = 1$ *and*

$$\mathbf{K}^1 = \begin{pmatrix} -1 \\ -1 \\ 1 \end{pmatrix}. \tag{2.10}$$

From (2.7) *and* (2.9)*, we conclude*

$$k_1^1 \bar{c}_1^1 \bar{c}_2^1 = -a^1, \tag{2.11a}$$

$$k_2^1 \bar{c}_2^1 = -a^1, \tag{2.11b}$$

$$k_{3f}^1 \bar{c}_1^1 - k_{3b}^1 = \quad a^1. \tag{2.11c}$$

In order to solve this system, we express $\bar{c}_2^1$ *and* $\bar{c}_1^1$ *as a function of* a^1 *as follows*

$$\bar{c}_1^1 = \frac{a^1 + k_{3b}^1}{k_{3f}^1}, \tag{2.12a}$$

$$\bar{c}_2^1 = -\frac{a^1}{k_2^1}. \tag{2.12b}$$

The substitution of these two expressions in (2.11a)*, yields*

$$\begin{aligned} -a^1 &= -\frac{k_1^1}{k_2^1 k_{3f}^1} a^1 (a^1 + k_{3b}^1), \\ 0 &= a^1 \left(a^1 - \frac{k_2^1 k_{3f}^1 - k_1^1 k_{3b}^1}{k_1^1} \right). \end{aligned} \tag{2.13}$$

Finally, from (2.12b) *and* (2.12a) *we have that the two equilibrium points of this network are*

$$\textbf{Off steady state :}\bar{\mathbf{c}}^{\mathbf{1}}_{\text{off}} = \begin{pmatrix} \frac{k^1_{3b}}{k^1_{3f}} & 0 \end{pmatrix}^T, \tag{2.14a}$$

$$\textbf{On steady state :}\bar{\mathbf{c}}^{\mathbf{1}}_{\text{on}} = \begin{pmatrix} \frac{k^1_2}{k^1_1} & \frac{k^1_{3b}}{k^1_2} - \frac{k^1_{3f}}{k^1_1} \end{pmatrix}^T. \tag{2.14b}$$

It is noteworthy that we can parametrise the solution of the augmented system (2.11) *by* a^1*, as shown in* (2.13)*. Moreover, we remark that the dimension of the null space of* $\mathbf{N}^1$ *is 1, so we only require one scalar,* a^1*, to represent the linear combination that spans Null*$(\mathbf{N}^1)$*. In addition, the name* off *and* on steady *state, follows from the absence or presence of active protein concentration in the respective equilibrium point.*

In the following example, as a generalisation of the previous example, we obtain the equilibrium points of the circular and sequential autoactivation depicted in Figure 2.1.

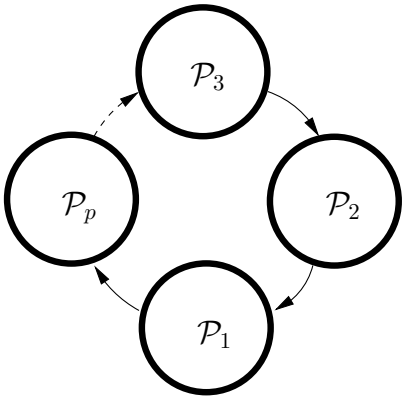

Figure 2.1: *Sequential protein activation network. The active version of each protein* A^{i+1} *(arrows) activates the protein* P^i*, as described by the reaction network (circles) in* (2.15)*.*

Example 2.2. *In this example we obtain the equilibria set for a sequential protein activation and carry forward the notation from the previous example. Consider an activation loop of* p*-tier, as shown in Figure 2.1, where the last active protein* A^1 *activates the first inactive protein* P^p*. Therefore, the index* i *should be understood as having modulo* p*. In addition we will consider that the* $i + 1^{th}$ *active protein* A^{i+1} *activates the* i^{th} *inactive protein* P^i*, by means of the the*

forthcoming reaction network

$$P^i + A^{i+1} \xrightarrow{k_1^i} A^i + A^{i+1}, \tag{2.15a}$$

$$A^i \xrightarrow{k_2^i} 0, \tag{2.15b}$$

$$P^i \underset{k_{3b}^i}{\overset{k_{3f}^i}{\rightleftharpoons}} 0. \tag{2.15c}$$

By letting

$$\mathbf{c} = \begin{pmatrix} \mathbf{c}^1 \\ \vdots \\ \mathbf{c}^p \end{pmatrix} \tag{2.16}$$

and

$$\mathbf{c}^i = \begin{pmatrix} [P^i] \\ [A^i] \end{pmatrix}, \tag{2.17}$$

the stoichiometric matrix and reaction rate vector are given by

$$\mathbf{N} = \begin{pmatrix} \mathbf{N}^1 & \mathbf{0} & \dots & \mathbf{0} \\ \mathbf{0} & \mathbf{N}^2 & \dots & \mathbf{0} \\ \vdots & \vdots & \ddots & \vdots \\ \mathbf{0} & \mathbf{0} & \dots & \mathbf{N}^p \end{pmatrix}, \tag{2.18a}$$

$$\mathbf{v}(\mathbf{c}) = \begin{pmatrix} \mathbf{v}\left(\mathbf{c}^1, \mathbf{c}^2\right) \\ \mathbf{v}\left(\mathbf{c}^2, \mathbf{c}^3\right) \\ \vdots \\ \mathbf{v}\left(\mathbf{c}^p, \mathbf{c}^1\right) \end{pmatrix}. \tag{2.18b}$$

Note that the same reaction topology holds for all tiers, and therefore $\mathbf{N}^1 = \mathbf{N}^2 = \ldots = \mathbf{N}^p$. *Moreover,* $\mathbf{N}^1$ *has already been defined in* (2.8)*. In turn*

$$\mathbf{v}\left(\mathbf{c}^i, \mathbf{c}^{i+1}\right) = \begin{pmatrix} k_1^i c_1^i c_2^{i+1} \\ k_2^i c_2^i \\ k_{3f}^i c_1^i - k_{3b}^i. \end{pmatrix}$$

A basis for Null$(\mathbf{N})$ *is given by*

$$\mathbf{K} = \begin{pmatrix} \mathbf{K}^1 & \mathbf{0} & \dots & \mathbf{0} \\ \mathbf{0} & \mathbf{K}^2 & \dots & \mathbf{0} \\ \vdots & \vdots & \ddots & \vdots \\ \mathbf{0} & \mathbf{0} & \dots & \mathbf{K}^p \end{pmatrix}.$$

Similarly to $\mathbf{N}$*, we note that* $\mathbf{K}^1 = \mathbf{K}^2 = \ldots = \mathbf{K}^p$*. The definition of* $\mathbf{K}^1$ *is given in* (2.10)*. Now, the equilibrium set satisfies*

$$\mathbf{N}\mathbf{v}(\bar{\mathbf{c}}) = \mathbf{0} \quad \Longrightarrow \quad \mathbf{N}^i\mathbf{v}\left(\bar{\mathbf{c}}^i, \bar{\mathbf{c}}^{i+1}\right) = \mathbf{0}\ \forall\, i \in [1, p],$$

which, in terms of the $\mathbf{N}^i$*s null space, becomes*

$$\mathbf{K}^i\mathbf{a}^i = \mathbf{v}\left(\bar{\mathbf{c}}^i, \bar{\mathbf{c}}^{i+1}\right).$$

Or in extenso

$$k_1^i \bar{c}_1^i \bar{c}_2^{i+1} = -a^i, \tag{2.19a}$$

$$k_2^i \bar{c}_2^i = -a^i, \tag{2.19b}$$

$$k_{3f}^i \bar{c}_1^i - k_{3b}^i = \quad a^i. \tag{2.19c}$$

Analogously to the one-tier feedback, we conclude that the solution for the equation above can be parametrized by a^i*, as follows. From* (2.19c)

$$\bar{c}_1^i = \frac{a^i + k_{3b}^i}{k_{3f}^i}, \tag{2.20a}$$

and from (2.19b)

$$\bar{c}_2^i = -\frac{a^i}{k_2^i}. \tag{2.20b}$$

Whence, substituting (2.20) *into* (2.19a)*, we obtain*

$$a^{i+1} = \frac{\alpha^i a^i}{1 + \beta^i a^i}. \tag{2.21}$$

Where we have defined

$$\alpha^i = \frac{k_2^{i+1} k_{3f}^i}{k_1^i k_{3b}^i}, \tag{2.22a}$$

$$\beta^i = \frac{1}{k_{3b}^i}; \tag{2.22b}$$

To find a closed-form expression for all a^i, we note that a^2, a^3 and a^4 can be expressed in terms of a^1, as follows

$$\begin{aligned}
a^2 &= \alpha^1 \frac{a^1}{1 + \beta^1 a^1}, \\
a^3 &= \alpha^1 \alpha^2 \frac{a^1}{1 + \left[\beta^1 + \alpha^1 \beta^2\right] a^1}, \\
a^4 &= \frac{a^1 \prod_{j=1}^{3} \alpha^j}{1 + \left[\beta^1 + \alpha^1 \beta^2 + \alpha^1 \alpha^2 \beta^3\right] a^1}.
\end{aligned}$$

From which we conclude

$$a^{i+1} = \frac{a^1 \prod_{j=1}^{i} \alpha^j}{1 + \left[\sum_{k=1}^{i} \beta^k \prod_{j=1}^{k-1} \alpha^j\right] a^1}. \tag{2.23}$$

When $i = p$, the expression above becomes

$$a^1 = \frac{a^1 \prod_{j=1}^{p} \alpha^j}{1 + \left[\sum_{k=1}^{p} \beta^k \prod_{j=1}^{k-1} \alpha^j\right] a^1}. \tag{2.24}$$

By letting

$$\begin{aligned}
\lambda &= \prod_{j=1}^{p} \alpha^j, \\
\sigma &= \sum_{k=1}^{p} \beta^k \prod_{j=1}^{k-1} \alpha^j,
\end{aligned}$$

we can rewrite (2.24) *as*

$$a^1 \left(a^1 - \frac{\lambda - 1}{\sigma}\right) = 0, \tag{2.25}$$

which is a second order polynomial in a^1, with a trivial solution. Let $n(z)$ and $d(z)$ denote the numerator and denominator of the rational term z. In term of the parameters, the non-trivial

root becomes

$$\frac{\lambda-1}{\sigma}=\frac{n(\lambda)-d(\lambda)}{d(\lambda)\,\sigma},$$
$$\frac{\lambda-1}{\sigma}=\frac{\prod_{j=1}^{p}k_2^{j+1}k_{3f}^{j}-\prod_{j=1}^{p}k_1^{j}k_{3b}^{j}}{\sum_{k=1}^{p}k_1^{k}\prod_{j=1}^{k-1}k_2^{j+1}k_{3f}^{j}\prod_{j=k+1}^{p}k_1^{j}k_{3b}^{j}}.$$

Where we have used the definition of α^i *in* (2.22a)*. The solution for the remaining* a^i*s can be found explicitly through* (2.23)*, as follows*

$$a^{i+1}=\frac{n(a^1)\prod_{j=1}^{i}\alpha^j}{d(a^1)+\left[\sum_{k=1}^{i}\beta^k\prod_{j=1}^{k-1}\alpha^j\right]n(a^1)}.$$

Considering a^1*'s non-trivial root in* (2.25)*, we have*

$$\begin{aligned}a^{i+1}=&\frac{(\lambda-1)\prod_{j=1}^{i}\alpha^j}{\sigma+\left[\sum_{k=1}^{i}\beta^k\prod_{j=1}^{k-1}\alpha^j\right](\lambda-1)}\\=&\frac{\prod_{j=1}^{p}n(\alpha^j)-\prod_{j=1}^{p}d(\alpha^j)}{\prod_{j=1}^{i}d(\alpha^j)\sum_{k=i+1}^{p}\left(k_1^k\prod_{j=i+1}^{k-1}n(\alpha^j)\prod_{j=k+1}^{p}d(\alpha^j)\right)+}\\&\frac{}{+\prod_{j=i+1}^{p}n(\alpha^j)\sum_{k=1}^{i}\left(k_1^k\prod_{j=1}^{k-1}n(\alpha^j)\prod_{j=k+1}^{i}d(\alpha^j)\right)}.\end{aligned}\tag{2.26}$$

Finally, to obtain a closed form expression of the equilibrium points, we substitute the former expression in (2.20)*. It is noteworthy, that despite having an arbitrary number of intermediate activation steps* p*, this reaction network has only two steady states, characterised by* $a^{i+1}=0$ *or by the expression in* (2.26)*, respectively. From* (2.20) *we therefore have*

$$\textbf{Off steady state}:\bar{\mathbf{c}}_{\text{off}}^{\mathbf{i+1}}=\begin{pmatrix}\frac{k_{3b}^{i+1}}{k_{3f}^{i+1}} & 0\end{pmatrix}^T,\tag{2.27a}$$
$$\textbf{On steady state}:\bar{\mathbf{c}}_{\text{on}}^{\mathbf{i+1}}=\begin{pmatrix}\frac{a^{i+1}+k_{3b}^{i+1}}{k_{3f}^{i+1}} & -\frac{a^{i+1}}{k_2^{i+1}}\end{pmatrix}^T,\tag{2.27b}$$

Since all kinetic parameters k_j^i *are positive, all inactive proteins of the* off steady state *have positive concentrations. As per definition of this state, the concentration of all active proteins*

are zero. Therefore, all concentration of proteins are non-negative and this state is biologically meaningful. The existence condition for a meaningful on steady state *is more subtle and depends on the choice of kinetic parameters. In particular, we note that from* (2.19a)*,* $\bar{c}_1^i$ *may be expressed as the ratio of positive terms (see the definition of* $d\left(a^{i+1}\right)$ *in* (2.26)*):*

$$\begin{aligned}\bar{c}_1^i &= \frac{k_2^{i+1}}{k_1^i}\frac{a^i}{a^{i+1}},\\ \bar{c}_1^i &= \frac{k_2^{i+1} d\left(a^{i+1}\right)}{k_1^i d\left(a^i\right)}.\end{aligned} \tag{2.28}$$

Hence, we can assure that all concentrations of the inactive proteins for the on steady state *are positive. In turn, for all the concentrations of the active proteins to be positive, we require* a^{i+1} *to be negative since the denominator of* a^{i+1} *in* (2.26) *is positive. For every* i*, the numerator of* a^{i+1} *is the same. Thus, all the active proteins are positive when*

$$\prod_{j=1}^{p} k_1^j k_{3b}^j - \prod_{j=1}^{p} k_2^j k_{3f}^j > 0. \tag{2.29}$$

Furthermore, this condition is independent of i*, therefore unspecific for the actual protein within the circular activation network and, consequently, a general condition for a meaningful* on steady state*. In the formula above, we have also replaced* $j+1$ *by* j *in the second product by exploiting the modularity of the product with respect to* p*.*

We conclude by stating that the existence of a biologically meaningful on steady state *requires that the product of all the synthesis and activation rates of the inactive proteins is greater than the product of all degradation rates of the active and inactive proteins.*

The previous two examples relate the equilibrium point with the null space of the stoichiometric matrix, yet requires the invertibility of the nonlinear map $\mathbf{v}\left(\bar{\mathbf{c}}\right)$. A different approach, which relies on a suitable linear coordinate transformation, shows that the equilibrium set of the reaction network in (2.5) belongs to a lower dimensional space, spanned by the columns of the stoichiometric matrix associated to nonlinear reaction rates. We explore these ideas in the following.

2.3.1 Equilibria Set in a Lower Dimensional Space

Here, we consider all reactions to be unidirectional. Consequently, we will represent a reversible reaction as two different reactions. This will allow us to split the reaction vector in nonlinear,

linear and constant functions, i.e.,

$$\mathbf{v}(\mathbf{c}) = \begin{pmatrix} \mathbf{v_{NL}} \\ \mathbf{v_L} \\ \mathbf{v_0} \end{pmatrix} : \mathbb{R}^n_+ \to \mathbb{R}^{m_1+m_2+m_3}. \tag{2.30}$$

It will be convenient to express $\mathbf{v_L}$ as a linear combination of the state $\mathbf{c}$

$$\mathbf{v_L} = \mathbf{G}\mathbf{c}, \tag{2.31}$$

where $\mathbf{G} \in \mathbb{R}^{m_2 \times n}$. The partition of the reaction rate vector $\mathbf{v}(\mathbf{c})$ induces the following order in the stoichiometric matrix

$$\mathbf{N} = \begin{pmatrix} \mathbf{N_{NL}} & \mathbf{N_L} & \mathbf{N_0} \end{pmatrix} \in \mathbb{R}^{n \times (m_1+m_2+m_3)}. \tag{2.32}$$

We will focus on finding all states $\bar{\mathbf{c}}$ such that

$$\mathbf{N}\mathbf{v}(\bar{\mathbf{c}}) + \mathbf{B}\bar{\mathbf{u}} = \mathbf{0}. \tag{2.33}$$

For the sake of simplicity, in the rest of this section we assume that $\mathbf{N_{NL}}$ is full column rank. The extension otherwise, is straightforward. Consider a linear transformation $\mathbf{z} = \mathbf{T}\mathbf{c}$, defined as

$$\begin{pmatrix} \mathbf{z_1} \\ \mathbf{z_2} \end{pmatrix} = \begin{pmatrix} \mathbf{N_{NL}}^{\perp} \\ \mathbf{N_{NL}}^{T} \end{pmatrix} \mathbf{c}. \tag{2.34}$$

Consequently

$$\mathbf{c} = \begin{pmatrix} \mathbf{N_{NL}}^{\perp +} & \mathbf{N_L}^{T+} \end{pmatrix} \mathbf{z}. \tag{2.35}$$

We note that $\mathbf{N_{NL}}^{\perp}$ vanishes (that is, has dimension zero), except when $\mathbf{N_{NL}}$ is rank deficient. In other words, to have a non-trivial $\mathbf{N_{NL}}^{\perp}$ we require that the number of species exceed the number of nonlinear reactions ($n > m_1$). In the $\mathbf{z}$ coordinates, the dynamics of the system (2.5) takes the form

$$\frac{\mathrm{d}}{\mathrm{d}t}\mathbf{z_1} = \mathbf{N_{NL}}^{\perp}\mathbf{N_L}\mathbf{G}\mathbf{T}^{-1}\mathbf{z} + \mathbf{N_{NL}}^{\perp}\mathbf{N_0}\mathbf{v_0} + \mathbf{N_{NL}}^{\perp}\mathbf{B}\mathbf{u}, \tag{2.36a}$$

$$\frac{\mathrm{d}}{\mathrm{d}t}\mathbf{z_2} = \mathbf{N_{NL}}^{T}\mathbf{N_{NL}}\mathbf{v_{NL}}(\mathbf{z}) + \mathbf{N_{NL}}^{T}\mathbf{N_L}\mathbf{G}\mathbf{T}^{-1}\mathbf{z} + \mathbf{N_{NL}}^{T}\mathbf{N_0}\mathbf{v_0} + \mathbf{N_{NL}}^{T}\mathbf{B}\mathbf{u}. \tag{2.36b}$$

From (2.36a), the equilibrium for $\mathbf{z}_1$ satisfies

$$\mathbf{R}\bar{\mathbf{z}}_\mathbf{2} + \mathbf{S} = \bar{\mathbf{z}}_\mathbf{1}, \tag{2.37}$$

where have been defined

$$\begin{aligned} q = &\quad \text{nullity}\{{\mathbf{N}_{\mathbf{NL}}}^T\}, \\ \mathbb{R}^{q\times q} \quad \ni \quad &\mathbf{\Sigma} = -\left({\mathbf{N}_{\mathbf{NL}}}^{\perp}\mathbf{N}_\mathbf{L}\mathbf{G}{\mathbf{N}_{\mathbf{NL}}}^{\perp+}\right)^{-1}, \\ \mathbb{R}^{q\times(n-q)} \quad \ni \quad &\mathbf{R} = \mathbf{\Sigma}{\mathbf{N}_{\mathbf{NL}}}^{\perp}\mathbf{N}_\mathbf{L}\mathbf{G}{\mathbf{N}_{\mathbf{NL}}}^{T+}, \\ \mathbb{R}^{q} \quad \ni \quad &\mathbf{S} = \mathbf{\Sigma}{\mathbf{N}_{\mathbf{NL}}}^{\perp}\left(\mathbf{N_0}\mathbf{v_0} + \mathbf{B}\bar{\mathbf{u}}\right) \end{aligned}$$

By substituting (2.37) in (2.36b) and rearranging terms, we obtain

$$\mathbf{P}\mathbf{v}_{\mathbf{NL}}(\mathbf{R}\bar{\mathbf{z}}_\mathbf{2} + \mathbf{S}, \bar{\mathbf{z}}_\mathbf{2}) + \mathbf{Q}\bar{\mathbf{z}}_\mathbf{2} + \mathbf{W} = \mathbf{0}. \tag{2.38}$$

Here

$$\begin{aligned} \mathbb{R}^{(n-q)\times(n-q)} \quad \ni \quad &\mathbf{P} = {\mathbf{N}_{\mathbf{NL}}}^T\mathbf{N}_{\mathbf{NL}}, \\ \mathbb{R}^{(n-q)\times(n-q)} \quad \ni \quad &\mathbf{Q} = {\mathbf{N}_{\mathbf{NL}}}^T\mathbf{N}_\mathbf{L}\mathbf{G}\left({\mathbf{N}_{\mathbf{NL}}}^{\perp+}\mathbf{R} + {\mathbf{N}_\mathbf{L}}^{T+}\right), \\ \mathbb{R}^{(n-q)} \quad \ni \quad &\mathbf{W} = {\mathbf{N}_{\mathbf{NL}}}^T\left(\mathbf{N}_\mathbf{L}\mathbf{G}{\mathbf{N}_{\mathbf{NL}}}^{\perp+}\mathbf{S} + \mathbf{N_0}\mathbf{v_0} + \mathbf{B}\bar{\mathbf{u}}\right). \end{aligned}$$

As we can see from (2.38), we only need to solve a system of $(n-q)$ nonlinear equations with $(n-q)$ independent variables comprised in $\bar{\mathbf{z}}_\mathbf{2}$, in contrast to the original formulation in (2.33) in which we require to solve n nonlinear equations in n variables. In the next section we will consider the diffusion of species in a spatial domain to obtain a dynamical model that describes the species concentration dynamics in time and space.

2.4 Reaction-Diffusion Systems

Although the solution to the model in (2.5) represents the temporal profile of a system, it fails to reproduce some behaviours in which the parameter uncertainty [40], the spatial behaviour [41, 2], and/or boundary conditions are of interest. All these effects can be modelled by Partial Differential Equations (PDE), which, in contrast to the ODEs, are functions which include

derivatives with respect to more than one variable. Here we will focus on the spatio-temporal behaviour of the reaction network, driven by the diffusion of species in only one spatial direction. We note that the PDE formulation and the results derived in the rest of the thesis can be extended to more spatial coordinates. However, we prefer an unidimensional spatial approach to ease our presentation.

The effect of diffusion will be modelled by Fick's laws [42], which in general states that the net flux of the species $\mathbf{c}$ across an area of interest is proportional to the species concentrations gradient. Consequently its mathematical form is

$$\mathbf{J}(t,x) = -\mathbf{D}\frac{\partial}{\partial x}\mathbf{c}(t,x), \tag{2.39}$$

where the matrix $\mathbf{D}$ will be assumed to be constant in the spatial direction denoted by $x \in \Omega \subset \mathbb{R}$. To include the diffusion of molecules in addition to the reaction of species, consider a control volume whose start point is 0 and end point is $\xi \in \Omega$, with constant transversal area A. The time rate of change of mass is given by

$$\frac{\partial}{\partial t}\text{mass} = \text{Net flux of mass} + \text{Rate of conversion of mass due to reaction.}$$

Using the relationships (2.5) and (2.39)

$$\begin{aligned}\frac{\partial}{\partial t}\mathbf{c}(t,x)A\xi &= (\mathbf{J}(t,0) - \mathbf{J}(t,x))A + (\mathbf{N}\mathbf{v}(\mathbf{c}(t,x)) + \mathbf{B}\mathbf{u})A\xi \\ \frac{\partial}{\partial t}\mathbf{c}(t,x)\xi &\approx \mathbf{D}\frac{\partial^2}{\partial x^2}\mathbf{c}(t,x)\xi + (\mathbf{N}\mathbf{v}(\mathbf{c}(t,x)) + \mathbf{B}\mathbf{u})\xi,\end{aligned}$$

where the approximation $\mathbf{J}(t,x) \approx \mathbf{J}(t,0) + \frac{\partial}{\partial x}\mathbf{J}(t,x)\xi$ was used. Letting $\xi \to 0$, the foregoing equation becomes

$$\frac{\partial}{\partial t}\mathbf{c}(t,x)d\xi = \mathbf{D}\frac{\partial^2}{\partial x^2}\mathbf{c}(t,x)d\xi + (\mathbf{N}\mathbf{v}(\mathbf{c}(t,x)) + \mathbf{B}\mathbf{u})d\xi.$$

Integration over the spatial domain yields

$$\int_0^x \frac{\partial}{\partial t}\mathbf{c}(t,x)d\xi = \int_0^x \mathbf{D}\frac{\partial^2}{\partial x^2}\mathbf{c}(t,x)d\xi + \int_0^x (\mathbf{N}\mathbf{v}(\mathbf{c}(t,x)) + \mathbf{B}\mathbf{u})d\xi.$$

Since this equation is valid for any selection of $x \leq \xi$, we can conclude that the integrand

satisfies

$$\frac{\partial}{\partial t}\mathbf{c}(t,x) = \mathbf{D}\frac{\partial^2}{\partial x^2}\mathbf{c}(t,x) + \mathbf{N}\mathbf{v}(\mathbf{c}(t,x)) + \mathbf{B}\mathbf{u}. \tag{2.40}$$

In the following we will prefer the symbol ∇^2 to denote the Laplacian operator $\frac{\partial^2}{\partial x^2}$. Of major relevance in the modelling with PDEs is the correct selection of the boundary conditions, since this describes the physical constrains that the surroundings exert over the system analysed. The initial and boundary conditions may be represented by the expressions

$$\mathbf{c}(0,x) = \mathbf{c}_0(x) \; \forall \; x \in \Omega \subset \mathbb{R}, \tag{2.41}$$

$$m(t,\partial\Omega) = p(t,\partial\Omega)\mathbf{c}(t,\partial\Omega) + q(t,\partial\Omega) \left.\frac{\partial \mathbf{c}(t,x)}{\partial \mathbf{n}}\right|_{x=\partial\Omega} \quad \forall \; t \in \mathbb{R}_+, \tag{2.42}$$

where $\mathbf{n}$ is the outward normal vector to the boundary of Ω, denoted as $\partial\Omega$. The expression in (2.42) is the generic form of the boundary conditions (Robin boundary conditions). In particular, when $q(t,\partial\Omega) = 0$ or $p(t,\partial\Omega) = 0$ it used to represent Dirichlet or Neumann boundary conditions respectively.

In Section 2.3 we considered the equilibrium points of the reaction network in (2.5). When we account for the diffusion of species along with the reaction of the species, usually two types of equilibrium points are considered: $i)$ a spatially independent steady state (homogeneous steady state) and $ii)$ a steady state that depends on the spatial dimension (inhomogeneous or heterogeneous). For the first one, the steady states and the local stability analysis are the same as for the ODE case. For the later one, the steady states are, in general, computed by the solution of a $2n$th order ordinary differential equation subject to the boundary conditions of the original PDE. For the sake of completeness, we review the definitions of both steady states from the literature [2, 43].

2.4.1 Homogeneous Steady State

In [2] a homogeneous steady state, $\bar{\mathbf{c}}$, is defined as a state of a reaction-diffusion system that is invariant w.r.t. time and space, i.e.,

$$\frac{\partial}{\partial t}\bar{\mathbf{c}} = \nabla^2\bar{\mathbf{c}} = \mathbf{0}. \tag{2.43}$$

From (2.40) we conclude that $\mathbf{N}\mathbf{v}(\bar{\mathbf{c}}) = \mathbf{0}$, hence the homogeneous steady state of a reaction-diffusion PDE coincides with those of the model for the reaction system.

2.4.2 Heterogeneous Steady State

In general, PDEs are also capable of presenting equilibria that although temporally invariant, vary with the spatial dimension. For instance, morphogenes present a concentration gradient in equilibrium that promote downstream protein activation or synthesis in a spatial-dependent rate, leading to a different activation intensity in downstream pathways over all the spatial range of the cell [43]. This spatial-dependent steady state may be determined by assuming that there exist $\tilde{\mathbf{c}} = \tilde{\mathbf{c}}(x)$ such that

$$\frac{\partial}{\partial t}\tilde{\mathbf{c}} = \mathbf{0}.$$

Consequently, from (2.40) it follows that for any steady state

$$\nabla^2\tilde{\mathbf{c}} = -\mathbf{D}^{-1}\mathbf{N}\mathbf{v}(\tilde{\mathbf{c}}), \tag{2.44}$$

with the appropriate boundary conditions. Note that this resembles the nonhomogeneous Laplace equation [44]. Since $\tilde{\mathbf{c}}$ depends only on x, the expression in (2.44) is an ordinary differential equation in x with boundary conditions.

$$\frac{\mathrm{d}}{\mathrm{d}x}\mathbf{w_1} = \quad \mathbf{w_2}, \tag{2.45a}$$

$$\frac{\mathrm{d}}{\mathrm{d}x}\mathbf{w_2} = -\mathbf{D}^{-1}\mathbf{N}\mathbf{v}(\mathbf{w_1}). \tag{2.45b}$$

Here $\mathbf{w_1} = \tilde{\mathbf{c}}$ and $\mathbf{w_2} = \frac{\mathrm{d}}{\mathrm{d}x}\tilde{\mathbf{c}}$, and the initial and boundary conditions are those of (2.44). We note that, since the ODEs in (2.45) are nonlinear, an analytical description of the possible heterogeneous steady states is in general difficult.

2.5 Error Coordinates

Having characterised the equilibrium set of the reaction(-diffusion) system, we can avail of a translation of coordinates to express the dynamical model of the reaction network so that the linear and nonlinear parts of the model appear explicitly. Consider the following change of

coordinates:

$$\mathbf{e}(t,x) = \mathbf{c}(t,x) - \bar{\mathbf{c}}. \tag{2.46}$$

Differentiation with respect to time yields

$$\frac{\partial}{\partial t}\mathbf{e}(t,x) = \frac{\partial}{\partial t}\mathbf{c}(t,x).$$

In terms of the coordinate $\mathbf{e}(t,x)$, the model in (2.40) is

$$\frac{\partial}{\partial t}\mathbf{e}(t,x) = \mathbf{D}\nabla^2\left\{\mathbf{e}+\bar{\mathbf{c}}\right\} + \mathbf{N}\mathbf{v}(\mathbf{e}+\bar{\mathbf{c}}) + \mathbf{B}\mathbf{u}.$$

Here we have considered, without loss of generality, that the external input in steady state is zero. If it were not zero, we could express the input as deviation from the one in steady state value and express the dynamical model in terms of this deviation coordinates for the input.

Accounting for the partition of the reaction rate vector $\mathbf{v}(\mathbf{c})$ and stoichiometric matrix $\mathbf{N}$, as given in (2.30) and (2.32), respectively, the foregoing equation becomes

$$\begin{aligned}\frac{\partial}{\partial t}\mathbf{e}(t,x) &= \mathbf{D}\nabla^2\left\{\mathbf{e}+\bar{\mathbf{c}}\right\} + \mathbf{N}_{\mathbf{NL}}\mathbf{v}_{\mathbf{NL}}\left(\mathbf{e}+\bar{\mathbf{c}}\right) + \mathbf{N}_{\mathbf{L}}\mathbf{G}\left(\mathbf{e}+\bar{\mathbf{c}}\right) + \mathbf{N}_{\mathbf{0}}\mathbf{v}_{\mathbf{0}},\\ &= \mathbf{D}\nabla^2\mathbf{e} + \mathbf{N}_{\mathbf{NL}}\left[\mathbf{v}_{\mathbf{NL}}\left(\mathbf{e}+\bar{\mathbf{c}}\right) - \mathbf{v}_{\mathbf{NL}}\left(\bar{\mathbf{c}}\right)\right] + \mathbf{N}_{\mathbf{NL}}\mathbf{G}\mathbf{e},\end{aligned} \tag{2.47}$$

where we have exploited the definition of the equilibrium:

$$\mathbf{0} = \mathbf{D}\nabla^2\bar{\mathbf{c}} + \mathbf{N}_{\mathbf{NL}}\mathbf{v}_{\mathbf{NL}}\left(\bar{\mathbf{c}}\right) + \mathbf{N}_{\mathbf{NL}}\mathbf{G}\bar{\mathbf{c}} + \mathbf{N}_{\mathbf{0}}\mathbf{v}_{\mathbf{0}}.$$

The expression in (2.47), accounts for any nonlinear reaction rate $\mathbf{v}_{\mathbf{NL}}$. Although we wont consider in the rest of this thesis any prescribed form for the nonlinearities $\mathbf{v}_{\mathbf{NL}}$, we shall use the following assumptions to obtain a simpler form of (2.47).

Assumption 2.1. *Let*

A1. All the nonlinear reactions have at most two reactants;

A2. All the stoichiometric coefficients for the reactants are one; and

A3. The reaction rates $\mathbf{v}_{\mathbf{NL}}$ are modelled with the Mass Action Law.

Under these assumptions, the vector $\mathbf{v_{NL}}$ is composed of monomials of order two that can be expressed as a quadratic form, i.e.,

$$v_{NLi}(\mathbf{c}) = \mathbf{c}^T \mathbf{Y}_i \mathbf{c},$$

for a suitable selection of the elements in $\mathbf{Y}_i = \mathbf{Y}_i^T \in \mathbb{R}^{n \times n}$. Hence the vector $\mathbf{v_{NL}}(\mathbf{c})$ can be expressed as

$$\mathbf{v_{NL}}(\mathbf{c}) = \left(\mathbf{I}_{m_1} \otimes \mathbf{c}^T\right) \mathbf{Y}\mathbf{c}, \tag{2.48}$$

where $\mathbf{Y} = (\mathbf{Y}_1 \quad \mathbf{Y}_2 \quad \dots \quad \mathbf{Y}_{m_1})^T$ and $\otimes$ denotes the Kronecker product. The definition and properties of this product can be found in [45, 46], for instance. Since $\mathbf{c} = \mathbf{e} + \bar{\mathbf{c}}$, Equation (2.48) becomes

$$\begin{aligned}
\mathbf{v_{NL}}(\mathbf{e} + \bar{\mathbf{c}}) &= \left(\mathbf{I}_{m_1} \otimes (\mathbf{e} + \bar{\mathbf{c}})^T\right) \mathbf{Y} (\mathbf{e} + \bar{\mathbf{c}}), \\
&= \left(\mathbf{I}_{m_1} \otimes \mathbf{e}^T\right) \mathbf{Y}\mathbf{e} + \left(\mathbf{I}_{m_1} \otimes \bar{\mathbf{c}}^T\right) \mathbf{Y}\bar{\mathbf{c}} + 2\left(\mathbf{I}_{m_1} \otimes \mathbf{e}^T\right) \mathbf{Y}\bar{\mathbf{c}}, \\
\mathbf{v_{NL}}(\mathbf{e} + \bar{\mathbf{c}}) &= \mathbf{v_{NL}}(\mathbf{e}) + \mathbf{v_{NL}}(\bar{\mathbf{c}}) + 2\left(\mathbf{I}_{m_1} \otimes \bar{\mathbf{c}}^T\right) \mathbf{Y}\mathbf{e}.
\end{aligned} \tag{2.49}$$

Hence, under the Assumptions 2.1, we can rewrite (2.47) as

$$\frac{\partial}{\partial t}\mathbf{e} = \mathbf{D}\nabla^{\mathbf{2}}\mathbf{e} + \mathbf{A}\mathbf{e} + \mathbf{N_{NL}}\mathbf{v_{NL}}(\mathbf{e}) + \mathbf{B}\mathbf{u}, \tag{2.50}$$

where

$$\mathbf{A} = \mathbf{N_L}\mathbf{G} + 2\mathbf{N_{NL}}\left(\mathbf{I}_{m_1} \otimes \bar{\mathbf{c}}^T\right) \mathbf{Y}. \tag{2.51}$$

The dynamical system in (2.50) explicitly shows the linear and nonlinear terms for the special case of the nonlinearities $\mathbf{v_{NL}}$described in the Assumptions 2.1. Nevertheless, a similar form for the dynamical system can be obtained for any kind of nonlinearities in $\mathbf{v_{NL}}$. This follows for the Taylor expansion around $\bar{\mathbf{c}}$ of the reaction rates in $\mathbf{v}(\mathbf{c})$ in (2.40). This expansion leads to

$$\frac{\partial}{\partial t}\mathbf{e} = \mathbf{D}\nabla^2\mathbf{e} + \mathbf{A}\mathbf{e} + \mathbf{N_{NL}}\mathbf{g}(\mathbf{e}) + \mathbf{B}\mathbf{u}. \tag{2.52}$$

Here $\mathbf{A}$ is the Jacobian of $\mathbf{N}\mathbf{v}(\mathbf{c})$ and $\mathbf{g}(\mathbf{e})$ has all the higher order terms of the Taylor expansion of $\mathbf{v_{NL}}$ around $\bar{\mathbf{c}}$. Although this is not a closed form expression for the dynamical system, it

makes explicit the linear part of the model. Both expressions of the dynamical system (2.40) in the error coordinates (2.46) will be used in the subsequent chapters, to analyse different aspects of the reaction networks dynamics.

When we consider the nonhomogeneous steady state $\tilde{\mathbf{c}}$, we can derive an analogous transformation to that in (2.46). In the resulting coordinates the differential equation that governs the (spatio-)temporal dynamics has the form of (2.52), yet the matrix $\mathbf{A}$ and the vector $\mathbf{g}(\mathbf{e})$ will depend on the spatial variable since the Taylor expansion will be around the space-dependent heterogeneous steady state $\tilde{\mathbf{c}}(x)$. We also note that when we neglect the diffusion of species, the models in deviation coordinates have the form of (2.50) or (2.52), by letting $\mathbf{D} = \mathbf{0}$ and changing the partial derivative w.r.t time to absolute derivatives.

2.6 Summary

We conclude this chapter with a summary of the content in this chapter. Firstly, we presented mathematical models of biochemical reaction networks and extended them to include the diffusion of the species. Secondly, we characterised, in a general framework, the equilibrium set of these reaction(-diffusion) networks. We then presented a linear transformation that allow us to obtain a coupled linear algebraic system along with a nonlinear one. Having characterised the equilibrium set of the reaction network, we introduced a simple coordinate transformation that explicitly shows the linear and nonlinear terms of the dynamical model. In the following section, we will analyse some basic dynamical properties of the reaction networks such as local stability.

Chapter 3

Basic Dynamical Properties

Contents

In this chapter we analyse two biochemical networks to determine aspects of their basic dynamical behaviour, such as local stability. The first system is the cyclic protein autoactivation introduced in Example 2.2. We perform a local stability analysis by representing the reaction network as the interconnection of p linear systems. By applying the Small Gain Theorem we derive conditions for the local stability of both fixed points of this reaction network. The second system analysed is a single protein autoactivation, where, under a biologically-motivated scenario, we derive closed-form expressions that describe its spatio-temporal evolution.

In the previous section we determined the Differential Equations (DEs) that arise from a reaction (-diffusion) network. Although these DEs govern the rate of change of the concentrations in space and/or time, further analysis should be performed to characterise the properties of the solutions of such DEs.

Usually, a first attempt to analyse these dynamics is to obtain a numerical solution of the DE. With this numerical approach we obtain the behaviour of the system under a chosen set of initial

conditions, inputs and parameters. Although shedding some light on the dynamic characteristics of the system, it becomes difficult to determine whether the outcome of the computations is a result of the chosen conditions for the simulation or are structural properties of the network or consequence of fine-tuned kinetic parameters [21, 47].

Hence, to provide a deeper characterisation of the solutions we wish to analyse systems properties in terms of the parameters of the reaction network. One of the most insightful properties in the analysis of DEs is to characterise the stability of the equilibrium set. For instance, to determine whether or not the trajectories of the system will converge to an equilibrium point of the system when the initial condition is close to the equilibrium.

In general the study of stability is a difficult task, given that we are dealing with nonlinear differential equations. Notwithstanding this difficulty, there are results available in the literature which deal with specific classes of systems. In our first case-study we deal with a class of block circulant matrices. In [48] and references therein, the authors provided the 'secant condition' as a necessary and sufficient condition to ensure the diagonal stability of a reaction network, whose linear dynamical system can be described by circulant matrix. Also, [49] extended the results of [48] to reaction diffusion systems, where they ruled out diffusion driven instability arising from diffusion coefficients of different magnitudes [16, 2].

In the forthcoming section, we will study the ODE of the reaction network introduced in Example 2.2, by representing it as the interconnection of p linear systems. By further computation of each system's input-output gain, we avail of the Small Gain Theorem [50] to derive local stability conditions. A comparable approach using the Small Gain Theorem has recently been provided for local instability analysis to conclude periodic oscillations in a different class of systems, namely gene regulatory networks in [51].

3.1 Local Stability Analysis of a Circular Protein Activation

In this section, we revisit the system studied in Example 2.2 and analyse the local stability of each of its two fixed points. For this purpose, we avail of the notion of input-output stability along with the Small Gain Theorem. These preliminaries are given below.

Firstly, we note that this analysis will be performed on the linearisation of (2.5), which is an

ODE of the form

$$\frac{\mathrm{d}}{\mathrm{d}t}\mathbf{e} = \mathbf{A}\mathbf{e} + \mathbf{B}\mathbf{u}, \tag{3.1a}$$

$$\mathbf{y} = \mathbf{C}\mathbf{e} + \mathbf{D}\mathbf{u}. \tag{3.1b}$$

Here $\mathbf{e}$ represents the deviation coordinates from the equilibrium point, defined as $\mathbf{e}(t) = \mathbf{c}(t) - \bar{\mathbf{c}} : \mathbb{R}_+ \to \mathbb{R}^n$ and $\mathbf{u}(t) : \mathbb{R}_+ \to \mathbb{R}^w$, and the matrices $\mathbf{B}$, $\mathbf{C}$, and $\mathbf{D}$, have the appropriate dimensions.

We will use an input-output approach to perform the stability analysis. When the initial conditions are zero, the transfer function [52, 53] for the system in (3.1) is defined as

$$\mathbf{H}(s) = \mathbf{D} + \mathbf{C}(s\mathbf{I} - \mathbf{A})^{-\mathbf{1}}\mathbf{B}. \tag{3.2}$$

This formula arises from the Laplace transform of the linear system (3.1), representing this model in the frequency domain s. This allows us to express the ODE (3.1) as an algebraic relationship that describes the output of the system as a function of the input. This relationship is explicitly given by the transfer function (3.2). For further discussion and details on this derivation, we refer the interested reader to [52, 53].

The basic notion of input-output stability is that a small input $\mathbf{u}$ will yield a small output $\mathbf{y}$. In order to characterise the input-output properties of the system (3.1), we require a means to measure the 'size' of a signal. For this purpose, we define the $\mathcal{L}_z$ norm of a signal as

$$||\mathbf{u}||_{\mathcal{L}_z} := \left(\int_0^\infty \left(||\mathbf{u}(t)||_z \right)^z \, \mathrm{d}t \right)^{1/z}, \tag{3.3}$$

where $||\mathbf{u}(t)||_z$ is the z-norm of $\mathbf{u}$ defined as

$$||\mathbf{u}(t)||_z := \left(\sum_{i=1}^{w} \left(u_i(t) \right)^z \right)^{1/z}.$$

When $||\mathbf{u}||_{\mathcal{L}_z}$ is finite , we say that this signal belongs to the $\mathcal{L}_z$ space. However, the definition in (3.3) is a bit restrictive, since there are many signals (e.g. a constant function) that do not belong to the $\mathcal{L}_z$ space. To consider a less restrictive space, we consider the time truncation of a

signal:

$$\mathbf{u}_\tau(t) := \begin{cases} \mathbf{u}(t) & : t < \tau, \\ 0 & : t \geq \tau. \end{cases} \tag{3.4}$$

If $||\mathbf{u}_\tau||_{\mathcal{L}_z} < \infty \; \forall \, \tau < \infty$, we say that the signal belongs to the Extended $\mathcal{L}_z$ space: $\mathcal{L}_{ze}$.

In the remainder of this chapter, we will focus on the $\mathcal{L}_2$ norm of the signals for which a tight bound on the gain γ can be readily computed. This bound is given by the following theorem.

Theorem 3.1. [50] *Consider the linear time-invariant system in* (3.1)*, where all the eigenvalues of* $\mathbf{A}$ *have negative real part, and its transfer function* $\mathbf{H}(j\omega) \in \mathbb{C}^{q \times w}$ *is given in* (3.2)*. Then the* $\boldsymbol{\mathcal{L}_2}$ ***gain*** *of the system is*

$$\gamma := \sup_{\omega \in \mathbb{R}_+} ||\mathbf{H}(j\omega)||_2 = \sup_{\omega \in \mathbb{R}_+} \sqrt{\bar{\lambda}\left(\mathbf{H}^*(j\omega)\mathbf{H}(j\omega)\right)},$$

where $\bar{\lambda}\left(\mathbf{X}\right)$ *denotes the maximum eigenvalue of* $\mathbf{X}$*.*

The proof of the theorem above can be found in [50]. For a single-input single-output transfer function, i.e. $h(j\omega) \in \mathbb{C}$, its gain γ can, thus, be computed as

$$\gamma := \sup_{\omega \in \mathbb{R}_+} |h(j\omega)| = \sup_{\omega \in \mathbb{R}_+} \sqrt{h^*(j\omega)h(j\omega)}. \tag{3.5}$$

Having characterised the input-output gain, we avail of the Small Gain Theorem below, to

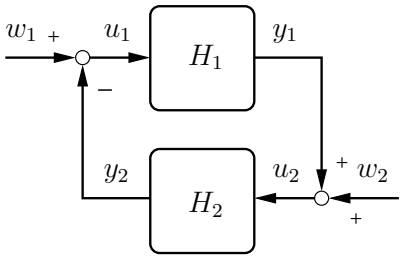

Figure 3.1: *Interconnection of two dynamical systems.*

provide sufficient conditions for stability of an interconnection of systems, whose gain γ and bias term β are known.

Theorem 3.2 (Small Gain Theorem)**.** [50] *Consider an interconnection of systems as depicted*

in Figure 3.1, where

$$||\mathbf{y_1}||_{\mathcal{L}_z} \leq \gamma_1 ||\mathbf{u_1}||_{\mathcal{L}_z} + \beta_1,$$
$$||\mathbf{y_2}||_{\mathcal{L}_z} \leq \gamma_2 ||\mathbf{u_2}||_{\mathcal{L}_z} + \beta_2.$$

And assume that the signals $\mathbf{y_1}, \mathbf{y_2}, \mathbf{u_1}, \mathbf{u_2}$*, have a finite* $\mathcal{L}_z$ *norm. Then, the feedback connection is finite gain* $\mathcal{L}_z$ *stable if*

$$\gamma_1 \gamma_2 < 1.$$

The proof of the two theorems above can be found in [50], for instance. Now, we revisit the reaction network introduced in Example 2.2 to characterise the local stability of the equilibrium set.

Example 3.1. *In Example 2.2, we computed the equilibria set of the reaction network in* (2.15)*. Our main task here is to derive stability conditions in terms of the parameters. Although a global characterisation of stability is desirable, in general this is very difficult to determine for a nonlinear system with a locally Lipschitz nonlinearity. For this reason we start the stability analysis via the linearisation of the model* (2.5)*. This linearisation is given by*

$$\frac{\mathrm{d}}{\mathrm{d}t}\mathbf{e} = \mathbf{A}\mathbf{e}, \tag{3.6}$$

where $\mathbf{e} = \mathbf{c} - \bar{\mathbf{c}}$ *stands for deviation coordinates from the equilibrium, and* $\mathbf{A} \in \mathbb{R}^{n \times n}$ *is the Jacobian of the system* (2.5)*. With the definitions of the stoichiometric matrix and reaction rate given in* (2.18)*, this Jacobian is given by*

$$\mathbf{A} := \frac{\mathrm{d}}{\mathrm{d}\mathbf{c}}\mathbf{N}\mathbf{v}(\mathbf{c}) = \begin{pmatrix} \mathbf{A}^{11} & \mathbf{A}^{12} & \mathbf{0} & \dots & \mathbf{0} \\ \mathbf{0} & \mathbf{A}^{22} & \mathbf{A}^{23} & \dots & \mathbf{0} \\ \ddots & \ddots & \ddots & \ddots & \ddots \\ \mathbf{A}^{p1} & \mathbf{0} & \mathbf{0} & \dots & \mathbf{A}^{pp} \end{pmatrix}, \tag{3.7}$$

with the block matrices defined as

$$\mathbf{A}^{ii} := \frac{\mathrm{d}}{\mathrm{d}\mathbf{c}^i}\mathbf{N}^i\mathbf{v}^i\left(\mathbf{c}^i, \mathbf{c}^{i+1}\right) = \begin{pmatrix} -\left(k_1^i\bar{c}_2^{i+1} + k_{3f}^i\right) & 0 \\ k_1^i\bar{c}_2^{i+1} & -k_2^i \end{pmatrix} \tag{3.8a}$$

$$\mathbf{A}^{ii+1} := \frac{\mathrm{d}}{\mathrm{d}\mathbf{c}^{i+1}}\mathbf{N}^i\mathbf{v}^i\left(\mathbf{c}^i, \mathbf{c}^{i+1}\right) = k_1^i\bar{c}_1^i\begin{pmatrix} 0 & -1 \\ 0 & 1 \end{pmatrix}, \tag{3.8b}$$

Note that $\mathbf{A}^{ii+1}$ *can be expressed as the product* $\mathbf{A}^{ii+1} = \mathbf{B}^i\mathbf{C}$*, where*

$$\mathbf{B}^i := k_1^i\bar{c}_1^i\begin{pmatrix} -1 \\ 1 \end{pmatrix}, \tag{3.9a}$$

$$\mathbf{C} := \begin{pmatrix} 0 & 1 \end{pmatrix}. \tag{3.9b}$$

Therefore, the linearisation in (3.6) *can be expressed as the interconnection of* p *systems of the form (cf. Eq.* (3.1)*)*

$$\frac{\mathrm{d}}{\mathrm{d}t}\mathbf{e}^i = \mathbf{A}^{ii}\mathbf{e}^i + \mathbf{B}^i u^i, \tag{3.10a}$$

$$y^i = \mathbf{C}\mathbf{e}^i. \tag{3.10b}$$

Here $\mathbf{e}^i = \mathbf{c}^i - \bar{\mathbf{c}}^i$ *is the species concentration referred to the steady state* $\bar{\mathbf{c}}_i$*. From the interconnection topology in* (2.15)*, we note that*

$$u^i = y^{i+1}. \tag{3.11}$$

By splitting the linearisation of the reaction network in (3.6) *into* p *subsystems of the form* (3.10)*, we can analyse the input-output behaviour of* p *systems separately and, then, infer conditions on the stability of each steady state of the entire interconnected system* (3.6)*. These ideas will lead to conditions for the* $\mathcal{L}_2$ *small gain stability of* (3.6) *and are summarised below in Proposition 3.1. In this Proposition, for the analysis of the* on steady state*, we make some assumptions on inequality relationships between the reaction parameters. The strategy of the proof is to obtain the transfer function of the system* (3.10) *and estimate its* $\mathcal{L}_2$ *gain. Once the gain for the* p *isolated systems is obtained, we avail of the Small Gain Theorem* (3.2) *to obtain conditions on the parameters that ensure local stability of the interconnected systems. In what follows we denote* $\mathbf{A}_{\text{off}}$ *as the Jacobian in* (3.7) *evaluated in the* off steady state*, defined in* (2.27)*. The*

definition of $\mathbf{A}_{\text{on}}$ *follows similarly.*

Proposition 3.1. *Consider the system in* (3.6)*. For the* on steady state*,* $\forall\, i \in [1, p]$ *suppose that one of the following conditions (*(3.12a)*,* (3.12b)*) holds*

$$k_{3f}^i > k_2^i \quad \text{or} \tag{3.12a}$$

$$k_2^i > k_{3f}^i, \quad \mu^i > k_{3f}^i, \quad \text{and} \quad \frac{1}{\left(k_{3f}^i\right)^2} < \frac{1}{\left(k_2^i\right)^2} + \frac{1}{\left(\mu^i\right)^2} \tag{3.12b}$$

with μ^i *defined for the* on steady state *in* (2.20) *as*

$$\sigma^i := k_1^i \bar{c}_1^i = k_2^{i+1} \frac{d\left(a^{i+1}\right)}{d\left(a^i\right)} > 0, \tag{3.13a}$$

$$\mu^i := k_1^i \bar{c}_2^{i+1} + k_{3f}^i = \frac{d\left(\alpha^i\right)}{\sigma^i} > 0. \tag{3.13b}$$

These definitions follow from the expressions in (2.19)*. Then the system in* (3.6) *is* $\mathcal{L}_2$ *stable if and only if*

1. ***Off Steady State***

$$\det\left(\mathbf{A}_{\text{off}}\right) = \prod_{i=1}^{p} k_2^i k_{3f}^i - \prod_{i=1}^{p} k_1^i k_{3b}^i \; > 0. \tag{3.14a}$$

2. ***On Steady State***

$$\det\left(\mathbf{A}_{\text{on}}\right) = \prod_{i=1}^{p} k_1^i k_{3b}^i - \prod_{i=1}^{p} k_2^i k_{3f}^i \; > 0. \tag{3.14b}$$

Proof.

The closed-form expressions of $\det\left(\mathbf{A}_{\text{off}}\right)$ and $\det\left(\mathbf{A}_{\text{on}}\right)$ in (3.14a) and (3.14b), respectively, are derived in Lemma A.2 in Appendix A. The rest of the proof follows by noting that the transfer function of the system in (3.10), as defined in (3.2), is given by

$$h^i(s) = k_1^i \bar{c}_1^i \frac{s + k_{3f}^i}{(s + k_1^i \bar{c}_2^{i+1} + k_{3f}^i)(s + k_2^i)}. \tag{3.15}$$

Then, from Theorem 3.1, the $\mathcal{L}_2$ gain of the system above is

$$\gamma^i = \left|k_1^i \bar{c}_1^i\right| \sup_{\omega \in \mathbb{R}} \sqrt{\frac{\omega^2 + \left(k_{3f}^i\right)^2}{\left[w^2 + \left(k_1^i \bar{c}_2^{i+1} + k_{3f}^i\right)^2\right]\left[\omega^2 + \left(k_2^i\right)^2\right]}}. \tag{3.16}$$

By recalling that $y^{i+1} = u^i$ and assuming zero initial conditions, we have the following bound

$$\begin{gathered} ||y^1||_{\mathcal{L}_2} \leq \gamma^1 ||u^1||_{\mathcal{L}_2} \ , \quad ||y^2||_{\mathcal{L}_2} \leq \gamma^2 ||u^2||_{\mathcal{L}_2} \quad \text{and} \\ \therefore \ ||y^1||_{\mathcal{L}_2} \leq \gamma^1 \gamma^2 ||u^2||_{\mathcal{L}_2} \ . \end{gathered}$$

Iterating from 1 to $p-1$, we have

$$||y^1||_{\mathcal{L}_2} \leq \prod_{i=1}^{p-1} \gamma^i \left|\left|u^{p-1}\right|\right|_{\mathcal{L}_2} \ .$$

In turn, the $\mathcal{L}_2$ gain of the pth system is also given by the expression in (3.16). Hence, by the Small Gain Theorem 3.2, the closed loop system is finite gain stable if

$$\prod_{i=1}^{p} \gamma^i < 1. \tag{3.17}$$

The expression above, with the appropriate γ^i, gives a sufficient condition for either of the steady states to be stable. For later use, we will require the closed-loop transfer function of the system, given by:

$$h(s) = \frac{h^p}{1 - \prod_{i=1}^{p} h^i(s)}. \tag{3.18}$$

In the following, we derive specific expressions for each steady state.

1. **Off Steady State**

   The *off steady state* is given in (2.27a). Substituting (2.27a) into (3.16) yields

$$\gamma_{\text{off}}^i := \frac{k_1^i k_{3b}^i}{k_2^i k_{3f}^i}. \tag{3.19}$$

Consequently, the stability condition in (3.17) takes the form,

$$\gamma_{\text{off}} := \prod_{i=1}^{p} \frac{k_1^i k_{3b}^i}{k_2^i k_{3f}^i} < 1, \tag{3.20}$$

or equivalently:

$$\prod_{i=1}^{p} k_2^i k_{3f}^i - \prod_{i=1}^{p} k_1^i k_{3b}^i > 0,$$

as stated in (3.14a). For the proof of the necessity, let us assume that $\gamma_{\text{off}} \geq 1$. From (3.18), the characteristic equation is given by

$$\begin{aligned} q_{\text{off}}(s) :&= 1 - \prod_{i=1}^{p} h_{\text{off}}^i(s), \\ &= 1 - \prod_{i=1}^{p} \frac{k_1^i k_{3b}^i}{k_{3f}^i} \frac{1}{s + k_2^i}, \end{aligned}$$

where we have used the definition of the transfer function in (3.15), evaluated in the *off steady state*. The limit of the equation above as s approaches to $+\infty$ and 0 are

$$\begin{aligned} q_{\text{off}}(+\infty) &= 1 \\ q_{\text{off}}(0) &= 1 - \gamma_{\text{off}} \leq 0. \end{aligned}$$

Hence, there must be a real root of the characteristic equation with a non-negative real part, when $\gamma_{\text{off}} \geq 1$.

2. **On Steady State**

The *on steady state* is given by (2.27b), which is parametrised by a^{i+1} defined in (2.26). Firstly, we note that (2.20b) allows us to write

$$k_1^i \bar{c}_2^{i+1} + k_{3f}^i = \frac{k_2^{i+1} k_{3f}^i \mathrm{d}\left(a^{i+1}\right) - k_1^i \mathrm{n}\left(a^{i+1}\right)}{k_2^{i+1} \mathrm{d}\left(a^{i+1}\right)}. \tag{3.21}$$

Furthermore, we claim

$$k_2^{i+1} k_{3f}^i \mathrm{d}\left(a^{i+1}\right) = \mathrm{d}\left(\alpha^i\right) \mathrm{d}\left(a^i\right) + k_1^i \mathrm{n}\left(a^{i+1}\right). \tag{3.22}$$

We provide a proof of this statement in Claim A.1, in Appendix A. By substituting (2.28),

(3.21), (3.22), we can express the transfer function of the ith system as

$$h^i_{\text{on}}(s) = \sigma^i \frac{s + k^i_{3f}}{(s + \mu^i)\left(s + k^i_2\right)}, \tag{3.23}$$

where we used the definitions in (3.13). Moreover, the gain of the ith system in (3.16) is

$$\gamma^i_{\text{on}} = \sigma^i \sup_{\omega \in \mathbb{R}} \sqrt{\frac{\omega^2 + \left(k^i_{3f}\right)^2}{\left[w^2 + \left(\mu^i\right)^2\right]\left[\omega^2 + \left(k^i_2\right)^2\right]}}. \tag{3.24}$$

Now, we note that the square root function is a monotonically increasing function of its argument. Hence, the supremum of the square root in (3.24) is given by the square root of the supremum of the argument. That is to say,

$$\gamma^i_{\text{on}} = \sigma^i \sqrt{\sup_{\omega \in \mathbb{R}} \frac{\omega^2 + \left(k^i_{3f}\right)^2}{\left[\omega^2 + \left(\mu^i\right)^2\right]\left[\omega^2 + \left(k^i_2\right)^2\right]}}.$$

Let us define $\mathbb{R}_{\geq 0} \ni \Omega = \omega^2$. In order to find the critical points Ω^*, we apply the natural logarithm to the argument of the square root and differentiate with respect to Ω:

$$\frac{\mathrm{d}}{\mathrm{d}\Omega}\left\{\ln\left(\Omega + \left(k^i_{3f}\right)^2\right) - \ln\left(\Omega + \left(\mu^i\right)^2\right) - \ln\left(\Omega + \left(k^i_2\right)^2\right)\right\}\Big|_{\Omega=\Omega^*} = 0.$$

Solving the foregoing equation for Ω^*, yields

$$\Omega^* = -\left(k^i_{3f}\right)^2 \pm \sqrt{\left[\left(k^i_{3f}\right)^2 - \left(k^i_2\right)^2\right]\left[\left(k^i_{3f}\right)^2 - \left(\mu^i\right)^2\right]}. \tag{3.25}$$

Considering the conditions in (3.12), we conclude that there is no positive real solution for Ω^* to the expression above. To see this, suppose that condition (3.12a) holds, then if $i)$ $k^i_{3f} \geq \mu^i$ the radicand will be less than $(k^i_{3f})^4$, leading to a negative Ω^*. On the contrary, if $ii)$ $k^i_{3f} \leq \mu^i$ the radicand in (3.25) is negative, hence leading to a complex Ω^*. On the other hand, when $k^i_2 > k^i_{3f}$ and $\mu^i > k^i_{3f}$, the radicand in (3.25) is positive. However, we note that Ω^* is negative if

$$\left(k^i_{3f}\right)^2 < \sqrt{\left[\left(k^i_{3f}\right)^2 - \left(k^i_2\right)^2\right]\left[\left(k^i_{3f}\right)^2 - \left(\mu^i\right)^2\right]},$$

which is equivalent to

$$\frac{1}{\left(k_{3f}^{i}\right)^{2}} > \frac{1}{\left(k_{2}^{i}\right)^{2}} + \frac{1}{\left(\mu^{i}\right)^{2}}.$$

That is to say, under the conditions in (3.12), the supremum in equation (3.24) is obtained for $\Omega = 0$ or $\Omega = \infty$. Indeed, by substitution the maximum value is achieved for $\Omega = 0$. From (3.24) we obtain

$$\gamma_{\text{on}}^{i} = \sigma^{i} \left| \frac{k_{3f}^{i}}{\mu^{i} k_{2}^{i}} \right|.$$

Taking into account the definitions in (3.13), the formula for γ^{i} becomes

$$\gamma_{\text{on}}^{i} = \frac{k_{2}^{i+1} k_{3f}^{i}}{k_{1}^{i} k_{3b}^{i}} \frac{k_{2}^{i+1}}{k_{2}^{i}} \left[\frac{\mathrm{d}\left(a^{i+1}\right)}{\mathrm{d}\left(a^{i}\right)} \right]^{2}. \tag{3.26}$$

We further note that

$$\gamma_{\text{on}} := \prod_{i=1}^{p} \gamma_{\text{on}}^{i} = \prod_{i=1}^{p} \frac{k_{2}^{i+1} k_{3f}^{i}}{k_{1}^{i} k_{3b}^{i}}. \tag{3.27}$$

Consequently, the small gain stability condition in (3.17) is equivalent to

$$\prod_{i=1}^{p} k_{1}^{i} k_{3b}^{i} - \prod_{i=1}^{p} k_{2}^{i} k_{3f}^{i} > 0,$$

where we have taken into account the modularity of the superindex i in k_{2}^{i+1}. Finally, we provide proof of necessity following the argument provided in the proof of the *off steady state*. Now, let us assume that $\gamma_{\text{on}} > 1$. Moreover, the characteristic equation of the closed loop transfer function in (3.18) is given by

$$q_{\text{on}}(s) : = 1 - \prod_{i=1}^{p} \sigma^{i} \frac{s + k_{3f}^{i}}{\left(s + \mu^{i}\right)\left(s + k_{2}^{i}\right)},$$

where we have used the definition of the transfer function in (3.15), evaluated in the *off*

steady state. The limits of the equation above as s tends to $+\infty$ and 0 are

$$q_{\text{on}}(\infty) = 1$$
$$q_{\text{on}}(0) = 1 - \prod_{i=1}^{p} \sigma^i \frac{k_{3f}^i}{\mu^i k_2^i} = 1 - \gamma_{\text{on}} \leq 0.$$

Hence, there must be a real root of the characteristic equation with a positive real part, and, therefore, the system is unstable if $\gamma_{\text{on}} \geq 1$.

□

The conditions for the stability of each steady state, in the proposition above, are mutually exclusive. Hence, we can ensure that, under these conditions and for each parameter set that satisfies (3.12)*, exactly one of the steady states will be stable. Moreover, we note that by comparing* (3.14b) *and* (2.29)*, one of the conditions to ensure stability of the* on steady state *is the same that is required for this state to have positive concentrations.*

Although Proposition 3.1 provides full characterisation of the stability of the closed-loop system, to obtain this result we restricted the analysis of the on steady state *to the conditions on the kinetic parameters shown in* (3.12)*. In the Proposition 3.2 below, we relax this restriction and derive sufficient conditions for the stability of the* on steady state*. The proof of this proposition and the subsequent remark can be found in Claim A, in Appendix A. The outline of the proof relies on the fact that when $k_2^i > k_{3f}^i$ for some i, the peak frequency Ω^* in* (3.25) *might have a positive real solution. Further analysis yields the stability results summarised in the following proposition.*

Proposition 3.2. *Let for some $i \in [1, p]$*

$$k_2^i > k_{3f}^i, \tag{3.28a}$$
$$\mu^i > k_{3f}^i, \tag{3.28b}$$
$$\frac{1}{\left(k_{3f}^i\right)^2} > \frac{1}{\left(k_2^i\right)^2} + \frac{1}{\left(\mu^i\right)^2}. \tag{3.28c}$$

Then the on steady state *of the system in* (3.6) *is $\mathcal{L}_2$ stable if for all i*

$$\prod_{i=1}^{p} \frac{k_2^{i+1} k_{3f}^i}{k_1^i k_{3b}^i} < \prod_{i=1}^{p} \theta^i, \tag{3.29}$$

where

$$\theta^i = \begin{cases} \frac{k_{3f}^i}{\mu^i}\sqrt{1-\left(\frac{k_{3f}^i}{k_2^i}\right)^2} + \frac{k_{3f}^i}{k_2^i}\sqrt{1-\left(\frac{k_{3f}^i}{\mu^i}\right)^2} & ,\forall\, i \textit{ which satisfy } (3.28) \\ 1 & ,\textit{otherwise.} \end{cases} \tag{3.30}$$

Moreover, the on steady state *will be unstable if* (3.14b) *does not hold.*

The following remark presents a more conservative, yet tractable, stability criterion of the system in (3.6)*.*

Remark 3.1. *Consider the linear system in* (3.6)*, and let for some* $i \in [1, p]$ *the conditions* (3.28) *be satisfied, then the* on steady state *of the system in* (3.6) *is* $\mathcal{L}_2$ *stable if*

$$\prod_{i=1}^{p} \frac{k_2^{i+1} k_{3f}^i}{k_1^i k_{3b}^i} < \prod_{i=1}^{p} \nu^i, \tag{3.31}$$

where,

$$\nu^i = \begin{cases} \left(\frac{k_{3f}^i}{k_2^i}\right)^2, & \forall\, i \textit{ which satisfy } (3.28) \\ 1, & \textit{otherwise.} \end{cases} \tag{3.32}$$

Both conditions (3.29) *and* (3.31)*, provide a criterion for determining the stability of the* on steady state*, when some of the subsystems in the loop satisfy the conditions in* (3.28)*. However, we remark that there exist some parameters which do not satisfy* (3.29) *and* (3.31)*, and do not violate* (3.14b)*; that is to say, under the conditions* (3.28)*, there are some parameters for which we cannot determine the stabilty of* (3.6)*, from this perspective.*

Of note, when $k_2^i > k_{3f}^i$ *we can use the stability criterion in* (3.31) *for all* i*. Although this might be very conservative, it provides a straightforward stability test since we avoid checking conditions* (3.12) *and* (3.28) *to determine which one of the propositions above we require.*

Summarising, in the previous example we presented the *local* stability analysis of (3.6), by considering two different cases. The one described in Proposition 3.1 provides necessary and sufficient conditions for stability of the *off* and *on steady state* under certain restrictions on the kinetic parameters. In turn, Proposition 3.2 present sufficient stability conditions of the *on steady state*, for the cases that Proposition 3.1 does not account for. Of note, as we only performed a *local* stability analysis, we have not rigorously ruled out the existence of strange attractors or

chaotic behaviours [54]. However, we did not observe such behaviour in our computational simulations.

In the following section, we consider the characterisation of the dynamical response of PDEs. Firstly, we obtain the closed-form expression for the solution of a linear first order PDE, so as to study its spatio-temporal behaviour. And secondly, we present a result from the literature that provides a means to analyse the linearisation of a PDE, which allows us to extend the results in Example 3.1.

3.2 PDE Solutions via Green's Functions

It is well known that the solution of an ODE exists and is unique within a non-trivial window of time when the ODE is locally Lipschitz continuous. It is remarkable that this statement still holds when the system analysed is nonlinear. For the PDE case, the mere proof of existence is a more subtle topic, since there is no unifying theory that provides an easy answer to the problem. However, there are well studied classes of PDEs for which the analytical solution may be derived once the kernel of the solution space is found. Examples of these well characterised equations are the Laplace, Wave and Heat Equations. The kernel that constructs the solution space, is commonly denoted as a *Green's function*.

Formally, a Green's function is the solution to the Fredholm integral equation with the kernel defined by the specific differential operator under study [55, 56]. Specific forms of Fremhold integral equations are Laplace and Fourier transforms. The Green's function has the following property with respect to a linear differential operator L:

$$LG(x,\xi) = \delta(x-\xi).$$

Here, $\delta(z)$ is the Dirac Delta. A consequence of this property is that multiplying the expression above by a well behaved function $f(\xi)$ and integrating over all $x \in \Omega$, we note

$$\int_\Omega LG(x,\xi)f(\xi)\,\mathrm{d}\xi = \int_\Omega \delta(x-\xi)f(\xi)\,\mathrm{d}\xi = f(x)$$

Let $Lu(x) = \int_\Omega LG(x,\xi)f(\xi)\,\mathrm{d}\xi$, a possible choice for $u\,(x)$ is

$$u(x) = \int_\Omega G(x,\xi)f(\xi)\,\mathrm{d}\xi.$$

This equation is known as the Fredholm integral equation. In general, this equation is difficult to solve analytically. However, the Green's functions associated with some well-known linear differential operators are available in the literature, see for example [44].

As an example of the use of the Green's functions, let us perform a simple dynamical analysis in a simple protein activation mechanism in the presence of diffusion of the species. We will pay special attention to the spatio-temporal evolution of the dynamical system when the initial conditions have been represented by its Fourier representation.

Example 3.2. *Consider the following reaction network*

$$P + A \xrightarrow{k_1} 2A \tag{3.33a}$$

$$A \xrightarrow{k_2} 0 \tag{3.33b}$$

$$P \underset{k_{3b}}{\overset{k_{3f}}{\rightleftharpoons}} 0 \tag{3.33c}$$

$$A + I \xrightarrow{k_4} 0 \tag{3.33d}$$

$$I \underset{k_{5b}}{\overset{k_{5f}}{\rightleftharpoons}} 0. \tag{3.33e}$$

Here P represents the inactive form of a protein, whereas A is the active form. In turn, I stands for the inhibitor of A, which avoids further reaction of A.

Defining the vector $\mathbf{c} = (c_1\ c_2\ c_3)^T := ([P]\ [A]\ [I])^T \in \mathbb{R}^3_+$, and using the mass-action reaction mechanism, we obtain the following set of coupled bilinear ODEs

$$\dot{c}_1 = -k_{3f}c_1 - k_1c_1c_2 + k_{3b} \tag{3.34a}$$

$$\dot{c}_2 = -k_2c_2 + k_1c_1c_2 - k_4c_2c_3 \tag{3.34b}$$

$$\dot{c}_3 = -k_{5f}c_3 - k_4c_2c_3 + k_{5b}. \tag{3.34c}$$

Moreover, when the inhibitor's turnover is faster than the reaction of the species rates we can consider its concentration constant and equal to $\bar{c}_3$, hence we can further reduce the dynamical system above to a two states model:

$$\dot{c}_1 = -k_{3f}c_1 - k_1c_1c_2 + k_{3b} \tag{3.35a}$$

$$\dot{c}_2 = -k_2c_2 + k_1c_1c_2. \tag{3.35b}$$

We note that the system in (3.35) *is the same as that studied in Example 2.1. Hence the steady*

states are given by (2.14)*:*

$$\textbf{Off steady state} : \bar{\mathbf{c}}_{\text{off}} = \begin{pmatrix} \frac{k_{3b}^1}{k_{3f}^1} & 0 \end{pmatrix}^T, \tag{3.36}$$

$$\textbf{On steady state} : \bar{\mathbf{c}}_{\text{on}} = \begin{pmatrix} \frac{k_2^1}{k_1^1} & \frac{k_{3b}^1}{k_2^1} - \frac{k_{3f}^1}{k_1^1} \end{pmatrix}^T. \tag{3.37}$$

A precise characterisation of the stability of the linearisation of (3.35) *can be achieved by examining the characteristic polynomial of the Jacobian of* (3.35)*:*

$$p(s) \quad = \quad s^2 + \left(k_1 \left[\bar{c}_2 - \bar{c}_1\right] + k_2 + k_{3f}\right) s + k_1 \left(k_2 \bar{c}_2 - k_{3f} \bar{c}_1\right) + k_2 k_{3f}.$$

The Routh-Hurwitz criterion applied to a second order polynomial, states that the roots of such a polynomial are negative, when all the coefficients have the same sign [52]. From this criterion, we conclude that the off steady state *is locally stable if and only if* $k_1/k_2 < k_{3f}/k_{3b}$*; in turn, for the* on steady state *to be stable, we require* $k_1/k_2 > k_{3f}/k_{3b}$*.*

Figure 3.2(a) depicts the location and stability of the steady states for c_2 *as a function of* k_1*. Similar results can be obtained for analysing the stability of both states in terms of other kinetic parameters. We conclude that an activation of* A *is not always present, but requires the condition* $k_2/k_1 < k_{3b}/k_{3f}$ *to be fulfilled. Figures 3.2(b-d) show trajectories with two different initial conditions, when the* on steady state *is stable. In Figure 3.2(d), the solid line represents an orbit of the system that converges to the stable steady state. Similarly, the orbit, represented by the dotted line, will converge to the stable steady state even if its initial condition is very close to the unstable steady state. In contrast, the orbit whose initial condition lies in the axis* $c_2(t) = 0$ *will converge to the unstable steady state. This shows that this unstable steady state is a saddle point. In turn, the stable steady state is a focus.*

Now we analyse the spatial and temporal dynamics of the active form $c_2(t, x)$*. We will consider a one-dimensional spatiotemporal model, which resemble a long cell, such as a skeletal muscle cell or a neurons axon, and that the initial condition has been conveyed to the intracellular domain by means of membrane receptors.*

By including the diffusion of species in a unidimensional spatial domain with zero-flux

boundary conditions, the system in (3.34) *becomes the following set of PDEs:*

$$\frac{\partial}{\partial t}c_1 = d_1\nabla^2 c_1 - k_{3f}c_1 - k_1 c_1 c_2 + k_{3b}, \tag{3.38a}$$

$$\frac{\partial}{\partial t}c_2 = d_2\nabla^2 c_2 - k_2 c_2 + k_1 c_1 c_2 - k_4 c_2 c_3, \tag{3.38b}$$

$$\frac{\partial}{\partial t}c_3 = d_3\nabla^2 c_3 - k_{5f}c_3 - k_4 c_2 c_3 + k_{5b}, \tag{3.38c}$$

with the diffusion constants d_1, d_2, d_3 *for inactive form, active form and inhibitor, respectively.*

Firstly, we note that the homogeneous steady states are the same as for the ODE case in (3.38). *Nevertheless, the stability of such fixed points become a more subtle topic in this spatiotemporal frame. We will comment on their stability, once we derive the analytical solutions. Again, the system* (3.38) *is nonlinear and a straightforward analytical solution is not possible.*

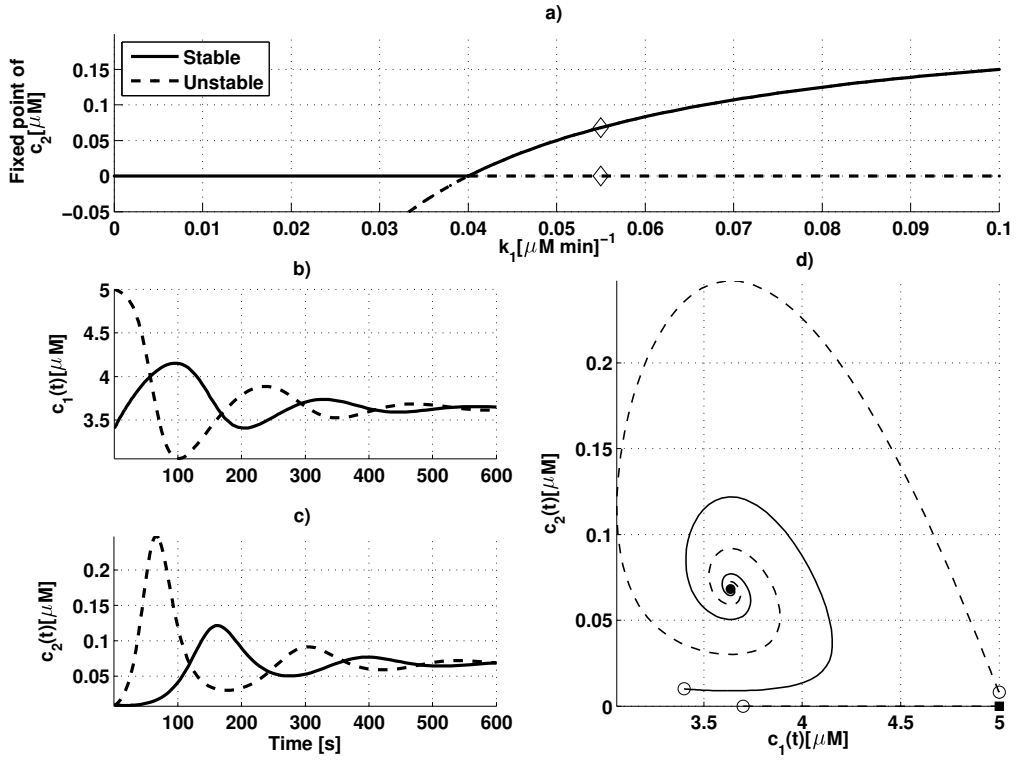

Figure 3.2: *Trajectories and phase portrait due to two different initial conditions for the system in* (3.35). *Panel* ***a)*** *shows the fixed point loci of the active enzyme A concentration* ($\bar{c}_2$) *as a function of* k_1. *In turn, Panels* ***b)*** *and* ***c)*** *depict* $c_1(t)$ *and* $c_2(t)$, *respectively, with different initial conditions. Finally,* ***d)*** *shows a phase portrait where we plot the active form* $c_2(t)$ *vs the inactive form* $c_1(t)$. *The dot (square) represents (un-) stable steady state and the circles, the initial conditions for each orbit. Parameters* $\{k_1, k_2, k_{3f}, k_{3b}\} = \{0.055, 0.2, 0.01, 0.05\}[(\mu M s)^{-1}]$.

We therefore analyse biological scenarios that allow for an analytical solution under simplifying assumptions: We will assume that a temporal profile for $c_1(t)$ is given for all time. This can represent cases in which the synthesis rate of this protein is controlled by other processes such as the genetic machinery or an external influx large enough so as to render the reaction of $c_1(t)$ negligible. Moreover, for the sake of simplicity, we will assume that the concentration of the inhibitor $c_3(t,x)$ is constant and equal to $\bar{c}_3$, which can represent the case in which the turnover is faster than the reaction of the species rates. Under this assumptions, we can describe the systems dynamics by the reduced model

$$\frac{\partial}{\partial t}c_2 = d_2\nabla^2 c_2 + \alpha(t)c_2. \tag{3.39}$$

Here

$$\alpha(t) = k_1 c_1(t) - k_4\bar{c}_3 - k_2. \tag{3.40}$$

In order to cope with the term $\alpha(t)$, we introduce an auxiliary variable $\phi(t)$, that satisfies

$$\frac{\mathrm{d}}{\mathrm{d}t}\phi(t) = \alpha(t)\phi(t), \phi(0) = 1, \phi(t) \neq 0 \,\forall\, t \geq 0. \tag{3.41}$$

This allows us to define the change of variables from $c_2(t,x)$ to $u(t,x)$ as

$$c_2(t,x) = \phi(t)u(t,x), \tag{3.42}$$

which leads to the PDE

$$\begin{aligned}\frac{\partial}{\partial t}\{\phi(t)u(t,x)\} &= d_2\nabla^2\{\phi(t)u(t,x)\} + \alpha(t)\phi(t)u(t,x)\\ \frac{\partial}{\partial t}u(t,x) &= d_2\nabla^2 u(t,x).\end{aligned} \tag{3.43}$$

Expressions (3.42) *and* (3.41) *imply that the initial conditions given to $u(t,x)$, are the same initial conditions as those given to $c_2(t,x)$. This can be seen as follows*

$$c_2(0,x) = \phi(0)u(0,x) = u(0,x). \tag{3.44}$$

The equation in (3.43) *is the Homogeneous Heat Equation with the given initial condition $u(0,x) = g(x)$ in an infinite spatial domain [55]. Using the Green's function approach [44],*

some solutions to (3.43) *are given by*

$$u(t,x) = \int_{-\infty}^{\infty} g(\xi) G(t,x,\xi) d\xi, \tag{3.45}$$

where $G(t,x,\xi)$ *is a Green's function defined as*

$$G(t,x,\xi) = \frac{1}{2\sqrt{\pi dt}} \exp\left(-\frac{(x-\xi)^2}{4dt}\right).$$

We consider two initial conditions, for the reaction diffusion network in (3.38)*:*

IC1. ***Gaussian initial condition:*** *Here the initial concentration has a Gaussian shape, that is*

$$g(x) = \frac{k}{\sqrt{\pi\sigma^2}} \exp\left(-\frac{(x-\mu)^2}{\sigma^2}\right) =: k\mathcal{N}(x-\mu,\sigma^2),$$

where μ *is the location of maximum activation and* σ *is the activation spread. Substitution of this initial condition into* (3.45)*, leads to*

$$u(t,x) = \frac{k}{2\pi\sigma\sqrt{2d_2t}} \int_{-\infty}^{\infty} k \exp\left(-\left[\frac{\sigma^2(x-\xi)^2 + 2d_2t(\xi-\mu)^2}{4d_2t\sigma^2}\right]\right) d\xi$$
$$u(t,x) = \frac{k}{\sqrt{2\pi(2d_2t+\sigma^2)}} \exp\left(-\frac{(x-\mu)^2}{4d_2t+2\sigma^2}\right).$$

Substituting this last solution into (3.42)*, the spatio-temporal profile for* $c_2(t,x)$ *gives*

$$c_2(t,x) = k\phi(t)\mathcal{N}(x-\mu, 2d_2t+\sigma^2). \tag{3.46}$$

We note that Equations (3.43) *and* (3.45) *translate an initial Gaussian function into a Gaussian with a maximum at the same location whose amplitude is modulated by* $\phi(t)$*. Due to the linearity of* (3.43)*, any composition of Gaussian functions as initial condition, yields a composition of Gaussian functions. To show this, consider the initial condition*

$$g(x) = \sum_{i=1}^{N} k_i \mathcal{N}(x-\mu_i, \sigma_i^2).$$

Which leads to

$$c_2(t,x) = \phi(t) \sum_{i=1}^{N} k_i \mathcal{N}(x-\mu_i, 2d_2t+\sigma_i^2). \tag{3.47}$$

IC2. ***Periodic initiator signal:*** *We consider an arbitrary* $2\pi-$*periodic signal by means of its*

Fourier series. Let this representation be given by the infinite series

$$g(x) = \frac{a_0}{2} + \sum_{n=1}^{\infty} \left(a_n \cos(nx) + b_n \sin(nx)\right), \tag{3.48}$$

where the coefficients a_n *and* b_n *are given by*

$$\begin{aligned} a_0 &= \frac{1}{\pi} \int_{-\pi}^{\pi} g(\xi) d\xi, \\ a_n &= \frac{1}{\pi} \int_{-\pi}^{\pi} g(\xi) \cos(n\xi) d\xi, \\ b_n &= \frac{1}{\pi} \int_{-\pi}^{\pi} g(\xi) \sin(n\xi) d\xi. \end{aligned}$$

Although this specific series requires the restriction to 2π *periodic signals, rescaling of the space variable* x *allows us to generalise the analysis to any periodicity of the initial signal* $g(x)$*.*

From (3.42) *and* (3.45) *follows,*

$$u(t,x) = \frac{a_0}{2} + \sum_{n=1}^{\infty} \exp(-d_2 t n^2) \left(a_n \cos(nx) + b_n \sin(nx)\right),$$

which leads to

$$c_2(t,x) = \frac{a_0}{2}\phi(t) + \sum_{n=1}^{\infty} \phi(t) \exp(-d_2 t n^2) \left(a_n \cos(nx) + b_n \sin(nx)\right). \tag{3.49}$$

To depict the effect of the diffusion process in the spatio-temporal evolution of the system, let us consider that $\alpha(t)$ *in* (3.40) *is a constant over time. Hence,* $\phi(t)$ *in* (3.41) *becomes*

$$\phi(t) = \exp(\alpha t). \tag{3.50}$$

Substituting the expression above in (3.49)*, yields*

$$c_2(t,x) = \frac{a_0}{2} \exp(\alpha t) + \sum_{n=1}^{\infty} \exp(\alpha t) \exp(-d_2 t n^2) \left(a_n \cos(nx) + b_n \sin(nx)\right). \tag{3.51}$$

The solution to (3.45) *driven by the initial condition in* (3.48)*, preserves the original infinite-series form. However, while the exponential damping factor in* (3.51) *varies lin-*

Table 3.1: *Conditions for the stability of the solutions to Equation* (3.39) *when* $\alpha(t) = \alpha$.

Initial Condition	**Stability condition**
Gaussian initial condition	$\bar{c}_1 < \frac{k_2+k_4\bar{c}_3}{k_1} + \frac{x^2}{k_1(4d_2t+2\sigma^2)t}$
Arbitrary periodic signal	$\bar{c}_1 < \frac{k_2+k_4\bar{c}_3}{k_1}$

early in time, it depends quadratically on the frequency (n). *Consequently, the system* (3.39) *acts as a* low-pass filter. *In particular, for high* n *(high spatial frequency), the series in* (3.51) *shows that these components decay rapidly with time. This filtering effect can be seen in Figure 3.3(a) and (b), which show a low "frequency" sinusoidal signal (small* n*) and a 'noisy' sinusoidal signal (high* n*), respectively. After an initial transient, we note that they yield the same dynamical response given in Figure 3.3(c) and (d), respectively.*

In turn, Figure 3.3(c) depicts a 'noisy' Gaussian function as an initial condition, represented as

$$g_2(x) = \mathcal{N}(x - \mu, \sigma^2) + 0.005 \sin(10x).$$

Due to the linearity of the heat equation, the solution (3.42) *with the foregoing initial condition will be the sum of two terms:*

$$c_2(t, x) = \exp(\alpha t)\mathcal{N}(x - \mu, 2d_2t + \sigma^2) + 0.005 \exp((\alpha - 100d_2)t) \sin(10x).$$

Again, we note that the filtering effect of the heat equation will decrease the spatial fluctuations, since the second element of the sum will decrease in magnitude very quickly as time increases, as noted in the previous example. The solution for $t = t_f = 0.15[s]$ *is given in Figure 3.3(f). In all cases, we note that the effect of the high-frequency noise vanishes, as time proceeds.*

For both initial conditions, we note that the solution's magnitude is modulated by the function $\phi(t)$. *As we noted before, when* α *is a constant,* $\phi(t) = \exp(\alpha t)$. *Hence, to ensure the boundedness of the solutions, we just require* $\alpha < 0$. *Conditions for* $\alpha < 0$ *are shown in Table 3.1, which are derived from the definition of* α *in* (3.40) *and the solutions for both initial conditions in* (3.46) *and* (3.51).

In the foregoing example, we were able to determine a significant amount of dynamical characteristics of the system by means of obtaining a closed-form expression for the solution of the governing PDE. However, deriving a formula that represents the solutions is only possible in

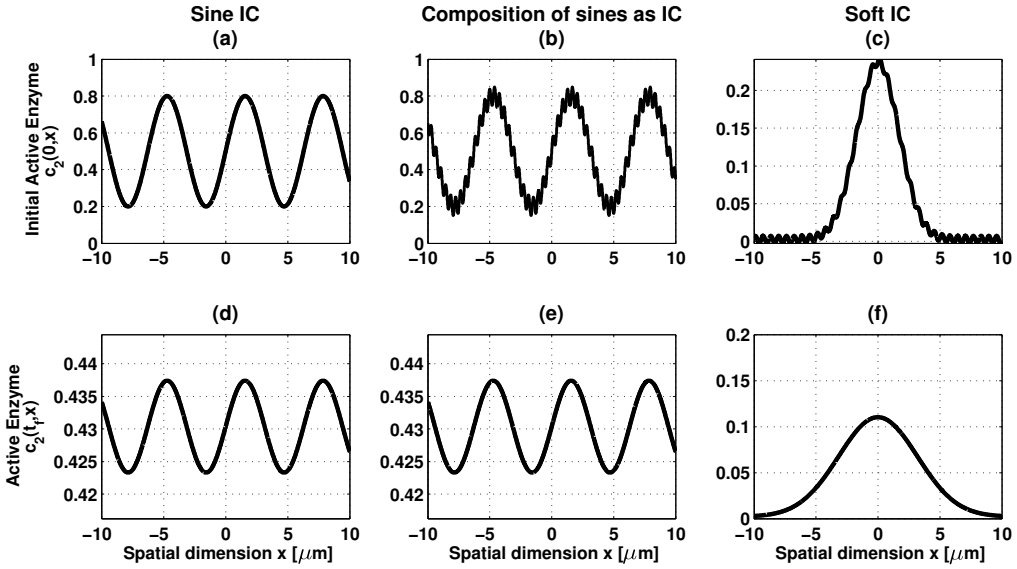

Figure 3.3: *Initial conditions and the solution for* (3.39)*. Panel (a) depicts a sinusoidal signal of a single frequency; in turn, panel (b) shows a sum of low and high frequency sine functions; finally, panel (c) shows a 'noisy' Gaussian function with* $\mu = 0$ *and* $\sigma^2 = 1.7$*. The panels (d-f) depict the solution to* (3.39) *at* $t = t_f = 0.15[s]$ *for the initial conditions (a-c), respectively. Parameters:* $\{k_1, k_2, k_{3f}, k_{3b}, k_4\} = \{k_2/5, 0.2, 0.01, 0.05\}[(\mu M s)^{-1}]$, $k_{in} = 0.5$, $d_2 = 24[\mu m^2/s]$, $\sigma = 1.7, \alpha = -1$.

some special cases; when the DE is more specific, a rigorous treatment to develop such formulas becomes quickly intractable. Nevertheless, it is possible to deduce some dynamical behaviours, without the need of explicitly solving the PDE set. For the sake of completeness, in the following section, we present a result taken from the literature.

3.3 PDEs Local Stability Analysis

As in the ODE case, the linearisation of a PDE provides a means to deduce the stability in a neighbourhood of the fixed points. The forthcoming theorem shows a criterion to determine this local stability. Let us consider the linearisation of the of the PDE (2.40), given by

$$\frac{\partial}{\partial t}\mathbf{e} = \mathbf{D}\nabla^2\mathbf{e} + \mathbf{A}\mathbf{e}, \tag{3.52}$$

here $\mathbf{e} = \mathbf{c} - \bar{\mathbf{c}}$ and $\mathbf{A} = \mathbf{N}\nabla_{\mathbf{c}}\mathbf{v}(\mathbf{c})|_{\mathbf{c}=\bar{\mathbf{c}}}$. The forthcoming Theorem relates the linearisation in (3.52) with the local stability of a homogeneous steady state.

Theorem 3.3. [57, 19] *Consider the system in* (3.52) *and an orthonormal set of eigenfunctions*

$\{\phi_i\}$, $i \in \mathbb{N}$ invariant w.r.t. the Laplacian operator, that is to say,

$$\langle \phi_i, \phi_j \rangle = \quad \delta_{ij} \tag{3.53a}$$

$$\nabla^2 \phi_j = -\lambda_j \phi_j, \quad \lambda_j \in \mathbb{R}_+, \quad 0 < \lambda_j < \lambda_{j+1} \tag{3.53b}$$

Where δ_{ij} represents the Kronecker delta. We consider zero-flux boundary conditions: $\partial \mathbf{e}/\partial x|_{x=\partial\Omega} = 0$. Then, the steady state $\mathbf{e} = \mathbf{0}$ of (3.52) *is stable, if, for all j, all the eigenvalues of*

$$\mathbf{A}_j = \mathbf{A} - \lambda_j \mathbf{D} \tag{3.54}$$

have negative real part.

From Theorem 3.3, we note that if $\mathbf{D} = d\,\mathbf{I}$ and $\mathbf{A}$ is stable, the matrix $\mathbf{A}_j$ will always be stable, since the eigenvalues of $\mathbf{A}_j$ are those of $\mathbf{A}$ but shifted $d\,\lambda_j$ units to the left. This remark gives us a simple, yet powerful way to extend the stability results for a linear ODE to the spatio-temporal setup. In the following, we will avail of Theorem 3.3 to extend the results in Example 3.1, when the diffusion of the species is relevant. For this, we will also use a link between the $\mathcal{L}_2$ stability of the p isolated subsystems and their open loop stability. This link is specified by

Lemma 3.1 (Bounded Real Lemma)**.** *Consider a strictly proper linear time invariant system of the form* (3.1) *with $\mathbf{D} = \mathbf{0}$, whose minimal realisation transfer function $\mathbf{H}(s)$ is defined in* (3.2)*, along with a positive constant $\gamma > 0$. Then, the following statements are equivalent*

1. $||\mathbf{H}(s)||_\infty < \gamma$,
2. $\exists \quad \mathbf{P} = \mathbf{P}^T > \mathbf{0}$ *such that*

$$\begin{pmatrix} \mathbf{PA} + \mathbf{A}^{\mathrm{T}}\mathbf{P} + \mathbf{C}^{\mathrm{T}}\mathbf{C} & \mathbf{PB} \\ \mathbf{PB}^{\mathrm{T}} & -\gamma^2\mathbf{I} \end{pmatrix} < \mathbf{0}$$

We will also make use of the following theorem found in [58, p. 120], which relates the sign definitiveness of a matrix with the sign definitiveness of the submatrices that compose it.

Theorem 3.4. [58] *Let a square matrix $\mathbf{M}$ be defined by blocks:*

$$\mathbf{M} = \begin{pmatrix} \mathbf{M_{11}} & \mathbf{M_{12}} \\ \mathbf{M_{12}^{T}} & \mathbf{M_{22}} \end{pmatrix},$$

where $\mathbf{M_{11}}$ *and* $\mathbf{M_{22}}$ *are symmetric. Then* $\mathbf{M}$ *is positive definite if and only if*

$$\mathbf{M_{11}} > \mathbf{0}, \qquad \mathbf{M_{22}} > \mathbf{0},$$
$$\mathbf{M_{11}} - \mathbf{M_{12}}\mathbf{M_{22}^{-1}}\mathbf{M_{12}^{T}} > \mathbf{0}, \qquad \mathbf{M_{22}} - \mathbf{M_{12}^{T}}\mathbf{M_{11}^{-1}}\mathbf{M_{12}} > \mathbf{0}.$$

Now, we revisit Example 3.1 extending its formulation to the spatio-temporal case. To include the effect of the species diffusion, it is necessary to define the diffusion matrix $\mathbf{D}$ in (3.52):

$$\mathbf{D} = \operatorname{diag}\left\{\mathbf{D^1}, \mathbf{D^2}, \dots \mathbf{D}^p\right\}, \tag{3.55a}$$
$$\mathbf{D}^i = \begin{pmatrix} d_1^i & 0 \\ 0 & d_2^i \end{pmatrix}. \tag{3.55b}$$

Moreover, we assume zero-flux boundary conditions and that we have available the eigenfunctions ϕ_i and eigenvalues λ_i in (3.53) for a spatial domain. Let us consider the case in which the diffusion coefficients of the i^{th}active and inactive species are equal, but not necessarily the same to j^th active and inactive proteins. That is to say, let the diffusion constants satisfy the following assumption.

Assumption 3.1. *Let the diffusion constant for each one of the* p *subsystems satisfy*

$$d_1^i = d_2^i = d^i \quad \forall\, i \in [1, p].$$

With this formulation, we have the following proposition.

Proposition 3.3. *Consider the matrix* (3.54)*, where* $\mathbf{A}$ *is as in* (3.7) *and* $\mathbf{D}$ *has been defined in* (3.55)*, and satisfies Assumption 3.1. Then the stability conditions of the diffusion-less formulation characterised in Propositions 3.1 and 3.2 also guarantee local stability of* (3.52)*.*

Proof. In Propositions 3.1 and 3.2, we characterised the $\mathcal{L}_2$ gain of the individual subsystems that comprise the Jacobian matrix $\mathbf{A}$ in (3.7). Henceforth, we will consider that the gains γ^i, satisfy with either of these results. Hence, the Bounded Real Lemma (3.1) guarantees that there exists $\mathbf{P}^i = \left(\mathbf{P}^i\right)^T > 0$ such that

$$\dot{\tau}^i(t) := \begin{pmatrix} \mathbf{e}^i \\ u^i \end{pmatrix}^T \begin{pmatrix} \mathbf{P}^i\mathbf{A}^{ii} + \left(\mathbf{A}^{ii}\right)^{\mathrm{T}}\mathbf{P}^i + \mathbf{C}^{\mathrm{T}}\mathbf{C} & \mathbf{P}^i\mathbf{B}^i \\ \left(\mathbf{P}^i\mathbf{B}^i\right)^{\mathrm{T}} & -\left(\gamma^i\right)^2 \end{pmatrix} \begin{pmatrix} \mathbf{e}^i \\ u^i \end{pmatrix} < 0, \tag{3.56}$$

where $\mathbf{B}^i$, $\mathbf{C}$ and γ^i have been defined in (3.9a), (3.9b) and (3.19) and (3.26), for the *on* and *off steady states*, respectively. From (3.56) we note that

$$\sum_{i=1}^{p} \zeta^i \dot{\tau}^i(t) < 0 \quad \forall\, \zeta^i > 0. \tag{3.57}$$

In addition, from Theorem 3.4 we can conclude that

$$\mathbf{P}^i \mathbf{A}^{ii} + \left(\mathbf{A}^{ii}\right)^{\mathrm{T}} \mathbf{P}^i + \mathbf{C}^{\mathrm{T}}\mathbf{C} < \mathbf{0},$$

which implies that

$$\mathbf{P}^i \mathbf{A}^{ii} + \left(\mathbf{A}^{ii}\right)^{\mathrm{T}} \mathbf{P}^i := -\mathbf{Q}^i < \mathbf{0}. \tag{3.58}$$

Now the time integral of (3.56) is given by

$$\tau^i(t) = \left(\mathbf{e}^i\right)^T \mathbf{P}^i \mathbf{e}^i + \left|\left|y^i\right|\right|^2_{\mathcal{L}_2} - \left(\gamma^i\right)^2 \left|\left|u^i\right|\right|^2_{\mathcal{L}_2} .$$

By recalling that $u^i = y^{i+1}$, we note

$$\begin{aligned} &\tau^i(t) + \left(\gamma^i\right)^2 \tau^{i+1}(t) = \\ &\left(\mathbf{e}^i\right)^T \mathbf{P}^i \mathbf{e}^i + \left|\left|y^i\right|\right|^2_{\mathcal{L}_2} + \left(\gamma^i\right)^2 \left(\mathbf{e}^{i+1}\right)^T \mathbf{P}^{i+1} \mathbf{e}^{i+1} - \left(\gamma^i \gamma^{i+1}\right)^2 \left|\left|u^{i+1}\right|\right|^2_{\mathcal{L}_2} . \end{aligned} \tag{3.59}$$

Where we have defined

$$\zeta^i := \prod_{k=1}^{i-1} \left(\gamma^k\right)^2 . \tag{3.60}$$

Iterating (3.59) from 1 to p, we have

$$\begin{aligned} V(t) := \sum_{i=1}^{p} \zeta^i \tau^i(t) &= \sum_{i=1}^{p} \zeta^i \left(\mathbf{e}^i\right)^T \mathbf{P}^i \mathbf{e}^i + \left(1 - \prod_{i=1}^{p} \left(\gamma^i\right)^2\right) \left|\left|y^1\right|\right|^2_{\mathcal{L}_2} \\ &> \sum_{i=1}^{p} \zeta^i \left(\mathbf{e}^i\right)^T \mathbf{P}^i \mathbf{e}^i \\ &> 0. \end{aligned} \tag{3.61}$$

Where, we have considered that $\prod_{i=1}^{p} \gamma^i < 1$, to ensure stability according to Propositions 3.1 and 3.2. So far, we have shown that the functional $V(t)$ in (3.61) is a Lyapunov function for the

Jacobian matrix $\mathbf{A}$ in (3.7). However, when we account for the diffusion of species, we have to analyse the family of linear systems parametrised by the eigenvalue λ_j:

$$\dot{\mathbf{e}}^i = \left(\mathbf{A}^{ii} - \lambda_j \mathbf{D}^i\right) \mathbf{e}^i + \mathbf{B}^i u^i. \tag{3.62}$$

From Theorem 3.3, we need to show the stability of the system above for all j, to ensure the local stability of the reaction diffusion system. Differentiation in time of the functional $\tau^i(t)$ along the lines of the field (3.62) yields

$$\begin{aligned}\dot{\tau}^i_j(t) :&= \begin{pmatrix}\mathbf{e}^i \\ u^i\end{pmatrix}^T \begin{pmatrix}-\mathbf{Q}^i + \mathbf{C}^{\mathrm{T}}\mathbf{C} & \mathbf{P}^i\mathbf{B}^i \\ \left(\mathbf{P}^i\mathbf{B}^i\right)^{\mathrm{T}} & -\left(\gamma^i\right)^2\end{pmatrix}\begin{pmatrix}\mathbf{e}^i \\ u^i\end{pmatrix} - \lambda_j \left(\mathbf{e}^i\right)^T \left[\mathbf{D}^i\mathbf{P}^i + \left(\mathbf{D}^i\mathbf{P}^i\right)^T\right]\mathbf{e}^i \\ &= \dot{\tau}^i(t) - \lambda_j \left(\mathbf{e}^i\right)^T \left[\mathbf{P}^i\mathbf{D}^i + \left(\mathbf{P}^i\mathbf{D}^i\right)^T\right]\mathbf{e}^i,\end{aligned}$$

which is negative if $\mathbf{P}^i\mathbf{D}^i + \left(\mathbf{P}^i\mathbf{D}^i\right)^T > \mathbf{0}$. In particular by considering Assumption 3.1, we have

$$\dot{\tau}^i_j(t) = \dot{\tau}^i(t) - 2d^i\lambda_j \left(\mathbf{e}^i\right)^T \mathbf{P}^i\mathbf{e}^i \leq \dot{\tau}^i(t) < 0.$$

Hence for all j

$$\sum_{i=1}^{p} \zeta^i \dot{\tau}^i_j(t) < 0,$$

where ζ^i has been defined in (3.60). That is to say, $V(t)$ in (3.61) is a Lyapunov function for the family of systems in (3.62). □

In the result above, we extended the stability results in Propositions 3.1 and 3.2, by means of assuming the relationship on the diffusion constants described in Assumption 3.1. In the propositions below we conclude, under some conditions on the parameters, the stability for the linearisation of the PDE in (3.52).

Proposition 3.4. *Consider the matrix* (3.54)*, where* $\mathbf{A}$ *is as in* (3.7) *and* $\mathbf{D}$ *has been defined in* (3.55)*. Moreover, let*

$$\tilde{k}^i_2 := k^i_2 + \lambda_j d^i_2 \tag{3.63a}$$

$$\tilde{k}^i_2 := k^i_{3f} + \lambda_j d^i_1. \tag{3.63b}$$

In addition, assume that

$$\tilde{k}_{3f}^{i} > \tilde{k}_{2}^{i} \qquad \forall\ i,j \quad \text{and} \tag{3.64}$$

$$k_{3f}^{i} d_{2}^{i} > k_{2}^{i} d_{1}^{i}. \tag{3.65}$$

Then, the PDE in (3.52) *is locally stable if the conditions in* (3.14) *hold.*

Proof. Under the definitions in (3.63) the matrix $\mathbf{A}_{j}^{ii}$ comprised in (3.54) becomes

$$\mathbf{A}_{j}^{ii} = \begin{pmatrix} -\left(k_{1}^{i}\bar{c}_{2}^{i+1} + \tilde{k}_{3f}^{i}\right) & 0 \\ k_{1}^{i}\bar{c}_{2}^{i+1} & -\tilde{k}_{2}^{i} \end{pmatrix}. \tag{3.66}$$

Note that it has the same structure as the case in which the diffusion of species is not taken into account (cf. (3.8a)). Hence, we will follow the main plot of Proposition 3.1. There we found an expression for the $\mathcal{L}_2$ input-output gain for the ith system (3.16). Here, however, by taking the definition of the Jacobian matrix in (3.66), this gain becomes

$$\tilde{\gamma}^{i} = \left|k_{1}^{i}\bar{c}_{1}^{i}\right| \sup_{\omega\in\mathbb{R}} \sqrt{\frac{\omega^{2} + \left(\tilde{k}_{3f}^{i}\right)^{2}}{\left[\omega^{2} + \left(k_{1}^{i}\bar{c}_{2}^{i+1} + \tilde{k}_{3f}^{i}\right)^{2}\right]\left[\omega^{2} + \left(\tilde{k}_{2}^{i}\right)^{2}\right]}}. \tag{3.67}$$

Now, we consider each of the steady states.

1. **Off Steady State**

   The *off steady state* is given in (2.27a). Substituting (2.27a) into (3.16) yields

   $$\tilde{\gamma}_{\text{off}}^{i} := \frac{k_{1}^{i}k_{3b}^{i}}{\tilde{k}_{2}^{i}k_{3f}^{i}}.$$

   Consequently, the stability condition in (3.17) takes the form,

   $$\prod_{i=1}^{p} \frac{k_{1}^{i}k_{3b}^{i}}{\tilde{k}_{2}^{i}k_{3f}^{i}} \leq \prod_{i=1}^{p} \frac{k_{1}^{i}k_{3b}^{i}}{k_{2}^{i}k_{3f}^{i}} < 1.$$

   Hence, from the equation above, we have

   $$\prod_{i=1}^{p} k_{2}^{i}k_{3f}^{i} - \prod_{i=1}^{p} k_{1}^{i}k_{3b}^{i} > 0. \tag{3.14a}$$

Now we focus on the *on steady state*.

2. **On Steady State**

The definition of the *on steady state* is given in (2.27b). The argument in Proposition 3.1 showed that the gain for the ith system can be found when we evaluate (3.67) at $\omega^2 = \Omega^*$, which is the solution of

$$\Omega^* = -\left(\tilde{k}_{3f}^i\right)^2 \pm \sqrt{\left[\left(\tilde{k}_{3f}^i\right)^2 - \left(\tilde{k}_2^i\right)^2\right]\left[\left(\tilde{k}_{3f}^i\right)^2 - \left(\mu^i + \lambda_j d_1^i\right)^2\right]}. \tag{3.68}$$

Under the assumption (3.64), we conclude that Ω^* has no positive solution. Hence $\tilde{\gamma}_{on}^i$ in (3.67) is maximum when $\omega = 0$:

$$\begin{aligned}\tilde{\gamma}_{on}^i &= \sigma^i \frac{\tilde{k}_{3f}^i}{\left(\mu^i + d_1^i\lambda_j\right)\tilde{k}_2^i} \\ &= \left(\sigma^i\right)^2 \frac{\tilde{k}_{3f}^i}{\left(k_1^i k_{3b}^i + d_1^i\lambda_j\sigma^i\right)\tilde{k}_2^i}.\end{aligned}$$

Here μ^i and σ^i have been defined in (3.13). The product of all $\tilde{\gamma}_{on}^i$ yields

$$\prod_{i=1}^{p}\tilde{\gamma}_{on}^i = \prod_{i=1}^{p}\frac{k_{3f}^i + \lambda_j d_1^i}{k_2^i + \lambda_j d_2^i} \quad \frac{\left(k_2^{i+1}\right)^2}{k_{3b}^i k_1^i + d_1^i\lambda_j\sigma^i}. \tag{3.69}$$

The second product of the multiplication above is a monotonically decreasing function of λ_j. Whereas the derivative w.r.t. λ_j of the first product yields:

$$\frac{\mathrm{d}}{\mathrm{d}\lambda_j}\left\{\frac{k_{3f}^i + \lambda_j d_1^i}{k_2^i + \lambda_j d_2^i}\right\} = \frac{d_1^i k_2^i - d_2^i k_{3f}^i}{\left(k_2^i + d_2^i\lambda_j\right)^2},$$

which is negative for all j, when the the condition (3.65) is taken into account. This implies that (3.69) is a monotonically decreasing function of λ_j. Then, the biggest $\tilde{\gamma}_{on}^i$ is obtained when $j = 1$ or, respectively, when $\lambda_1 = 0$. Then, from the Small Gain Theorem and (3.69), we conclude that the condition for closed-loop stability is given by

$$\prod_{i=1}^{p} k_1^i k_{3b}^i - \prod_{i=1}^{p} k_2^i k_{3f}^i > 0. \tag{3.14b}$$

□

It is important to note that the conditions for stability in the foregoing proposition are the same as for the diffusion-less case, derived in Proposition 3.1. In fact, the previous two propositions conclude that the stability of the reaction-diffusion case is the same as the one for the ODE one, under different conditions on the parameters. Although this might seem an intuitive conclusion, it is not always the case that the reaction-diffusion network inherits the stability of the reaction network. Indeed, one of the characteristic dynamic behaviours of PDEs is the diffusion driven instability, which is of particular relevance in pattern formation of physiological characteristics [2, 16] and cell differentiation mechanisms [18]. However, it remains to be understood whether the instability due to diffusion might arise in the reaction network studied in Example 2.2.

3.4 Summary

In this chapter we analysed basic dynamical properties of two systems. In Example 3.1 we derived local stability conditions of a circular protein activation with an arbitrary number of intermediate activation steps, represented by a linear ODE set. These stability conditions are a function of the kinetic parameters of the reaction network. At a later stage we extended these results to the case in which the species diffuse, under some assumptions in the diffusion constants.

In turn, in Example 3.2 we found closed form solutions of a first order linear PDE, by means of the Green's function that spans the solution space of the homogeneous Heat Equation. In particular, we were able to expose the filtering behaviour of the system that gives rise to suppression of spatial fluctuations in species concentrations.

Up to now, all the analysis have been performed to derive closed-form expressions to quantify a particular performance index of interest. However, the continuous dependence on the spatial coordinate of PDEs hinder this exact analytical treatment. In the rest of this thesis, we will consider a class of methods to approximate a PDE set as an ODE set, at the cost of increasing the number of DE to solve, but keeping in mind the trade-off between accuracy and dimension.

Chapter 4

Reduction of Computational Load and Integrated Response for Classes of Reaction-Diffusion Systems

Contents

In this chapter we assume that the solutions to the reaction-diffusion PDEs belong to a Hilbert space. This allows us to express these solutions as a weighted sum of the basis functions which expand the solution space. By choosing these basis functions to be invariant with respect to the Laplacian operator, we will be able to derive an associated ODE set to the reaction-

diffusion PDE, at the cost of increasing the number of ODEs to solve. In the first instance, we use this associated ODE set along with the analytical solution for a linear combination of species concentration to reduce the computational load required for the numerical solution of a reaction diffusion network. At a later stage we avail of the projection method to derive analytical expressions of the time-integral of selected species in a reaction-diffusion network.

In this chapter we introduce a methodology available in the literature to express a PDE set as an infinite-dimensional ODE set. Applying this approach to reaction-diffusion models, we are able to further reduce the order of the resulting system, preserving dynamic characteristics of the system with an arbitrary accuracy. The cornerstone of the aforementioned method is to assume that the solutions to the PDE belong to a vector space. When we select the representation of the basis elements to be invariant with respect to the Laplacian operator, we obtain an explicit separation for the temporal and spatial dimensions of the expanded signal. This methodology is called the *Laplacian Spectral Decomposition* (LSD, for short) and is introduced in Section 4.1.

In Section 4.3, we will express a general nonlinear reaction-diffusion system as the interconnection of a linear and nonlinear PDEs. For the linear PDEs we are able to provide analytical solutions via the Green's function method, introduced in Section 3.2. Whereas the numerical simulation is only required for the nonlinear system. Here we avail of the LSD method to perform this simulation, so as to reduce the computational load. To asses this reduction, we compare the computational time required for the simulation by the methodology described above with a pure numerical approach as well as with the pure LSD approach. For a particular reaction network, the simulation results suggest that for the case of large densities in the spatial domain we can obtain a significant reduction of the computational time. In Section 4.4, we avail of the LSD method to compute the integral in time of the solutions of selected species in a class of reaction-diffusion systems.

4.1 Hilbert Spaces and LSD

A Hilbert space ($\mathbb{H}$) is a complete vector space endowed with an inner product. In the remaining of this chapter we will consider the standard inner product of a function vector space:

$$\langle \mathbf{f}(x), \mathbf{g}(x) \rangle = \int_{\Omega} \mathbf{g}^T(x)\mathbf{f}(x)\,\mathrm{d}x : \mathbb{H} \times \mathbb{H} \to \mathbb{R}_+,$$

where $\mathbf{f}(x)$ and $\mathbf{g}(x) : \Omega \to \mathbb{H}$. In general we can express the elements of a vector space as a linear combination of the elements of a basis that spans such a space. In addition, we recall that the representation of a vector space basis is not unique. This provides us with some degree of freedom to choose the elements of the basis.

When we focus on the reaction-diffusion equation

$$\frac{\partial}{\partial t}\mathbf{e} = \mathbf{D}\nabla^2\mathbf{e} + \mathbf{A}\mathbf{e} + \mathbf{N}_{\text{NL}}\mathbf{g}(\mathbf{e}) + \mathbf{B}\mathbf{u}, \tag{2.52}$$

with the appropriate initial and boundary conditions of the form

$$m(t, \partial\Omega) = p(t, \partial\Omega)\mathbf{c}(t, \partial\Omega) + q(t, \partial\Omega)\left.\frac{\partial \mathbf{c}(t,x)}{\partial \mathbf{n}}\right|_{x=\partial\Omega} \quad \forall\, t \in \mathbb{R}_+, \tag{2.42}$$

the LSD method suggests the choice of an orthonormal basis that is also invariant w.r.t. the Laplacian operator. In addition, the elements of the basis must comply with the boundary conditions of the reaction-diffusion under consideration, to be able to reproduce the solution of the PDE. In formal terms, we require the elements of the basis $\phi_i(x)$ to satisfy:

$$\langle \phi_i(x), \phi_j(x) \rangle = \quad \delta_{ij} \tag{4.1a}$$

$$\nabla^2\phi_i(x) = -\lambda_i\phi_i(x) \quad \text{subject to the boundary conditions in (2.42),} \tag{4.1b}$$

where $\lambda_i \in \mathbb{R}_+$ is denoted as the eigenvalue of the eigenfunction $\phi_i(x)$. Of note, for intricate spatial geometries the invariance condition in (4.1b) might be difficult to fulfil with an analytical expression. In those cases we can adopt a numerical approach to find the value of the basis elements in a discretisation of the spatial domain Ω. We call this a *local basis* [59, 60]. Nevertheless, in the remainder of this work we will consider simple geometries that allow for an analytical expression of the elements $\phi_i(x)$ of the *global* basis.

Once we have characterised the elements of the basis, we remark that the completeness of $\mathbb{H}$ allows us to express its elements as

$$c_i(t, x) = \sum_{i=1}^{\infty} w_i(t)\phi_i(x), \tag{4.2}$$

where $w_i(t)$ is the so-called mode of the eigenfunction $\phi_i(x)$. Here we note that the method proposed involves an explicit separation of the temporal and spatial dependencies [61]. In addition, as $c_i(t, x)$ is the solution of a PDE of the form (2.40) and we assume locally Lipschitz

nonlinearities, in [62, 63, 64] is shown that the eigenvalues λ_i diverge to infinity as i tends to infinity. Moreover, it is also shown that $0 < \lambda_i < \lambda_j \forall\, i < j$. This allows us to approximate the expression in (4.2) to the first ϑ elements of the series. That is to say, in a matrix formulation:

$$\mathbf{c}(t,x) \approx \sum_{i=1}^{\vartheta} \mathbf{w}_i(t)\phi_i(x) =: \mathbf{W^T}(t)\boldsymbol{\phi}(x), \tag{4.3}$$

were $\mathbf{W^T}(t) : \mathbb{R}_+ \to \mathbb{R}^{n\times\vartheta}$ and $\boldsymbol{\phi}(x) : \Omega \to \mathbb{R}^{\vartheta}$. Of note, we require all the vectors $c_i(t,x)$ to comply with the same boundary conditions, in order to be able to represent them with the common basis comprised in $\boldsymbol{\phi}(x)$. Furthermore, we remark that $\mathbf{W^T}(t)$ satisfies the following relationship, given the orthonormality of the entries in $\boldsymbol{\phi}(x)$:

$$\begin{aligned}\langle \mathbf{c}(t,x), \boldsymbol{\phi}(x)\rangle &= \left\langle \mathbf{W^T}(t)\boldsymbol{\phi}(x), \boldsymbol{\phi}(x)\right\rangle \\ &= \int_\Omega \mathbf{W^T}(t)\boldsymbol{\phi}(x)\boldsymbol{\phi^T}(x)\mathrm{d}x \\ \langle \mathbf{c}(t,x), \boldsymbol{\phi}(x)\rangle &= \mathbf{W^T}(t).\end{aligned} \tag{4.4}$$

In the following, for the sake of readability, we will frequently suppress the dependence on space and time in $\mathbf{W}(t)$ and $\boldsymbol{\phi}(x)$, respectively. In the next section, we avail of the explicit separation of the spatial and temporal dependencies in (4.3) to express the reaction-diffusion equation (2.40) as a first-order ODE set of dimension $n\vartheta$.

4.2 Associated ODE Set to a Reaction-Diffusion Equation

Here, we derive an ODE set that arises from the PDE in (2.40), when we consider the absence of the external input $\mathbf{u}(t,x)$. The next proposition, which relates the interaction of the vectorisation operation $\mathrm{vec}\,(\circ)$ and the Kronecker product $\otimes$ will be useful in what follows.

Proposition 4.1. [45]

$$\mathrm{vec}\,(\mathbf{AXB}) = \left(\mathbf{B^T}\otimes\mathbf{A}\right)\mathrm{vec}\,(\mathbf{X})\,.$$

The properties of the operations above as well as the proof of the theorem can be found in [45]. The following proposition shows how to express (2.52) as an associated first order ODE of dimension $n\vartheta$. Here we do not assume that the diffusion is the same for all the species nor a prescribed form of the nonlinear terms in $\mathbf{v_{NL}}(\mathbf{c})$.

Proposition 4.2. *Consider the PDE defined in* (2.40)*, with* $\mathbf{N}$ *and* $\mathbf{v}(\mathbf{c})$ *as defined in* (2.32) *and*

(2.30)*, respectively. The weights* $\mathbf{W}(t)$ *which satisfy* (4.3) *are the solution of the ODE set*

$$\frac{\mathrm{d}}{\mathrm{d}t}\mathrm{vec}\left(\mathbf{W^T}\right) = \mathbf{A_c}\mathrm{vec}\left(\mathbf{W^T}\right) + \mathbf{B_0}\mathrm{vec}\left(\mathbf{W_0^T}\right) + \mathbf{B_{NL}}\int_\Omega \mathrm{vec}\left(\mathbf{v_{NL}}\left(\mathbf{W^T}\boldsymbol{\phi}\right)\boldsymbol{\phi^T}\right)\mathrm{d}x. \quad (4.5)$$

Where

$$\mathbf{A_c} = (-\boldsymbol{\Lambda}\otimes\mathbf{D}) + (\mathbf{I}_\vartheta \otimes \mathbf{N_L G}), \quad (4.6a)$$

$$\mathbf{B_0} = \mathbf{I}_\vartheta \otimes \mathbf{N_0}, \quad (4.6b)$$

$$\mathbf{B_{NL}} = \mathbf{I}_\vartheta \otimes \mathbf{N_{NL}}, \quad (4.6c)$$

$$\mathbf{W_0^T} = (\mathbf{v}_0\ \mathbf{0}_{m_3\times(\vartheta-1)}). \quad (4.6d)$$

Here $\boldsymbol{\Lambda}\in\mathbb{R}^{\vartheta\times\vartheta}$ *is a diagonal matrix, whose* ii^{th} *entry is* λ_i*.*

Proof. Firstly, recall that our model has the form

$$\frac{\partial}{\partial t}\mathbf{c}(t,x) = \mathbf{D}\nabla^2\mathbf{c}(t,x) + \mathbf{N}\mathbf{v}(\mathbf{c}(t,x)), \quad (2.40)$$

when $\mathbf{u}(t,x) = \mathbf{0}$. Moreover, we partition the stoichiometric reaction rate vector and stoichiometric matrix as

$$\mathbf{v}(\mathbf{c}) = \begin{pmatrix}\mathbf{v_{NL}}\\ \mathbf{Gc}\\ \mathbf{v_0}\end{pmatrix} : \mathbb{R}_+\times\mathbb{R}_+^n \to \mathbb{R}^{m_1+m_2+m_3}, \quad (2.30)$$

$$\mathbf{N} = \begin{pmatrix}\mathbf{N_{NL}} & \mathbf{N_L} & \mathbf{N_0}\end{pmatrix} \in \mathbb{R}^{n\times(m_1+m_2+m_3)}. \quad (2.32)$$

When we express the species concentration vector $\mathbf{c}(t,x)$ as the truncated sum in (4.3) and postmultiply it by $\boldsymbol{\phi^T}$, (2.40) becomes

$$\begin{aligned}\frac{\partial}{\partial t}\mathbf{W^T}\boldsymbol{\phi}\boldsymbol{\phi^T} &= \mathbf{D}\mathbf{W^T}\nabla^2\boldsymbol{\phi}\boldsymbol{\phi^T} + \mathbf{N_L}\mathbf{G}\mathbf{W^T}\boldsymbol{\phi}\boldsymbol{\phi^T} + \mathbf{N_0}(\mathbf{v_z}\ \mathbf{0})\boldsymbol{\phi}\boldsymbol{\phi^T} + \mathbf{N_{NL}}\mathbf{v_{NL}}\left(\mathbf{W^T}\boldsymbol{\phi}\right)\boldsymbol{\phi^T},\\ &= -\mathbf{D}\mathbf{W^T}\boldsymbol{\Lambda}\boldsymbol{\phi}\boldsymbol{\phi^T} + \mathbf{N_L}\mathbf{G}\mathbf{W^T}\boldsymbol{\phi}\boldsymbol{\phi^T} + \mathbf{N_0}(\mathbf{v_z}\ \mathbf{0})\boldsymbol{\phi}\boldsymbol{\phi^T} + \mathbf{N_{NL}}\mathbf{v_{NL}}\left(\mathbf{W^T}\boldsymbol{\phi}\right)\boldsymbol{\phi^T};\end{aligned}$$

where we have used the invariance w.r.t. the Laplacian operator in (4.1b). Integrating over the

spatial domain, the equation above becomes

$$\frac{\mathrm{d}}{\mathrm{d}t}\mathbf{W^T} = -\mathbf{D}\mathbf{W^T}\mathbf{\Lambda} + \mathbf{N_L}\mathbf{G}\mathbf{W^T} + \mathbf{N_0}(\mathbf{v_z}\ \mathbf{0}) + \mathbf{N_{NL}}\int_\Omega \mathbf{v_{NL}}\left(\mathbf{W^T}\boldsymbol{\phi}\right)\boldsymbol{\phi^T}\mathrm{d}x.$$

Here we have used the orthonormality of the basis elements in (4.1a). Applying the vectorisation operation to the expression above, yields

$$\frac{\mathrm{d}}{\mathrm{d}t}\mathrm{vec}\left(\mathbf{W^T}\right) = \mathbf{A_c}\mathrm{vec}\left(\mathbf{W^T}\right) + \mathbf{B_0}\mathrm{vec}\left(\mathbf{W_0^T}\right) + \mathbf{B_{NL}}\int_\Omega \mathrm{vec}\left(\mathbf{v_{NL}}\left(\mathbf{W^T}\boldsymbol{\phi}\right)\boldsymbol{\phi^T}\right)\mathrm{d}x,$$

where the matrices $\mathbf{A_c}$, $\mathbf{B_0}$ and $\mathbf{B_{NL}}$ have been defined in (4.6). □

When we consider that $\mathbf{v_{nl}}(\mathbf{c})$ is a vector whose i^{th}component is a quadratic form (see Assumptions 2.1 in Section 2.5), we can express it as

$$\mathbf{v_{NL}}(\mathbf{c}) = \left(\mathbf{I}_{m_1} \otimes \mathbf{c}^T\right)\mathbf{Y}\mathbf{c}.$$

Representing $\mathbf{c}(t,x)$ as (4.3) and postmultipliying by $\boldsymbol{\phi^T}$, the vector $\mathbf{v_{nl}}(\mathbf{c})$ becomes

$$\begin{aligned}
\mathbf{v_{NL}}(\boldsymbol{W^T\phi})\boldsymbol{\phi^T} &= \begin{pmatrix} \boldsymbol{\phi^T}\mathbf{W}\mathbf{Y}_1\mathbf{W^T} \\ \vdots \\ \boldsymbol{\phi^T}\mathbf{W}\mathbf{Y}_{m_1}\mathbf{W^T} \end{pmatrix}\boldsymbol{\phi}\boldsymbol{\phi^T} \\
&= \left(\mathbf{I}_{m_1} \otimes \boldsymbol{\phi^T}\right)\begin{pmatrix} \mathbf{W}\mathbf{Y}_1\mathbf{W^T} \\ \vdots \\ \mathbf{W}\mathbf{Y}_{m_1}\mathbf{W^T} \end{pmatrix}\boldsymbol{\phi}\boldsymbol{\phi^T} \\
\mathbf{v_{NL}}(\boldsymbol{W^T\phi})\boldsymbol{\phi^T} &= \left(\mathbf{I}_{m_1} \otimes \boldsymbol{\phi^T}\right)\left(\mathbf{I}_{m_1} \otimes \mathbf{W}\right)\mathbf{Y}\mathbf{W^T}\boldsymbol{\phi}\boldsymbol{\phi^T}.
\end{aligned}$$

Here $\mathbf{Y} \in \mathbb{R}^{m_1 n \times n}$ has been defined in (2.48). Applying $\mathrm{vec}\,(\circ)$ to the expression above, we have

$$\mathrm{vec}\left(\mathbf{v_{nl}}(\boldsymbol{W^T\phi})\boldsymbol{\phi^T}\right) = \left(\boldsymbol{\phi}\boldsymbol{\phi^T} \otimes \mathbf{I}_{m_1} \otimes \boldsymbol{\phi^T}\right)\left(\mathbf{W} \otimes \mathbf{I}_{m_1} \otimes \mathbf{W}\right)\mathrm{vec}\left(\mathbf{Y}\right), \tag{4.7}$$

from which we note an explicit separation of the spatial and temporal dependencies. In the next section, we avail of the analytical solution of some species to reduce the number of PDEs, required to solve numerically.

4.3 Reduced Order PDE via Analytical Solution for a Class of Reaction-Diffusion Systems

In this section, we avail of the linear transformation presented in Section 2.3.1, which allows us to write the system in (2.40) as an interconnection of a linear and a nonlinear system. Under some conditions on the stoichiometric matrix and the Jacobian of the system, the analytical solution for the former will be found for an infinite spatial domain, hence the need for a numerical solution is only necessary for the nonlinear subsystem. Although the PDE problem might only be defined in a finite domain, we assume that the spatial domain in which the nonlinear PDE is being simulated is large enough so as to be able to assume it infinite. This assumption will allow us to derive a closed-form formula for an analytical solution of the linear part of the model. This analytical solution can be further analysed to infer some properties of the dynamics of the closed loop system. Towards the derivation of this analytical solution and further order reduction of the PDE, we first consider two preliminary results.

Lemma 4.1. *Consider a reaction-diffusion system of the form*

$$\frac{\partial}{\partial t}\mathbf{e} = d\nabla_x^2\mathbf{e} + \mathbf{A}\mathbf{e}. \tag{4.8}$$

The change of variables $\mathbf{e} = \exp(\mathbf{A}t)\boldsymbol{\psi}$ *in* (4.8) *gives*

$$\frac{\partial}{\partial t}\boldsymbol{\psi} = d\nabla_x^2\boldsymbol{\psi}. \tag{4.9}$$

The proof follows from the substitution of variables. Furthermore, we note that each element of (4.9) is a homogeneous Heat Equation, whose solution has been analysed in Section 3.2. Although the Heat Equation is similar to that of our interest, it does not include the nonlinearities of the system in (2.52), repeated here, for the sake of readability:

$$\frac{\partial}{\partial t}\mathbf{e} = \mathbf{D}\nabla^2\mathbf{e} + \mathbf{A}\mathbf{e} + \mathbf{N}_{\mathbf{NL}}\mathbf{g}(\mathbf{e}) + \mathbf{B}\mathbf{u}. \tag{2.52}$$

The next Lemma shows how a basis of the orthogonal complement of $\mathbf{N}_{\mathbf{NL}}$'s column space, denoted as $\mathbf{Q}$, can induce a linear transformation. The new coordinates will lead to a Heat Equation, and, hence, to an explicit formula for the solution can be found by means of (3.45). Let $r = \operatorname{colrank}(\mathbf{N}_{\mathbf{NL}})$. By the Rank-Nullity Theorem [39], $\mathbf{Q} \in \mathbb{R}^{(n-r)\times n}$.

Lemma 4.2. *Consider the system in* (2.52)*. If*

$$\mathbf{Q}\mathbf{N}_{\mathbf{L}}\mathbf{G} = \mathbf{\Theta}\mathbf{Q}, \tag{4.10}$$

where $\mathbf{\Theta} \in \mathbb{R}^{(n-r)\times(n-r)}$*, then the change of variables* $\exp(\mathbf{\Theta}t)\,\boldsymbol{\eta} = \mathbf{Q}\mathbf{e}$ *transforms* (2.52) *into an associated PDE set of order* $n-r$*, composed of homogeneous heat equations*

$$\frac{\partial}{\partial t}\boldsymbol{\eta} = d\nabla^2\boldsymbol{\eta}.$$

Proof. Premultiplying (2.52) by $\mathbf{Q}$ yields

$$\frac{\partial}{\partial t}\mathbf{Q}\mathbf{e} = d\nabla^2\mathbf{Q}\mathbf{e} + \mathbf{Q}\mathbf{A}\mathbf{e}.$$

If (4.10) holds, then

$$\frac{\partial}{\partial t}\mathbf{Q}\mathbf{e} = d\nabla^2\mathbf{Q}\mathbf{e} + \mathbf{\Theta}\mathbf{Q}\mathbf{e}.$$

Finally, by Lemma 4.1, the change of variables $\exp(\mathbf{\Theta}t)\,\boldsymbol{\eta} = \mathbf{Q}\mathbf{e}$ leads to the expression

$$\frac{\partial}{\partial t}\boldsymbol{\eta} = d\nabla^2\boldsymbol{\eta},$$

as desired. □

Furthermore, we remark that the conditions under which Property (4.10) holds, can be determined by computing

$$\mathbf{\Theta} = \mathbf{Q}\mathbf{N}_{\mathbf{L}}\mathbf{G}\mathbf{Q}^{+}. \tag{4.11}$$

Note that Lemma 4.2 suggest a linear transformation of the form

$$\begin{pmatrix}\mathbf{y}\\ \mathbf{z}\end{pmatrix} = \begin{pmatrix}\mathbf{Q}\\ \mathbf{M}\end{pmatrix}\mathbf{e}, \tag{4.12}$$

where $\mathbf{Q} \in \mathbb{R}^{(n-r)\times n}$ and $\mathbf{M} \in \mathbb{R}^{r\times n}$ is a matrix composed of r linearly independent rows of ${\mathbf{N}_{\mathbf{NL}}}^{T}$. The dynamics in these coordinates are

$$\frac{\partial}{\partial t}\mathbf{y} = d\nabla^2\mathbf{y} + \mathbf{\Theta}\mathbf{y} \tag{4.13a}$$

$$\frac{\partial}{\partial t}\mathbf{z} = d\nabla^2\mathbf{M}\mathbf{e} + \mathbf{M}\mathbf{A}\mathbf{e} + \mathbf{M}\mathbf{N}_{\mathbf{NL}}\mathbf{g}(\mathbf{e}). \tag{4.13b}$$

By Lemma 4.2, a closed form expression for $\mathbf{y}(t,x)$ can be found. With the inverse transformation

$$\mathbf{e} = \begin{pmatrix} \mathbf{Q}^+ & \mathbf{M}^+ \end{pmatrix} \begin{pmatrix} \mathbf{y} \\ \mathbf{z} \end{pmatrix},$$

we can express the PDE for $\mathbf{z}$ as

$$\frac{\partial}{\partial t}\mathbf{z} = d\nabla^2\mathbf{z} + \mathbf{M}\mathbf{A}\mathbf{M}^+\mathbf{z} + \mathbf{M}\mathbf{A}\mathbf{Q}^+\mathbf{y} + \mathbf{M}\mathbf{N}_{\mathbf{NL}}\mathbf{g}(\mathbf{y},\mathbf{z}). \tag{4.14}$$

As we see from Equation (4.13a) and Lemma 4.1, we have available the analytical solution for $\mathbf{y}(t,x)$. Hence it is only necessary to approximate the solution for $\mathbf{z}(t,x)$, in order to reconstruct the full state $\mathbf{c}(t,x)$. Towards this end, the following Proposition shows how the PDE for $\mathbf{z}(t,x)$ can be rewritten as a reduced order model (ROM) by means of the LSD.

Proposition 4.3. *Consider the PDE for* $\mathbf{z}(t,x)$ *as shown in* (4.14)*. Then* $\mathbf{z}(t,x)$ *can be approximated as*

$$\mathbf{z}(t,x) \approx \mathbf{W}_{\mathbf{z}}^{\mathbf{T}}(t)\boldsymbol{\phi}(x).$$

Here $\mathbf{W}_{\mathbf{z}}^{\mathbf{T}}$ *satisfies*

$$\frac{\mathrm{d}}{\mathrm{d}t}\mathrm{vec}\left(\mathbf{W}_{\mathbf{z}}^{\mathbf{T}}\right) = \tilde{\mathbf{A}}_{\mathbf{z}}\mathrm{vec}\left(\mathbf{W}_{\mathbf{z}}^{\mathbf{T}}\right) + \tilde{\mathbf{B}}_{\mathbf{y}}\mathrm{vec}\left(\mathbf{W}_{\mathbf{y}}^{\mathbf{T}}\right) + \tilde{\mathbf{B}}_{\mathbf{g}}\mathrm{vec}\left(\mathbf{W}_{\mathbf{g}}^{\mathbf{T}}\right), \tag{4.15}$$

$$\mathbf{W}_{\mathbf{g}}^{\mathbf{T}} = \int_{\Omega} \mathbf{g}\left(\mathbf{W}_{\mathbf{y}}^{\mathbf{T}}\boldsymbol{\phi}, \mathbf{W}_{\mathbf{z}}^{\mathbf{T}}\boldsymbol{\phi}\right)\boldsymbol{\phi}^{\boldsymbol{T}}\mathrm{d}x, \tag{4.16}$$

and

$$\tilde{\mathbf{A}}_{\mathbf{z}} = d(-\boldsymbol{\Lambda}\otimes\mathbf{I}_{\mathbf{r}}) + \left(\mathbf{I}_{\vartheta}\otimes\mathbf{M}\mathbf{A}\mathbf{M}^+\right) \tag{4.17a}$$

$$\tilde{\mathbf{B}}_{\mathbf{y}} = \left(\mathbf{I}_{\vartheta}\otimes\mathbf{M}\mathbf{A}\mathbf{Q}^+\right) \tag{4.17b}$$

$$\tilde{\mathbf{B}}_{\mathbf{g}} = (\mathbf{I}_{\vartheta}\otimes\mathbf{M}\mathbf{N}_{\mathbf{NL}}). \tag{4.17c}$$

Proof. We note that postmultiplication of the l.h.s in (4.14) by $\boldsymbol{\phi}^{\boldsymbol{T}}$ and integration over the spatial domain yield

$$\int_{\Omega}\frac{\partial}{\partial t}\mathbf{W}_{\mathbf{z}}^{\mathbf{T}}\boldsymbol{\phi}\boldsymbol{\phi}^{\boldsymbol{T}}\mathrm{d}x = \frac{\mathrm{d}}{\mathrm{d}t}\mathbf{W}_{\mathbf{z}}^{\mathbf{T}}.$$

Accordingly, the same operation applied to the r.h.s of (4.14) leads to

$$\frac{\mathrm{d}}{\mathrm{d}t}\mathbf{W}_{\mathbf{z}}^{\mathbf{T}} = -\mathbf{W}_{\mathbf{z}}^{\mathbf{T}}\mathbf{\Lambda} + \mathbf{M}\mathbf{A}\mathbf{M}^{+}\mathbf{W}_{\mathbf{z}}^{\mathbf{T}} + \mathbf{M}\mathbf{A}\mathbf{Q}^{+}\mathbf{W}_{\mathbf{y}}^{\mathbf{T}} + \mathbf{N}_{\mathbf{NL}}\mathbf{W}_{\mathbf{g}}^{\mathbf{T}},$$

where the properties in (4.1a) and (4.1b) along with the definition in (4.16) have been used. We note that $\frac{\mathrm{d}}{\mathrm{d}t}\mathbf{W}_{\mathbf{z}}^{\mathbf{T}}$ is a matrix in $\mathbb{R}^{r\times\vartheta}$. Applying $\mathrm{vec}\,(\circ)$ to the foregoing equation and Theorem 4.1 yield

$$\frac{\mathrm{d}}{\mathrm{d}t}\mathrm{vec}\left(\mathbf{W}_{\mathbf{z}}^{\mathbf{T}}\right) = \tilde{\mathbf{A}}_{\mathbf{z}}\mathrm{vec}\left(\mathbf{W}_{\mathbf{z}}^{\mathbf{T}}\right) + \tilde{\mathbf{B}}_{\mathbf{y}}\mathrm{vec}\left(\mathbf{W}_{\mathbf{y}}^{\mathbf{T}}\right) + \tilde{\mathbf{B}}_{\mathbf{g}}\mathrm{vec}\left(\mathbf{W}_{\mathbf{g}}^{\mathbf{T}}\right)$$

which is Equation (4.15) when the definitions in (4.17) are taken into account. □

Now we analyse a small reaction network. By focusing on the computational load, we give a comparison of the pure numerical, analytical/numerical, analytical/approximated, and approximated methods of solving the PDE.

Example 4.1. *We use of the procedures described above applied to the following biochemical reaction network*

$$A + B \xrightarrow{k_1} 2B \qquad B \xrightarrow{k_2} 0 \qquad A \underset{k_{3b}}{\overset{k_{3f}}{\rightleftharpoons}} 0.$$

By letting $\mathbf{c} = ([A] \quad [B])^T$*, the stoichiometric matrix and the reaction rate vector, according to the order proposed in* (2.32) *and* (2.30)*, are*

$$\mathbf{N} = \left(\begin{array}{c|cc|c} -1 & 0 & -1 & 1 \\ 1 & -1 & 0 & 0 \end{array}\right),$$
$$\mathbf{v}(\mathbf{c}) = \begin{pmatrix} k_1c_1c_2 & | & k_2c_2 & k_{3f}c_1 & | & k_{3b} \end{pmatrix}^T.$$

For this system, there exist two fixed points

$$\bar{\mathbf{c}}_{\mathbf{l}} = \begin{pmatrix} \frac{k_{3b}}{k_{3f}} & 0 \end{pmatrix}^T,$$
$$\bar{\mathbf{c}}_{\mathbf{h}} = \begin{pmatrix} \frac{k_2}{k_1} & \frac{k_{3b}}{k_2} - \frac{k_{3f}}{k_1} \end{pmatrix}^T.$$

For simplicity, we choose to make the Taylor expansion of the model around $\bar{\mathbf{c}}_{\mathbf{l}}$*. Hence, the*

Jacobian of $\mathbf{v}(\mathbf{c})$ *is*

$$\mathbf{J}(\bar{\mathbf{c}}_\mathbf{1}) = \left(\begin{array}{cc} 0 & \frac{k_1 k_{3b}}{k_{3f}} \\ \hline 0 & k_2 \\ k_{3f} & 0 \\ \hline 0 & 0 \end{array}\right).$$

In order to fully determine the PDE, we will consider that $x \in [0,1] = \Omega \subset \mathbb{R}$*, with the initial condition represented by*

$$\begin{pmatrix} c_1(0,x) \\ c_2(0,x) \end{pmatrix} = \begin{pmatrix} \bar{c}_1 \\ \mathcal{N}(x-\mu,\sigma^2) \end{pmatrix}.$$

Here $\mathcal{N}(\circ)$ *is a Gaussian function defined as*

$$\mathcal{N}(x-\mu,\sigma^2) = \frac{1}{\sqrt{2\pi\sigma^2}} \exp\left(-\frac{(x-\mu)^2}{2\sigma^2}\right). \tag{4.18}$$

Also, we account for zero-flux boundary conditions

$$\left.\frac{\partial \mathbf{c}(t,x)}{\partial \mathbf{n}}\right|_{x=\partial\Omega} = 0.$$

Reduction of Order via Analytical Solution for $y(t,x)$

With these definitions, the linear transformation in (4.12) *becomes*

$$\mathbf{T} = \begin{pmatrix} \mathbf{Q} \\ \mathbf{M} \end{pmatrix} = \left(\begin{array}{cc} 1 & 1 \\ \hline -1 & 1 \end{array}\right),$$

$$\mathbf{T}^{-1} = \begin{pmatrix} \mathbf{Q}^+ & \mathbf{M}^+ \end{pmatrix} = \frac{1}{2}\left(\begin{array}{c|c} 1 & -1 \\ 1 & 1 \end{array}\right),$$

which imply

$$\begin{pmatrix} y(t,x) \\ z(t,x) \end{pmatrix} = \begin{pmatrix} e_1(t,x) + e_2(t,x) \\ -e_1(t,x) + e_2(t,x) \end{pmatrix}.$$

Moreover, the corresponding initial conditions in the y, z variables are (recall that in this coordinates, $\bar{\mathbf{e}} = \mathbf{0}$):

$$\begin{pmatrix} y(0,x) \\ z(0,x) \end{pmatrix} = \begin{pmatrix} \mathcal{N}(x-\mu,\sigma^2) \\ \mathcal{N}(x-\mu,\sigma^2) \end{pmatrix}.$$

Hence Condition (4.10) *becomes*

$$\begin{pmatrix} k_{3f} & k_2 \end{pmatrix} = \begin{pmatrix} \frac{1}{2}[k_{3f}+k_2] & \frac{1}{2}[k_{3f}+k_2] \end{pmatrix}, \tag{4.19}$$

which is satisfied by letting $k_{3f} = k_2 = k$. Moreover, from Equation (4.11) *follows $\Theta = -k$.*

As stated in Section 4.3 we can compute the spatio-temporal profile of the system by a PDE of order $r = \operatorname{colrank}(\mathbf{N_{nl}}) = 1$. This reduced system is given by (4.14)*, which in our case is*

$$\frac{\partial}{\partial t} z(t,x) = d\nabla_x^2 z + \left(\frac{k_1 k_{3b}}{k} - k \right) z + \frac{k_1 k_{3b}}{k} y + \frac{1}{2} k_1 \left(y^2 - z^2 \right). \tag{4.20}$$

In turn, from Lemma 4.2 and (3.45)*, $y(t,x)$ satisfies*

$$\begin{aligned} y(t,x) &= \exp(-kt) \int_{-\infty}^{\infty} \mathcal{N}(x-\mu,\sigma^2)\mathcal{N}(x-\xi,2dt)\mathrm{d}\xi \\ y(t,x) &= \exp(-kt)\mathcal{N}(x-\mu,2dt+\sigma^2). \end{aligned} \tag{4.21}$$

Analytical Solution & LSD

Now, in order to perform the simulation via the analytical solution & LSD approach, it is necessary to compute the modes $\mathbf{w^T}(t)$ for $y(t,x)$ and $g(y,z)$, as noted in Proposition 4.3. For $\mathbf{w_y^T}(t)$ we prefer numerical computation to avoid the evaluation of a complex function in the code, hence reducing the computational load. In turn, from (4.16)*,*

$$\begin{aligned} \mathbf{w_g^T}(t) &= \int_\Omega g(\mathbf{w_y^T}\boldsymbol{\phi}, \mathbf{w_z^T}\boldsymbol{\phi})\boldsymbol{\phi^T}\mathrm{d}x \\ &= \frac{k_1}{2}\int_0^1 (\mathbf{w_y^T}\boldsymbol{\phi})^2\boldsymbol{\phi^T} - (\mathbf{w_z^T}\boldsymbol{\phi})^2\boldsymbol{\phi^T}\mathrm{d}x \\ \mathbf{w_g^T}(t) &= \frac{k_1}{2}\int_0^1 \boldsymbol{\phi^T}\left(\mathbf{w_y}\mathbf{w_y^T} - \mathbf{w_z}\mathbf{w_z^T}\right)\boldsymbol{\phi}\boldsymbol{\phi^T}\mathrm{d}x. \end{aligned} \tag{4.22}$$

The vectorised expression of the term $\boldsymbol{\phi}^{\boldsymbol{T}}\left(\mathbf{w}\mathbf{w}^{\mathbf{T}}\right)\boldsymbol{\phi}\boldsymbol{\phi}^{\boldsymbol{T}}$ *is*

$$\operatorname{vec}\left(\boldsymbol{\phi}^{\boldsymbol{T}}\left(\mathbf{w}\mathbf{w}^{\mathbf{T}}\right)\boldsymbol{\phi}\boldsymbol{\phi}^{\boldsymbol{T}}\right)=\left(\boldsymbol{\phi}\boldsymbol{\phi}^{\boldsymbol{T}}\otimes\boldsymbol{\phi}^{\boldsymbol{T}}\right)\operatorname{vec}\left(\mathbf{w}\mathbf{w}^{\mathbf{T}}\right),$$

from which we note an explicit separation of the spatial and temporal dependency. Each of the terms in the matrix $\boldsymbol{\phi}\boldsymbol{\phi}^{\boldsymbol{T}}\otimes\boldsymbol{\phi}^{\boldsymbol{T}}$ *is a product of three elements of the basis. Their integral over the spatial domain have this simple expression*

$$\int_0^1 \phi_i\phi_j\phi_k \mathrm{d}x=\begin{cases}1, & i=1, j=k\ \forall\ j,k\in[1,p]\\ 0, & \textit{otherwise.}\end{cases} \tag{4.23}$$

Then we can write the Equation (4.22) *as*

$$\operatorname{vec}\left(\mathbf{w}_{\mathbf{g}}^{\mathbf{T}}\right)(t)=\frac{k_1}{2}\left(\int_0^1 \boldsymbol{\phi}\boldsymbol{\phi}^{\boldsymbol{T}}\otimes\boldsymbol{\phi}^{\boldsymbol{T}}\,\mathrm{d}x\right)\left[\operatorname{vec}\left(\mathbf{w}_{\mathbf{y}}(t)\mathbf{w}_{\mathbf{y}}^{\mathbf{T}}(t)-\mathbf{w}_{\mathbf{z}}(t)\mathbf{w}_{\mathbf{z}}^{\mathbf{T}}(t)\right)\right]. \tag{4.24}$$

LSD

Finally, we assess the performance of the previous methods with the reduced order model obtained from (2.40)*. As stated in Section 4.1, the weights for this PDE satisfy*

$$\begin{aligned}\frac{\mathrm{d}}{\mathrm{d}t}\operatorname{vec}\left(\mathbf{W}^{\mathbf{T}}\right)=&\left[d\left(-\boldsymbol{\Lambda}\otimes\mathbf{I_2}\right)+\left(\mathbf{I}_{\vartheta}\otimes\mathbf{N_L}\mathbf{G}\right)\right]\operatorname{vec}\left(\mathbf{W}^{\mathbf{T}}\right)+\left(\mathbf{I}_{\vartheta}\otimes\mathbf{N_0}\right)\operatorname{vec}\left(\left(\mathbf{v_0}\ \mathbf{0}\right)\right)+\\&+\left(\mathbf{I}_{\vartheta}\otimes\mathbf{N}_{\mathbf{NL}}\right)\left(\int_{\Omega}\boldsymbol{\phi}\boldsymbol{\phi}^{\boldsymbol{T}}\otimes\boldsymbol{\phi}^{\boldsymbol{T}}\mathrm{d}x\right)\left(\mathbf{W}\otimes\mathbf{W}\right)\operatorname{vec}\left(\mathbf{Y}\right).\end{aligned} \tag{4.25}$$

Implementation and Results

The simulations were performed in a PC with a processor AMD A6-4455M APU and 3GB of RAM, running Kubuntu 12.10 64 bits and Matlab 2007b. Four different implementation were considered in order to compare the methods:

1. *Numerical Implementation. We avail of the function pdepe implemented in Matlab.*
2. *Analytical & Numerical. Using the expression for* $y(t,x)$ *in* (4.21)*, we simulated* (4.20) *with pdepe.*
3. *Analytical & LSD. We implemented* (4.15)*, where* $\mathbf{w}_{\mathbf{g}}^{\mathbf{T}}(t)$ *have been defined in* (4.24) *and* $\mathbf{w}_{\mathbf{y}}^{\mathbf{T}}(t)$ *are computed numerically. In this case, we used the ODE15s solver.*
4. *LSD. The implementation of* (4.25) *was simulated by the ODE15s solver.*

A global basis for Ω with zero-flux boundary conditions, which complies with (4.1b) *and* (4.1a) *is given by*

$$\phi_i(x) = k_i \cos(2\pi(i-1)x),$$
$$k_i = \begin{cases} 1 & , \quad i = 1 \\ \sqrt{2} & , \quad i \neq 1 \end{cases}.$$

In turn, the eigenvalues are

$$\lambda_i = [2\pi(i-1)]^2 \quad \forall\, i \in [1, \vartheta].$$

Figure 4.1 shows the surfaces obtained with the four different methods. In turn, Figure 4.3 shows the mean cpu time required by each solution method. To avoid variability of results, we repeated each simulation 100 times, and we show the associated error bar also in Figure 4.3. It is important to note that this result is for $\vartheta = 34$ number of eigenfunctions. We selected this number of eigenfunctions for the LSD methods as it provides an very accurate approximation of a Gaussian function, as shown in Figure 4.2. As the number of eigenfunctinos decreases, the LSD approach improves its performance w.r.t. the Analytical & LSD implementation and conversely. We also note a that the time required for pure LSD and Analytical & LSD methods tend to remain constant as the number of nodes varies, whereas the time required those method based on the function pdepe of Matlab seems to grow linearly as the number of nodes grows.

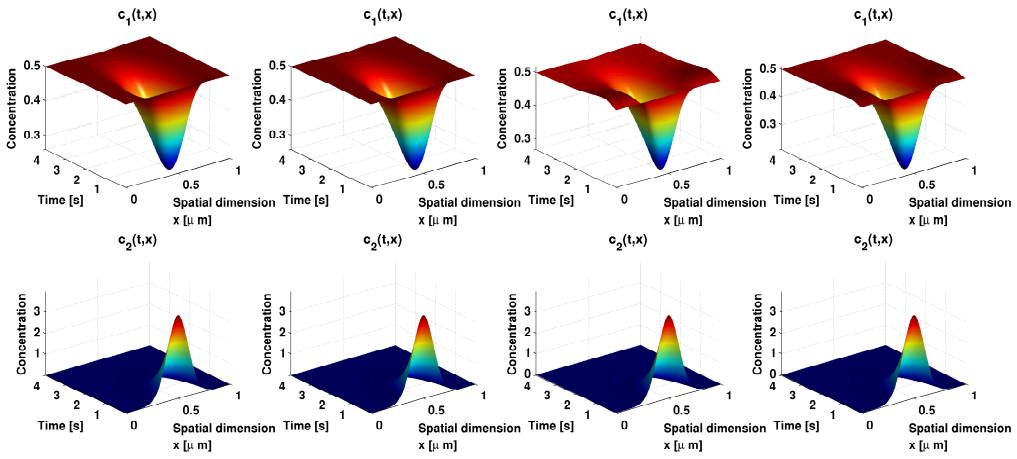

Figure 4.1: *Comparison of the methods for solving the PDE in the case study. From left to right this figure depicts the surface obtained by numerical, analytical/numerical, analytical/LSD, and LSD approaches, respectively.*

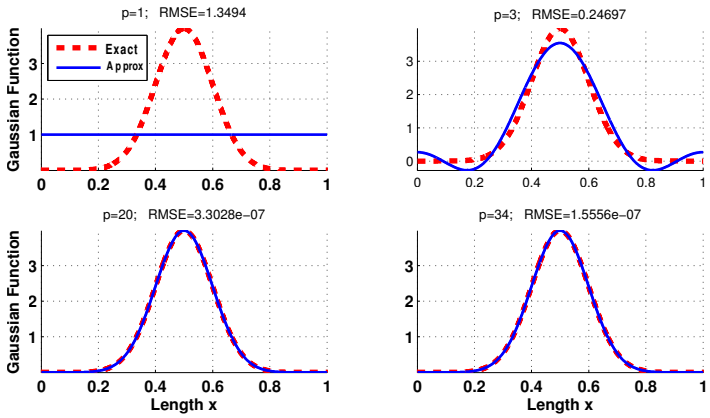

Figure 4.2: *Approximation of the Gaussian function in* (4.18) *as the number of eigenfunctions ϑ varies. The header of each panel shows the number ϑ used as well as the Root Mean Square Error (RMSE) between the approximation and the exact Gaussian function. Here we used $\sigma^2 = 0.01, \mu = 0.5$.*

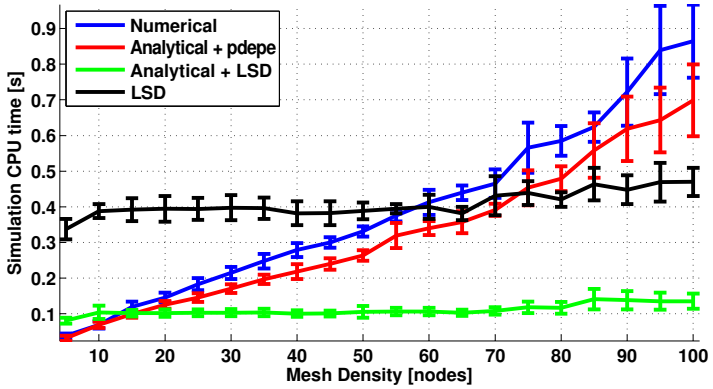

Figure 4.3: *CPU time assessment for the four methods to solve a PDE. The parameters used for the simulation are: $\vartheta = 34$, $\{k_1, k_2, k_{3b}, k_{3f}\} = \{1, 2, 2, 1\}$, $d = 0.001, \sigma^2 = 0.01, \mu = 0.5$.*

Although obtaining a solution of a reaction-diffusion system provides all the information about its dynamic response, the numerical solution only provides these characteristics for a particular set of initial and boundary conditions, diffusion constants, and kinetic parameters. Hence, approaches which include the analytical solution may be used to characterise some of the dynamic properties in terms of the parameters of the system. In light of this analytical treatment, in the forthcoming section, we will focus on the analytical computation of the integral of selected species in the biochemical network.

4.4 On the Temporal Integral of Solutions of Reaction-Diffusion Equations

The quantification of a signal's magnitude, may serve as a measure of the influence of such a signal in its environment. A possible choice of this magnitude quantification is the time-integral of the signal. In the biochemical context, the time-integral of the species concentration is one of the ways in which a cue may propagate its information through a signalling pathway [65].

For instance, in a spatio-temporal domain, the integrated response of morphogenes has been implicated in processes such as cellular growth and differentiation [66, 18, 43]. Moreover, by obtaining the integrated response of the erythropoietin receptor, a linear relationship of this receptor signal transmission has been suggested [67, 68]. Theoretical approaches towards the analytical computation of signal norms is presented in [69], where for a class of biochemical pathways the $\mathcal{L}_2$ norm of some signals can be computed by analysing an associated linear system.

This section focuses on the analytical computation of the integral in time of the reaction network concentrations, and its contents are a follow-up of this problem formulation originally posed in [70, 71]. The main idea is to find subspaces of the concentration space, which are orthogonal to the vectors associated to the nonlinear reaction rates. Once this subspace has been identified we derive analytical formulas for the integral of some species in the reaction network. We organise the presentation of these ideas in three different sections. Firstly, we show that the left null space of a matrix defined by the stoichiometric matrix and Jacobian of the system, determines linear combinations that present an integral constrain [25]. Secondly, we show sufficient conditions on the stoichiometric matrix, which allow us to compute the integrated response of single species. Finally, we extend this results to the reaction-diffusion case, as presented in [27].

Throughout this section, we will consider a reaction network expressed in terms of the error coordinates as presented in (2.52). Moreover, we adopt the following assumptions to ensure that the trajectories of the network have a finite integral.

Assumption 4.1. *Let the reaction-diffusion PDE and the influx of species* $\mathbf{u}(t, x)$ *satisfy*

A1. The model of the reaction network in (2.52) *has a unique exponentially stable fixed point,*

A2. moreover, the external inputs to the network $\mathbf{u}(t,x)$ *have a finite integral, that is to say*

$$\lim_{t\to\infty}\mathbf{u}(t,x)=\mathbf{0},$$
$$\int_0^\infty \mathbf{u}(t,x)\,\mathrm{d}t<\boldsymbol{\infty}.$$

4.4.1 Integral in Time of a Linear Combination of Species Concentration

As a motivation of the methodology to use, let us consider first the case in which the diffusion of species is negligible. Hence, the dynamics in the error coordinates in (2.52) are:

$$\frac{\mathrm{d}}{\mathrm{d}t}\mathbf{e}=\mathbf{A}\mathbf{e}+\mathbf{N}_{\mathbf{NL}}\mathbf{g}(\mathbf{e})+\mathbf{B}\mathbf{u}, \tag{4.26}$$

where $\mathbf{g}(\mathbf{e})$ comprises all the higher order terms of the Taylor expansion of the nonlinear reaction rates $\mathbf{v}_{\mathbf{NL}}(\mathbf{e})$. We note that we have not considered any particular functional form for the nonlinear reaction rates. Integration in time of (4.26) yields

$$\mathbf{e}(\infty)-\mathbf{e}(0)=\mathbf{A}\int_0^\infty \mathbf{e}\,\mathrm{d}t+\mathbf{N}_{\mathbf{NL}}\int_0^\infty \mathbf{g}(\mathbf{e})\,\mathrm{d}t+\mathbf{B}\int_0^\infty \mathbf{u}\,\mathrm{d}t.$$

Assumptions 4.1 ensure that the integrals are finite and $\mathbf{e}(\infty)=\mathbf{0}$. Hence,

$$\int_0^\infty \mathbf{e}\,\mathrm{d}t=-\mathbf{A}^{-1}\left(\mathbf{e}(0)+\mathbf{N}_{\mathbf{NL}}\int_0^\infty \mathbf{g}(\mathbf{e})\,\mathrm{d}t+\mathbf{B}\int_0^\infty \mathbf{u}\,\mathrm{d}t\right). \tag{4.27}$$

Now, let us define $\mathbf{y}=\mathbf{C}\mathbf{e}$ with $\mathbf{C}\in\mathbb{R}^{v\times n}$ and such that

$$\mathbf{C}\mathbf{A}^{-1}\mathbf{N}_{\mathbf{NL}}=\mathbf{0}. \tag{4.28}$$

Then

$$\int_0^\infty \mathbf{y}\,\mathrm{d}t=-\mathbf{C}\mathbf{A}^{-1}\left(\mathbf{e}(0)+\mathbf{B}\int_0^\infty \mathbf{u}\,\mathrm{d}t\right). \tag{4.29}$$

Condition (4.28) indicates that all the choices of $\mathbf{C}$ are linear combinations of the left null space of $\mathbf{A}^{-1}\mathbf{N}_{\mathbf{NL}}$. This null space allows us to identify algebraic constraints between the integral of the different species' concentrations, hence suggesting the existence of a constraint in the dynamics of the biochemical reaction network. However, this approach does not present conditions to compute the integral of specific species, which might provide more valuable information

for the downstream signalling. For the ODE case, we present these conditions in the following section.

4.4.2 Time-Integral of Selected Species Concentrations

In this section we will obtain conditions for which the analytical expression for the time-integral of some species can be obtained. Here, we still consider that the diffusion of species is negligible, and the dynamics of the species concentrations are governed by (4.26). Towards this end, let us split the state vector $\mathbf{c}(t)$ as

$$\mathbf{c}(t) = \begin{pmatrix} \mathbf{c_{NL}}(t) \\ \mathbf{c_{L}}(t) \end{pmatrix} \; : \; \mathbb{R}_+ \to \mathbb{R}^{k+(n-k)}. \tag{4.30}$$

The vector $\mathbf{c_{NL}}(t,x)$ is composed of the k species that are *exclusively* reactants or products of nonlinear reactions, whereas $\mathbf{c_{L}}(t,x)$ includes the rest of the species. Accordingly, the stoichiometric matrix, Jacobian, diffusion matrix, and input matrix in (4.26), and the deviation coordinate $\mathbf{e}(t)$, become

$$\mathbf{N} = \begin{pmatrix} \mathbf{N_1} & \mathbf{N_3} \\ \mathbf{N_2} & \mathbf{N_4} \end{pmatrix} \in \mathbb{R}^{(k+(n-k))\times(m_1+(m-m_1))},$$

$$\mathbf{J} = \begin{pmatrix} \mathbf{J_1} & \mathbf{J_2} \\ \mathbf{J_3} & \mathbf{J_4} \end{pmatrix} \in \mathbb{R}^{(m_1+(m-m_1))\times(k+(n-k))},$$

$$\mathbf{B} = \begin{pmatrix} \mathbf{B_1} \\ \mathbf{B_2} \end{pmatrix} \in \mathbb{R}^{(k+(n-k))\times q}, \tag{4.31a}$$

$$\mathbf{e}(t) = \begin{pmatrix} \mathbf{e_{NL}}(t) \\ \mathbf{e_{L}}(t) \end{pmatrix} \; : \; \mathbb{R}_+ \to \mathbb{R}^{k+(n-k)}. \tag{4.31b}$$

As a consequence of the definition of $\mathbf{e_{L}}(t)$, we note that $\mathbf{J_3} = \mathbf{N_3}^T = \mathbf{0}$, so the definitions for $\mathbf{N}$ and $\mathbf{J}$ above reduce to

$$\mathbf{N} = \begin{pmatrix} \mathbf{N_1} & \mathbf{0} \\ \mathbf{N_2} & \mathbf{N_4} \end{pmatrix}, \tag{4.32a}$$

$$\mathbf{J} = \begin{pmatrix} \mathbf{J_1} & \mathbf{J_2} \\ \mathbf{0} & \mathbf{J_4} \end{pmatrix}. \tag{4.32b}$$

Furthermore, we adopt the forthcoming assumption.

Assumption 4.2. *The number of nonlinear reaction rates equals that of elements in* $\mathbf{c}_{\mathbf{NL}}(t)$. *That is to say* $m_1 = k$.

Of course, this assumption limits the application of our methodology to a rather specific class of reaction networks. However, it allows us to obtain a closed-form expression for the integral in time of some species' concentrations. Under this assumption and the definitions in (4.31) and (4.32), we can express $\mathbf{A}^{-1}$ in (4.27) as

$$\mathbf{A}^{-1} = \begin{pmatrix} \mathbf{J}_1^{-1}\mathbf{N}_1^{-1} + \mathbf{J}_1^{-1}\mathbf{J}_2\left(\mathbf{N}_4\mathbf{J}_4\right)^{-1}\mathbf{N}_2\mathbf{N}_1^{-1} & -\mathbf{J}_1^{-1}\mathbf{J}_2\left(\mathbf{N}_4\mathbf{J}_4\right)^{-1} \\ -\left(\mathbf{N}_4\mathbf{J}_4\right)^{-1}\mathbf{N}_2\mathbf{N}_1^{-1} & \left(\mathbf{N}_4\mathbf{J}_4\right)^{-1} \end{pmatrix}. \tag{4.33}$$

Moreover, we note

$$\mathbf{A}^{-1}\mathbf{N}_{\mathbf{NL}} = \begin{pmatrix} \mathbf{J}_1^{-1} \\ \mathbf{0} \end{pmatrix}. \tag{4.34}$$

This implies that the time-integral of $\mathbf{e}_{\mathbf{L}}$ can be computed from (4.27) as

$$\int_0^\infty \mathbf{e}_{\mathbf{L}}\,\mathrm{d}t = \left(\mathbf{N}_4\mathbf{J}_4\right)^{-1}\mathbf{H}\left(\mathbf{e}(0) + \mathbf{B}\int_0^\infty \mathbf{u}\,\mathrm{d}t\right), \tag{4.35}$$

where

$$\mathbf{H} = \begin{pmatrix} \mathbf{N_2N_1^{-1}} & -\mathbf{I}_{n-k} \end{pmatrix}. \tag{4.36}$$

From (4.35), we note that the integral is directly proportional to the net flux of species integrated over time. The proportionality matrix is a function of the stoichiometry of the system and of the kinetic constants in $\mathbf{J}_4$; typically, $\mathbf{J}_4$ contains the degradation rates of the species in $\mathbf{e}_{\mathbf{L}}(t)$. In the forthcoming section, we derive in detail a similar result for the case in which the diffusion of the species in $\mathbf{e}_{\mathbf{L}}(t,x)$ is relevant. This methodology has assisted in the characterisation of the transduction properties of the erythropoietin membrane receptor [26].

4.4.3 Integral in Time of Selected Species Concentrations in a Reaction-Diffusion Network

In this section we extend the results derived in the previous section to a class of reaction-diffusion network. Here, we will make use of the LSD method introduced in Section 4.1, to derive a

formula for the time-integral of the species comprised in $\mathbf{e_L}(t,x)$. Moreover, we consider the expression of the reaction-diffusion model in the deviation coordinates form the homogeneous steady state given by

$$\frac{\partial}{\partial t}\mathbf{e} = \mathbf{D}\nabla^2\mathbf{e} + \mathbf{A}\mathbf{e} + \mathbf{N_{NL}}\mathbf{g}(\mathbf{e}) + \mathbf{B}\mathbf{u}. \tag{2.52}$$

Now, we consider the diffusion of species in a spatial domain Ω. Following the vector order for $\mathbf{c}(t,x)$ in (4.30), the diffusion matrix in (2.52) is

$$\mathbf{D} = \begin{pmatrix} \mathbf{D_1} & \mathbf{0} \\ \mathbf{0} & \mathbf{D_4} \end{pmatrix} \in \mathbb{R}^{(k+(n-k))\times(k+(n-k))}. \tag{4.37}$$

We also note that the modes $\mathbf{W_e^T}(t)$ are partitioned following the order given in (4.31b)

$$\mathbf{W_e^T}(t) = \begin{pmatrix} \mathbf{W_{NL}^T}(t) \\ \mathbf{W_L^T}(t) \end{pmatrix} \quad : \quad \mathbb{R}_+ \to \mathbb{R}^{(k+(n-k)\times\vartheta)}.$$

The forthcoming Proposition summarises the derivation of the time-integral of the species in $\mathbf{e_L}(t,x)$, when the reaction network satisfies Assumptions 4.1 and 4.2 along with assumption of no diffusivity for the species comprised in $\mathbf{e}_{NL}$. The later assumption models biological scenarios in which the species in $\mathbf{e}_{NL}$ are very big in comparison to the rest of the species in the network or when they are spatially fixed to the cell membrane, for instance.

Proposition 4.4. *Consider a reaction-diffusion system of the form given in* (2.52)*, that satisfy Assumptions 4.1 and 4.2. Moreover, let the diffusion of the species in* $\mathbf{e}_{NL}$ *be negligible:*

$$\mathbf{D}_1 = \mathbf{0}, \tag{4.38a}$$

and assume that all the functions in (2.52) *belong to the same Hilbert space. Then, the time integral of the species in* $\mathbf{e_L}(t,x)$ *is given by*

$$\int_0^\infty \mathbf{e_L}(t,x)\,\mathrm{d}t = \sum_{i=1}^{\vartheta} \left(-\lambda_i\mathbf{D}_4 + \mathbf{N}_4\mathbf{J}_4\right)^{-1}\mathbf{H}\left[\mathbf{w_e}(0)_i + \mathbf{B}\int_0^\infty \mathbf{w_u}_i\,\mathrm{d}t\right]\phi_i(x), \tag{4.39}$$

provided the inverse $\left(-\lambda_i\mathbf{D}_4 + \mathbf{N}_4\mathbf{J}_4\right)^{-1}$ *exists. Here* $\mathbf{H}$ *has been defined in* (4.36)*. In addition,* $-\lambda_i$ *and* $\phi_i(x)$ *are the ith eigenvalue and basis element of the Hilbert space to which the solutions of* (2.52) *belong. Moreover,* $\mathbf{w_e}(0)_i$ *and* $\mathbf{w_u}_i(t)$ *are the weights of the initial condition*

$\mathbf{e}(0)$ *and external influxes* $\mathbf{u}(t,x)$*, referred to the basis element* $\phi_i(x)$.

Proof. Firstly, we define

$$\mathbf{A} = \mathbf{NJ} = \begin{pmatrix} \mathbf{N_1 J_1} & \mathbf{N_1 J_2} \\ \mathbf{N_2 J_1} & \mathbf{N_2 J_2} + \mathbf{N_4 J_4} \end{pmatrix} =: \begin{pmatrix} \mathbf{A}_{11} & \mathbf{A}_{12} \\ \mathbf{A}_{21} & \mathbf{A}_{22} \end{pmatrix}. \tag{4.40}$$

Moreover, we note that, since we deal with an exponentially stable system, $\mathbf{e}(\infty) = \mathbf{0}$. Hence integration in time of (2.52) yields

$$\mathbf{0} - \mathbf{e}_0(x) = \mathbf{D}\nabla^2 \int_0^\infty \mathbf{e}\,\mathrm{d}t + \mathbf{A}\int_0^\infty \mathbf{e}\,\mathrm{d}t + \mathbf{N}_{\mathbf{NL}}\int_0^\infty \mathbf{g}(\mathbf{e})\,\mathrm{d}t + \mathbf{B}\int_0^\infty \mathbf{u}\,\mathrm{d}t.$$

Considering the partition of the state $\mathbf{e}(t,x)$ in (4.30) and $\mathbf{D}_1 = \mathbf{0}$, the equation above can be rewritten in partitioned form as:

$$-\mathbf{e}_{\mathbf{NL}0}(x) = \mathbf{A}_{11}\int_0^\infty \mathbf{e}_{\mathbf{NL}}\,\mathrm{d}t + \mathbf{A}_{12}\int_0^\infty \mathbf{e}_{\mathbf{L}}\,\mathrm{d}t + \mathbf{N_1}\int_0^\infty \mathbf{g}(\mathbf{e})\,\mathrm{d}t + \mathbf{B_1}\int_0^\infty \mathbf{u}\,\mathrm{d}t \tag{4.41a}$$

$$\begin{aligned} -\mathbf{e}_{\mathbf{L}0}(x) = \mathbf{D}_4\nabla^2 \int_0^\infty \mathbf{e}_{\mathbf{L}}\,\mathrm{d}t + \mathbf{A}_{21}\int_0^\infty \mathbf{e}_{\mathbf{NL}}\,\mathrm{d}t + \mathbf{A}_{22}\int_0^\infty \mathbf{e}_{\mathbf{L}}\,\mathrm{d}t + \\ + \mathbf{N_2}\int_0^\infty \mathbf{g}(\mathbf{e})\,\mathrm{d}t + \mathbf{B_2}\int_0^\infty \mathbf{u}\,\mathrm{d}t. \end{aligned} \tag{4.41b}$$

Since $\mathbf{e}_{\mathbf{NL}}(t,x)$, $\mathbf{e}_{\mathbf{L}}(t,x)$, $\mathbf{u}(t,x)$ belong to the same Hilbert space, we can approximate them as a truncated series in terms of the common basis $\boldsymbol{\phi}(x)$. Substituting these signals by its series representation and postmultiplying by $\boldsymbol{\phi}^T(x)$, the foregoing expressions become

$$\begin{aligned} -\mathbf{W}^{\mathbf{T}}_{\mathbf{NL}}(0)\boldsymbol{\phi}\boldsymbol{\phi}^T =& \mathbf{A}_{11}\int_0^\infty \mathbf{W}^{\mathbf{T}}_{\mathbf{NL}}\,\mathrm{d}t\boldsymbol{\phi}\boldsymbol{\phi}^T + \mathbf{A}_{12}\int_0^\infty \mathbf{W}^{\mathbf{T}}_{\mathbf{L}}\,\mathrm{d}t\boldsymbol{\phi}\boldsymbol{\phi}^T + \mathbf{N_1}\int_0^\infty \mathbf{g}(\mathbf{e})\,\mathrm{d}t\boldsymbol{\phi}^T + \\ &+ \mathbf{B_1}\int_0^\infty \mathbf{W}^{\mathbf{T}}_{\mathbf{u}}\,\mathrm{d}t\boldsymbol{\phi}\boldsymbol{\phi}^T \end{aligned}$$

$$\begin{aligned} -\mathbf{W}^{\mathbf{T}}_{\mathbf{L}}(0)\boldsymbol{\phi}\boldsymbol{\phi}^T =& \mathbf{D}_4\int_0^\infty \mathbf{W}^{\mathbf{T}}_{\mathbf{NL}}\,\mathrm{d}t\boldsymbol{\Lambda}\boldsymbol{\phi}\boldsymbol{\phi}^T + \mathbf{A}_{21}\int_0^\infty \mathbf{W}^{\mathbf{T}}_{\mathbf{NL}}\,\mathrm{d}t\boldsymbol{\phi}\boldsymbol{\phi}^T + \\ &+ \mathbf{A}_{22}\int_0^\infty \mathbf{W}^{\mathbf{T}}_{\mathbf{L}}\,\mathrm{d}t\boldsymbol{\phi}\boldsymbol{\phi}^T + \mathbf{N_2}\int_0^\infty \mathbf{g}(\mathbf{e})\,\mathrm{d}t\boldsymbol{\phi}^T + \mathbf{B_2}\int_0^\infty \mathbf{W}^{\mathbf{T}}_{\mathbf{u}}\,\mathrm{d}t\boldsymbol{\phi}\boldsymbol{\phi}^T, \end{aligned}$$

where the invariance w.r.t the Laplacian operator in (4.1b) has been used. By noting that the

orthonormality of the basis $\boldsymbol{\phi}(x)$ in (4.1a) implies $\int_\Omega \boldsymbol{\phi}\boldsymbol{\phi}^T \,\mathrm{d}x = \mathbf{I}_\vartheta$, integration over Ω yields

$$-\mathbf{W}_{\mathbf{NL}}^{\mathbf{T}}(0) = \mathbf{A}_{11}\int_0^\infty \mathbf{W}_{\mathbf{NL}}^{\mathbf{T}}\,\mathrm{d}t + \mathbf{A}_{12}\int_0^\infty \mathbf{W}_{\mathbf{L}}^{\mathbf{T}}\,\mathrm{d}t + +\mathbf{N_1F} + \mathbf{B_1}\int_0^\infty \mathbf{W}_{\mathbf{u}}^{\mathbf{T}}\,\mathrm{d}t \tag{4.42a}$$

$$\begin{aligned}-\mathbf{W}_{\mathbf{L}}^{\mathbf{T}}(0) = \mathbf{D}_4\int_0^\infty \mathbf{W}_{\mathbf{L}}^{\mathbf{T}}\,\mathrm{d}t\boldsymbol{\Lambda} + \mathbf{A}_{21}\int_0^\infty \mathbf{W}_{\mathbf{NL}}^{\mathbf{T}}\,\mathrm{d}t + \mathbf{A}_{22}\int_0^\infty \mathbf{W}_{\mathbf{L}}^{\mathbf{T}}\,\mathrm{d}t + \\ + \mathbf{N_2F} + \mathbf{B_2}\int_0^\infty \mathbf{W}_{\mathbf{u}}^{\mathbf{T}}\,\mathrm{d}t,\end{aligned} \tag{4.42b}$$

where we have defined $\mathbf{F} = \int_\Omega \int_0^\infty \mathbf{g}(\mathbf{e})\boldsymbol{\phi}^T(x)\,\mathrm{d}t\,\mathrm{d}x$. Given the stability of $\mathbf{A}$, we can ensure that its inverse exists and consequently $\mathbf{A}_{11}$ is nonsingular. Therefore, we can solve (4.42a) for $\int_0^\infty \mathbf{W}_{\mathbf{NL}}^{\mathbf{T}}(t)\,\mathrm{d}t$:

$$\int_0^\infty \mathbf{W}_{\mathbf{NL}}^{\mathbf{T}}\,\mathrm{d}t = -\mathbf{A}_{11}^{-1}\left(\mathbf{W}_{\mathbf{NL}}^{\mathbf{T}}(0) + \mathbf{A}_{12}\int_0^\infty \mathbf{W}_{\mathbf{L}}^{\mathbf{T}}\,\mathrm{d}t + \mathbf{N_1F} + \mathbf{B_1}\int_0^\infty \mathbf{W}_{\mathbf{u}}^{\mathbf{T}}\,\mathrm{d}t\right).$$

Since $m_1 = k$, $\mathbf{A}_{11}^{-1} = \mathbf{J_1}^{-1}\mathbf{N_1}^{-1}$ and the equation above becomes

$$\int_0^\infty \mathbf{W}_{\mathbf{NL}}^{\mathbf{T}}\,\mathrm{d}t = -\left(\mathbf{A}_{11}^{-1}\mathbf{W}_{\mathbf{NL}}^{\mathbf{T}}(0) + \mathbf{J_1}^{-1}\mathbf{J_2}\int_0^\infty \mathbf{W}_{\mathbf{L}}^{\mathbf{T}}\,\mathrm{d}t + \mathbf{J_1}^{-1}\mathbf{F} + \mathbf{A_{11}^{-1}B_1}\int_0^\infty \mathbf{W}_{\mathbf{u}}^{\mathbf{T}}\,\mathrm{d}t\right).$$

Substituting the equation above in (4.42b) and simplifying, yields

$$\mathbf{0}_{n\times\vartheta} = \mathbf{D}_4\int_0^\infty \mathbf{W}_{\mathbf{L}}^{\mathbf{T}}\,\mathrm{d}t\boldsymbol{\Lambda} + \mathbf{N_4J_4}\int_0^\infty \mathbf{W}_{\mathbf{L}}^{\mathbf{T}}\,\mathrm{d}t - \mathbf{H}\left(\mathbf{W}_{\mathbf{e}}^{\mathbf{T}}(0) + \mathbf{B}\int_0^\infty \mathbf{W}_{\mathbf{u}}^{\mathbf{T}}\,\mathrm{d}t\right),$$

where $\mathbf{H}$ is as in (4.36). We further consider the ith column of the matrix expression above:

$$\mathbf{0}_{n\times 1} = [-\lambda_i\mathbf{D}_4 + \mathbf{N_4J_4}]\int_0^\infty \mathbf{w}_{\mathbf{L}i}\,\mathrm{d}t - \mathbf{H}\left(\mathbf{w}_{\mathbf{e}i}(0) + \mathbf{B}\int_0^\infty \mathbf{w}_{\mathbf{u}i}\,\mathrm{d}t\right),$$

solving for $\int_0^\infty \mathbf{w}_{\mathbf{L}i}\,\mathrm{d}t$, leads to

$$\int_0^\infty \mathbf{w}_{\mathbf{L}i}\,\mathrm{d}t = [-\lambda_i\mathbf{D}_4 + \mathbf{N_4J_4}]^{-1}\,\mathbf{H}\left(\mathbf{w}_{\mathbf{e}i}(0) + \mathbf{B}\int_0^\infty \mathbf{w}_{\mathbf{u}i}\,\mathrm{d}t\right).$$

Multiplying each column by $\phi_i(x)$ and summing over all i (see Equation 4.3), gives the expression in (4.39). □

Now, we exemplify this result in a small biochemical reaction network.

Example 4.2. *In this example we compute the integral of some species of a biochemical reaction*

network, which represents the activation of the species S_3, in the presence of S_1 and S_2. We model this activation rate by means of a Power-Law reaction rate and consider a turn-over for S_2 and S_3. Furthermore, we assume that S_1 is a heavy molecule or that is attached to a fixed location and hence its diffusion is negligible.

Problem Definition

Consider the following biochemical reaction network

$$S_1 + S_2 \underset{\nwarrow}{\overset{v_1}{\rightleftharpoons}} S_3 \underset{\nwarrow}{\overset{v_2}{\rightleftharpoons}} 0 \underset{\nwarrow}{\overset{v_3}{\rightleftharpoons}} S_2. \tag{4.43}$$

We note that S_1 is the only species which reacts nonlinearly exclusively ($k = 1$), and further assume that this species does not diffuse in the spatial domain $[0,1] = \Omega \subset \mathbb{R}$. Let $\mathbf{c} = (\,[S_1] \;\big|\; [S_2] \quad [S_3]\,)^T$, and $\mathbf{v}(\mathbf{c}) = (v_1 \;\big|\; v_2 \quad v_3)^T$. Then the stoichiometric matrix, Jacobian matrix, reaction rate vector, and diffusion matrix are

$$\mathbf{N} = \left(\begin{array}{c|cc} -1 & 0 & 0 \\ \hline -1 & -1 & 0 \\ 1 & 0 & -1 \end{array}\right), \tag{4.44a}$$

$$\mathbf{v}(\mathbf{c}) = (k_{1f}c_1^{g_1}c_2^{g_2} - k_{1b}c_3 \,|\, k_{2f}c_2 - k_{2b} \quad k_{3f}c_3 - k_{3b})^T, \tag{4.44b}$$

$$\mathbf{J} = \left(\begin{array}{c|cc} k_{1f}g_1\bar{c}_1^{g_1-1}\bar{c}_2^{g_2} & k_{1f}g_2\bar{c}_1^{g_1}\bar{c}_2^{g_2-1} & -k_{1b} \\ \hline 0 & k_{2f} & 0 \\ 0 & 0 & k_{3f} \end{array}\right), \tag{4.44c}$$

$$\mathbf{D} = \left(\begin{array}{c|cc} 0 & 0 & 0 \\ \hline 0 & d_2 & 0 \\ 0 & 0 & d_3 \end{array}\right). \tag{4.44d}$$

The partition of the matrices above, follow the order proposed in (2.30) *and* (4.31)*. From the definitions above, the PDEs that govern the species concentration dynamics are*

$$\begin{aligned} \frac{\partial}{\partial t}c_1 &= \qquad\quad - k_{1f}c_1^{g_1}c_2^{g_2} + k_{1b}c_3 \\ \frac{\partial}{\partial t}c_2 &= d_2\nabla^2 c_2 - k_{1f}c_1^{g_1}c_2^{g_2} + k_{1b}c_3 - k_{2f}c_2 + k_{2b} \\ \frac{\partial}{\partial t}c_3 &= d_3\nabla^2 c_3 + k_{1f}c_1^{g_1}c_2^{g_2} - k_{1b}c_3 - k_{3f}c_3 + k_{3b}. \end{aligned}$$

We consider the initial conditions

$$\begin{pmatrix} c_1(0,x) \\ c_2(0,x) \\ c_3(0,x) \end{pmatrix} = \begin{pmatrix} \bar{c}_1 \cos(\alpha\pi x) + \bar{c}_1 \\ \bar{c}_2 \\ \bar{c}_3 \end{pmatrix} \alpha \in \mathbb{N},$$

and homogeneous Neumann boundary conditions

$$\left.\frac{\partial \mathbf{c}(t,x)}{\partial \mathbf{n}}\right|_{x=\partial\Omega} = 0.$$

This reaction network only has one homogeneous equilibrium point given by

$$\bar{\mathbf{c}} = \begin{pmatrix} \sqrt[g_1]{\frac{k_{1b}k_{3b}}{k_{1f}k_{3f}}\left(\frac{k_{2f}}{k_{2b}}\right)^{g_2}} \\ k_{2b}/k_{2f} \\ k_{3b}/k_{3f} \end{pmatrix}.$$

Integral Calculation

For the reaction network in (4.43)*, we have one species exclusively reacting nonlinearly and only one nonlinear reaction ($k = m_1 = 1$). Moreover, the species S_1 is assumed to have a negligible diffusion constant and all the species comply with homogeneous Neumann boundary conditions. Since the all hypotheses of Proposition 4.4 are fulfilled, we can compute the temporal integral of the species in $\mathbf{e_L}(t,x)$.*

Firstly, a global basis for Ω with homogeneous Neumann boundary conditions that complies with (4.1b) *and* (4.1a) *is given by*

$$\phi_i(x) = k_i \cos(\pi(i-1)x),$$
$$k_i = \begin{cases} 1 & , \quad i = 1 \\ \sqrt{2} & , \quad i \neq 1 \end{cases}.$$

In turn

$$\lambda_i = [\pi(i-1)]^2 \quad \forall\, i \in [1, \vartheta].$$

Moreover, we note that in the deviation coordinates $\mathbf{e} = \mathbf{c} - \bar{\mathbf{c}}$*, the initial conditions are*

$$\begin{pmatrix} e_1(0,x) \\ e_2(0,x) \\ e_3(0,x) \end{pmatrix} = \begin{pmatrix} \bar{c}_1 \cos(\alpha\pi x) \\ 0 \\ 0 \end{pmatrix},$$

and hence, all the columns of the matrix $\mathbf{W_e^T}(0)$ *are zero, except the* $\alpha + 1 - th$ *column, which is*

$$\mathbf{w_e}(0)_{\alpha+1} = \begin{pmatrix} \frac{\bar{c}_1}{\sqrt{2}} & 0 & 0 \end{pmatrix}^T.$$

From the expression above and the definitions in (4.44) *and* (4.36)*, the temporal integral of* $\mathbf{e_L}(t,x)$ *is given by* (4.39)*:*

$$\int_0^\infty \mathbf{e_L}(t,x)\,\mathrm{d}t = \frac{\bar{c}_1}{\sqrt{2}} \begin{pmatrix} \left[(\alpha\pi)^2 d_2 + k_{2f}\right]^{-1} \\ \left[(\alpha\pi)^2 d_3 + k_{3f}\right]^{-1} \end{pmatrix} \cos(\alpha\pi x). \tag{4.45}$$

The left column of Figure 4.4 depicts the simulation of the reaction network in (4.43)*, whereas the right column shows the comparison of the the numerical integration after simulation and the formula in* (4.45)*. It is noteworthy to mention that, despite having a complex dynamical behaviour, the expression for the integral in time of* $e_2(t,x)$ *and* $e_3(t,x)$ *are simple. Note that the magnitude of the elements in* (4.45) *will decrease quadratically in* α*. This observation has motivated the study of the filtering effect of the reaction diffusion systems, submitted as [28].*

4.5 Summary

In this section, we introduced a projection method which may be used to derive an associated ODE set from PDEs describing the dynamics of a reaction-diffusion system. In a class of reaction-diffusion systems, by means of the analytical solution of some coordinates of the PDE system, we were able to reduce the number of equations that require numerical solution. For a specific case study, we note a significant reduction of the computational load. However our methodology is based on the reduction of the number of PDEs to be solved numerically by obtaining the the analytical solution of some species. If the evaluation of this analytical solution represents a computational load larger than the required for obtaining the numerical solution of the original set of equations, our methodology will fail to provide a reduction on the computa-

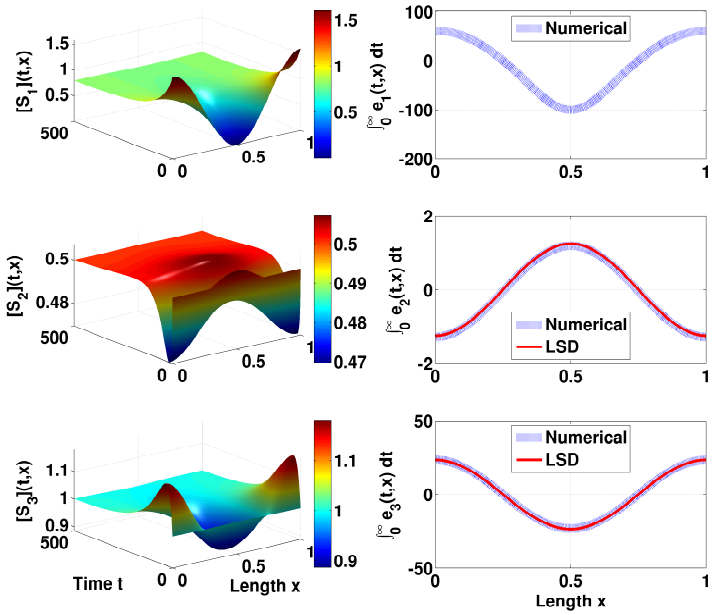

Figure 4.4: *Dynamics of the species in the case study and their integrals in time. The left column shows the spatio-temporal dynamics of the reactions in* (4.43)*. The right column shows the comparison of the analytical calculation (Continuous line) and the numerical integration after simulation (Discontinuous line). The parameters used are* $\{k_{1f}, k_{1b}, k_{2b}, k_{3f}, k_{3b}, k_{3f}, g_1, g_2\} = \{0.01, 0.005, 0.05, 0.025, 0.03, 0.03, 2, 0.35\}, \{d_2, d_3\} = \{0.015, 0.0001\}, \alpha = 2.$

tional load. Hence, there is a subtle trade-off between the evaluation of the analytical solution and the savings its use may represent. This further limits the application of our methodology, yet an better description of the cases in which this methodology may be useful remains to be studied.

Finally, we identified a class of reaction(-diffusion) systems for which the analytical formula of the time-integral of some species, can be obtained as a pure algebraical problem. For the spatio-temporal case, we stress out that the effect of the diffusion in the integrated response is that of a low pass filter. In the following chapter, we will derive some biological conclusions derived from the work presented up to now.

Chapter 5

Application to Selected Biochemical Reaction Networks

Contents

Up to now, we have considered general problems involved in the study of the DEs that describe the dynamics of reaction networks, and illustrated these results in particular examples. However, we haven't been explicit about the implications of this earlier work on the underlying biochemical systems. In this chapter, we close this gap by considering three biochemical pathways.

In this chapter, we present the application of the theoretical results obtained in the previous chapters to selected biochemical pathways. By linking the theoretical results with their biological implication, we achieve one of our main goals in this work: to provide a quantitative description of a particular phenomenon, as an analytical function of the parameters of the system.

In particular, in Section 5.1 we use the results obtained in Example 3.2 to characterise the activation of the Akt/mTOR complex via the insulin-like growth factor receptor, by identifying

biological scenarios that cast this activation in the reaction network (3.33). For a detailed discussion of this pathway, we refer the interested reader to [22], from which this case study has been extracted. In Section 5.2, we use the results derived in Examples 2.2 and 3.1 to characterise the equilibrium set of the caspase-6 mediated core apoptosis pathway, as modelled in [72]. These results have been reported in [23], currently under review. Finally, we present the computation of the integrated response of calcium cues in non-excitable cells.

5.1 Skeletal Muscle Growth

The Insulin-like growth factor (IGF-1) receptor pathway mediates cell growth and survival. Internalisation of insulin cues leads to phosphorylation and activation of the pro-survival kinase Akt and the subsequent activation of the the mammalian target of rapamycin (mTOR), which switches on anabolic processes such as protein or nucleotide production. In turn, it has been suggested that mTOR can phosphorylate and activate Akt [73, 74], thereby establishing a positive feedback loop (Figure 5.1.)

Recent reports suggested the IGF-1 mediated PI3K-/Akt-/mTOR pathway is a regulator of muscle cell growth. Overexpression of active AKT by genetic mutations or pharmacological activation gives rise to an increase in muscle fibre diameter (muscular hypertrophy), while muscle fibre diameter decreased upon inhibition of Akt or mTOR (muscular atrophy) [75, 76, 77]. Trophic factor receptors such as IGF-1 can be randomly and anisotropically distributed along the cell surface [78, 79, 80] and activation of Akt by PI3K has been determined to be localised at the receptors. This suggests that the Akt/mTOR positive feedback loop acts as a signal regenerator [81, 82, 83] in larger cells, so as to maintain a uniform signal progression.

In [22] it was shown how the IGF-1 mediated PI3K-/Akt-/mTOR pathway can be cast in the reaction network (3.33), studied in Example 3.2. There we concluded that, under a constant inactive concentration of the Akt/mTOR complex ($c_1(t,x)$), we observe a localised activation of the Akt/mTOR pool ($c_2(t,x)$). However, the effect of diffusion might assist the signal progression of $c_2(t,x)$. To show this, consider a Gaussian initial condition for the active Akt/mTOR pool, under constant concentrations of the inhibitor and inactive concentration of the Akt/mTOR complex. The spatio-temporal dynamics for $c_2(t,x)$ is given by

$$c_2(t,x) \quad = \quad \frac{k}{\sqrt{\pi(4d_2t+2\sigma^2)}}\exp\left(\alpha t - \frac{(x-\mu)^2}{4d_2t+2\sigma^2}\right), \tag{5.1}$$

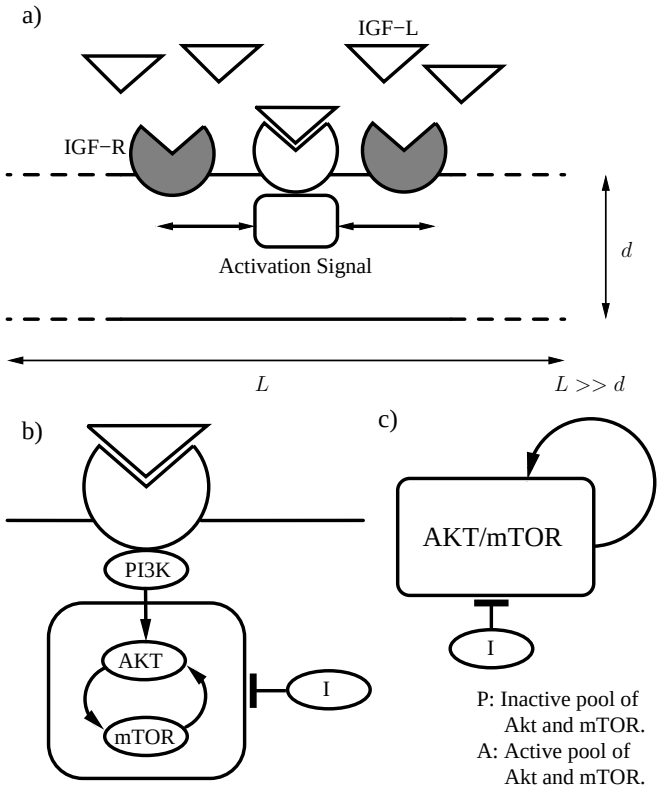

Figure 5.1: *AKT/mTOR pathway activation by IGF stimulation. Panel (**a**) shows an extended cell* $(L >> d)$*, with IGF receptors (IGF-R) that are activated by binding to IGF ligands (IGF-L). Upon binding, the active signal that originates at the receptor propagates through the cell. The diameter* d *of the cell is neglected. Panel (**b**) details how the receptors activation results in PI3 kinase activation and a subsequent positive feedback loop of Akt and mTOR. Moreover, the effect of an inhibitor* I *of such a pathway is considered. Panel (**c**) illustrates the abstraction of Akt and mTOR into one simple node which auto-activates itself as considered in this study. This auto-feedback is assumed to convert inactive versions of Akt/mTOR* (P) *to their respective active forms* (A)*.*

where σ represents the spread of the initial concentration of $c_2(0, x)$, μ the localisation of its maximum and k is the magnitude of the activation. In turn, d is the diffusion constant for the complex.

We depict this progression in Figure 5.2, where we show the effect of the interplay of the diffusion constants and Akt/mTOR inhibitors. To define the region of activation, we use a threshold on the $c_2(t, x)$ concentration. This threshold ($\tilde{c}_2$) might represent a value, which, if exceeded, triggers a downstream physiological event, such as muscular growth. We can find the region that is reached with the signal progression by comparing $\tilde{c}_2$ with (5.1).

$$\tilde{c}_2 \quad \leq \quad \frac{k}{\sqrt{\pi(4d_2t + 2\sigma^2)}} \exp\left(\alpha t - \frac{(x-\mu)^2}{4d_2t + 2\sigma^2}\right).$$

From the equation above, we can obtain the area around the original centre of activation μ where the threshold is exceeded at a certain time t

$$|x-\mu| \quad \leq \quad \sqrt{(4d_2t+2\sigma^2)\left[\alpha t - \frac{1}{2}\ln\left(k^{-2}\tilde{c}_2^2\pi(4d_2t+2\sigma^2)\right)\right]}. \tag{5.2}$$

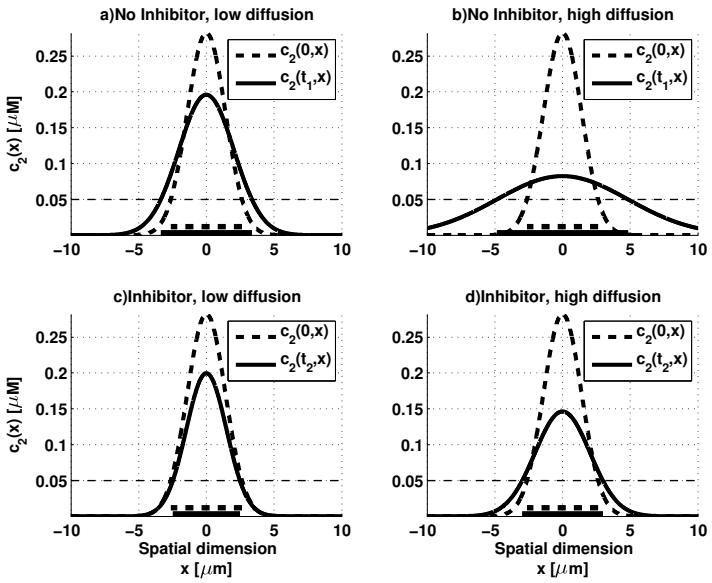

Figure 5.2: *Detecting spatial regions in which a concentration threshold (horizontal dotted line) is exceeded. We consider a Gaussian initial condition (depicted in a dotted line) with $\mu = 0$ and $\sigma^2 = 1.7$. The panel a) shows the behaviour of the active form $c_2(t_1, x)$ in the absence of inhibitor and with low diffusivity (d_l); in turn, b) depicts $c_2(t_1, x)$ without inhibitor, but with a higher diffusion constant (d_h). Accordingly, c) and d) represent $c_2(t_2, x)$ in the presence of inhibitor with low and high diffusion constants, respectively. The times t_1 and t_2, have been chosen close to the time in which the maximal signal propagation is observed. As we can see, an increase in the diffusion constant or the presence of an inhibitor lead to a decrease in the signal's spatial spread. Parameters: $\{k_1, k_2, k_4\} = \{0.04, 0.2, 8.3\}[(\mu M min)^{-1}]$; $\{d_l, d_h\} = \{30, 300\}[\mu m^2/min]$; $\{\sigma^2, \mu\} = \{1.7, 0\}$; $\{\bar{c}_1, \bar{c}_3\} = \{5, 10\}[\mu M]$; $\{t_1, t_2\} = \{0.0357, 0.0035\}[min]$.*

In Figure 5.2, we show the interplay of the magnitude of the diffusion constant and inhibitor with the progression of the signal in the spatial domain. We note that in the absence of inhibitor and high diffusion, the signal spreads in a broader range of the spatial domain (Figure 5.2.a), in contrast to the restrained spatial signal progression in the presence of inhibitor and low diffusion (Figure 5.2.c). In both cases, we have shown that the activation of the Akt/mTOR pool remains localised to the original location of the initial stimulus.

For a detailed derivation of these results and further discussion, we refer the interested reader to [22]. Having looked at an activation of the Akt/mTOR complex, modelled by a simple protein

auto-activation, we now consider a circular protein activation mechanism present in caspase-6 mediated apoptosis.

5.2 Apoptosis

Apotosis is an intracellular process that leads to cell destruction by means of the activation of caspase-3 [84, 85]. This process can be triggered by extracellular signals, through the activation of the Fas receptor [86], or by means of mitochondrial outer membrane permeabilization [87, 88, 89]. Moreover, many of the proteins involved in the apoptotic pathway are also related with non-apoptotic processes [90]. This along with the fatal outcome of this process, suggests that a tight regulation of the process is crucial for the normal cellular life cycle.

In general, apoptosis models highlight the activation of caspase-3 by its interaction with caspase-8/-9. However, there is evidence that in some cells the final caspase-3 activation may be mediated by caspase-6. In this loop, caspase-3 cleaves and activates caspase-6, while caspase-6 activates caspase-8 and caspase-8 closes the feedback by cleaving caspase-3 [91, 92] (Figure 5.3A). Moreover, caspase-6 has been shown to be expressed at lower levels compared to both other caspases [72, 93], suggesting the possibility it is a bottleneck in the loop.

This three-tier positive feedback loop, as modelled in [72], can be represented as the reaction network (2.15), analysed in Examples 2.2 and 3.1, when $p = 3$. In Example 2.2 we showed that this systems has two steady states. We denoted them as *off steady state*, when no activated caspases are present, and *on steady state*, otherwise. In addition, Example 3.1 derived conditions to determine the stability of each steady state.

As we mentioned above, caspase-6 might be a mediator of the final activation of the effector caspase. We therefore envisioned that small variations in such constants heavily affect the existence and the stability properties of the *on steady state* and the concentration of active proteins. In particular, we assumed that any bottleneck in this loop (such as a weak feedback link or a protein expressed at low levels) would significantly determine whether or not the loop would lead to an activation of the entire protein chain and how extensive the protein activation would be. To this end, we focused on apoptosis and illustrated how a three-tier feedback loop can act as a modulator of the magnitude of the caspase-3 activation. During apoptosis execution, a three-tier positive feedback has been shown to occur downstream to caspase-3 activation [72].

Hence, in the work under review [23], we investigated how fine tuning of the caspase-6 synthesis rate (k_{3b}^2), and therefore a small change in caspase-6 expression levels, influenced the

steady state expression levels of the major effector in this loop, the active caspase-3. We modelled this caspase-3/6/8 feedback as described previously [72] taking all kinetic constants from their supplementary data. We then varied the caspase-6 synthesis rate and studied the expression of active caspase-3 at steady state (Figure 5.3A; dashed arrow for variation of caspase-6; solid arrow for output of caspase-3). To calculate these equilibria we exploited our analytical formula (2.27) leading to the following expression for steady state levels of active caspase-3,

$$\bar{C}_{3a} = \frac{1.7843 \times 10^{25} k_{3b}^2 - 1.4925 \times 10^{15}}{2.2122 \times 10^{26} k_{3b}^2 + 4.8218}.$$

Figure 5.3C shows the steady state concentration of active caspase-3 (C_{3a}) under variation of the production rate of k_{3b}^2, depicted in Figure 5.3B. In the first case (panels B.1 and C.1), relatively small variation of the caspase-6 production rate k_{3b}^2 led to a pronounced change in the amount of active caspase-3 (at steady state) C_{3a} (Figure 5.3C.1). When the caspase-6 production rate (k_{3b}^2) was varied within a different, and in absolute terms even larger, concentration range Figure 5.3B.2, only a small effect in the expression levels of casapase-3 was observed. Taken together, these results suggest that within certain parameter ranges, an intermediary node in a feedback such as caspase-6 may act as an amplifier, similar to a molecular transistor. We finally remark that local stability condition for the *off steady state* is given by (see Proposition 3.1)

$$k_{3b}^2 < 8.36 \times 10^{-11} [\mu M/min].$$

When this threshold is exceeded, the *on steady state* is positive. In order to determine the stability of the *on steady state*, we remark that $k_2^i > k_{3f}^i$, as can be seen in the supplemental material of [72]. Hence, we may use the criterion in (3.31) for all i, to determine the stability of the *on steady state*. As a function of k_{3b}^2, (3.31) becomes

$$k_{3b}^2 > \frac{1}{k_{3b}^1 k_{3b}^3} \prod_{i=1}^{3} \frac{\left(k_2^i\right)^3}{k_1^i k_{3f}^i} = 9.0495 \times 10^{-10} [\mu M/min]. \tag{5.3}$$

As confirmed by the simulations in the panel Figure 5.3C, the variation of k_{3b}^2 proposed in panel Figure 5.3B, in agreement with the threshold in (5.3), yield stable *on steady states*.

Extracellular signals or signals coming from the mitochondria are responsible for the apoptosis onset. Especially, for the later case, cytosolic calcium is the cue that promotes the mitochondrial release of apoptotic promoters. In the following section, we study one of the characteristics of calcium cues that has been implicated in the triggering of diverse physiological processes: the

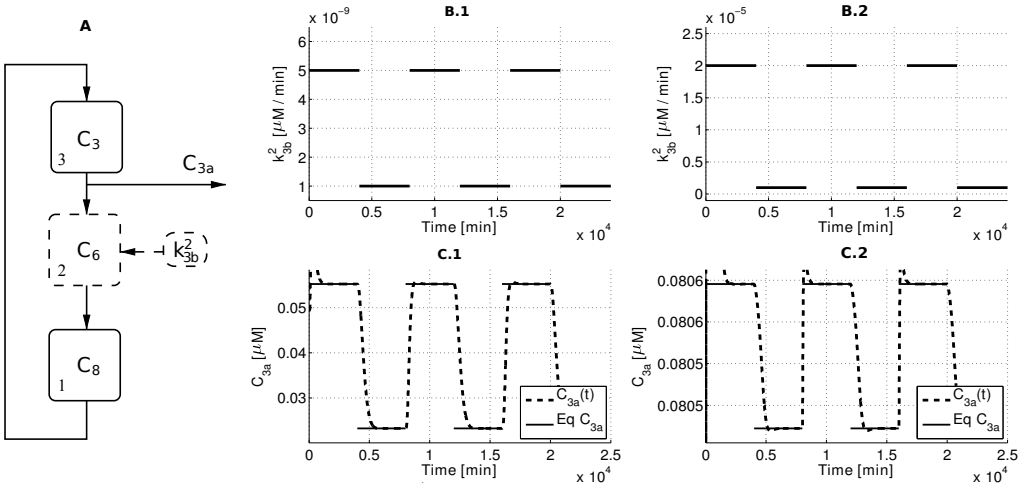

Figure 5.3: *Dynamical response of activate caspase-3 (C_{3a}) under variation of the synthesis of caspase-6 (k^2_{3b}), mimicking the switching behaviour of a transistor. The rest of the parameters were taken from the supplemental material of [72]. In panel **A** caspase-6 (C_6) activates caspase-8 (C_8), which further activates caspase-3 (C_3); to complete the loop, caspase-3 activates caspase-6. The detailed mechanism of activation for all panels is described in* (2.15)*. The sequence of activation (superindex i in* (2.15)*) is represented by the number adjacent to each box. The upper panels **B** show two variation regimes of synthesis rate of inactive caspase-6 k^2_{3b}. The lower panels **C** depict the concentration over time of C_{3a} in response to each parameter variation. The dashed line depicts the concentration of C_{3a} as a function of time, whereas the solid line shows the equilibrium point during variation of k^2_{3b}. Despite the absolute variation of the the parameter k^2_{3b} was lower in **B.1** than in **B.2**, the effect of this variation was much higher in the corresponding activation of caspase-3 C_{3a} **C.1** than in **C.2**. (Please, note the different scales in **B.1** and **B.2**). As consequence, in certain ranges, a small variation of k^2_{3b} yields a severe effect on the location of the equilibrium point of C_{3a}, similar to a 'molecular transistor'. Hence, a fine tuning of the synthesis of inactive caspase-6 is crucial for pronounced activation of caspase-3.*

time-integral of cytosolic calcium.

5.3 Calcium Homeostasis

Calcium ions (Ca^{2+}) are ubiquitous secondary messengers governing a large number of cellular functions, such as cell growth and differentiation, membrane excitability, and cell death [94]. In general, calcium-triggered-processes depend on the continuous presence of elevated cytosolic calcium and others just require certain calcium load to trigger downstream signals [95]. These two perspectives, are the principles of two main hypotheses suggesting how Ca^{2+} might trigger downstream reactions leading to events such as apoptosis, namely: "Calcium Load Hypothesis" and "Source-specificity Hypothesis" [96]. The former view suggests that degeneration is simply a function of the quantity of Ca^{2+} entering the cell, whereas in the latter hypothesis, Ca^{2+}-dependent processes are regulated separately through distinct signalling pathways linked

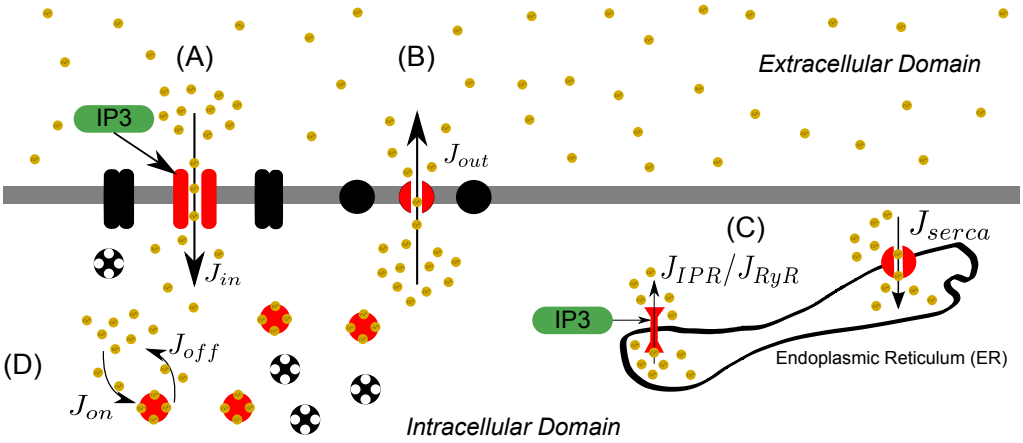

Figure 5.4: *Main Ca^{2+} fluxes in a non-excitable cell. Panel (**A**) depicts the IP3-mediated influx of Ca^{2+} to the intracellular domain (J_{in}); in turn, panel (**B**) shows the efflux of calcium due to membrane pumps (J_{out}), triggered by the presence of Na^{+} (not depicted); whereas Panel (**C**) shows the fluxes of calcium to/from the Endoplasmic or Sarcoplasmic Reticulum (J_{serca} and J_{IPR} or J_{RyR}). Finally, the Ca^{2+} buffering (J_{on}) and its release from the buffers (J_{off}) are shown in Panel (**D**).*

to specific routes of Ca^{2+} influx.

By building up a spatio-temporal model that accounts for the main Ca^{2+} fluxes, depicted in Figure 5.4, we focus on the computation of the time-integral of $[Ca^{2+}]_c$. Hence, analysing how Ca^{2+} signalling may trigger downstream processes in specific regions of the spatial domain. We focus on a unidimensional spatial domain, representing a long, thin cell. In this context, we consider the interplay of the cytosolic calcium (c_c), calcium in storage (c_s) and calcium buffers (b). We model this interaction with the following PDE

$$\frac{\partial}{\partial t}c_s = \gamma\left(-k_1(T+T_0)(c_s-c_c) + V_3\frac{c_c^2}{k_4^2+c_c^2}\right) \tag{5.4a}$$

$$\frac{\partial}{\partial t}c_c = d\nabla^2 c_c(x) - \gamma^{-1}\frac{\partial}{\partial t}c_s + \frac{\partial}{\partial t}b + \alpha c_c + \beta \tag{5.4b}$$

$$\frac{\partial}{\partial t}b = -k_2 c_c b + k_{m2}(b_{tot}-b), \tag{5.4c}$$

subject to Neumann boundary conditions for all the species:

$$\left[\frac{\partial c_s(x,t)}{\partial x}\right]_{x=0,L} = \left[\frac{\partial c_c(x,t)}{\partial x}\right]_{x=0,L} = \left[\frac{\partial b(x,t)}{\partial x}\right]_{x=0,L} = 0, \quad \forall t \in [0,\infty). \tag{5.4d}$$

Where we have defined

$$\alpha = \frac{\rho}{A}\left(k_5\left(T + T_0\right) + k_e\right) \tag{5.5a}$$

$$\beta = \frac{\rho}{A}\left(k_5\left(T + T_0\right)c_{\text{out}} + k_p\right). \tag{5.5b}$$

We have motivated the model (5.4) by the model in [97]. The definition of the parameters can be found (Table 1), repeated here, for the sake of readability. However, we have extended the model

Table 5.1: *Parameters definition*

Parameter	Definition
k_1	Rate of calcium release form the store
k_2	Rate of calcium association with the buffer
k_{m2}	Rate of calcium dissociation from the buffer
V_3	Maximum rate of calcium pumping into the store
k_4	Dissociation constant of the store calcium pump
c_{out}	Extracellular calcium concentration
b_{tot}	Total concentration of the calcium buffer
T_0	Basal fractional activity of the channels in the store
T	Fractional activity of the channels in the store

in [97] to include the diffusion of the cytosolic calcium. By considering the spatial dynamics, we also have to consider geometrical parameters of the spatial domain, namely L, ρ, A and γ represent the length, circumference, cross-sectional area, and the ratio of cytoplasmic to ER volumes, respectively.

The model in (5.4) has only one homogeneous fixed point, whose c_c coordinate is

$$\bar{c}_c = \frac{\beta}{\alpha}$$

Now, in order to compute the time-integral of the cytosolic calcium referred to its equilibrium concentration, we define the deviation coordinate $e_c = c_c - \bar{c}_c$, and note that the linear combination $e_c + \gamma^{-1}e_e - e_b$ leads to a linear PDE:

$$\frac{\partial}{\partial t}e_c + \gamma^{-1}\frac{\partial}{\partial t}e_e - \frac{\partial}{\partial t}e_b = d\nabla^2 e_c - \alpha e_c + g(t,x) \tag{5.6a}$$

$$\frac{\partial g}{\partial x} = \frac{\partial e_c}{\partial x} = 0 \qquad \text{at } x = 0 \text{ and } x = L. \tag{5.6b}$$

Here, we account for a perturbation $g(t,x)$ with a finite integral, which might arise from a

transitory perturbation of the parameters. Integrating (5.6a) over time, we have

$$e_c(0,x) + \gamma^{-1} e_e(0,x) - e_b(0,x) = \int_0^\infty \left(d\nabla^2 - \alpha\right) e_c(t,x)\,\mathrm{d}t + \int_0^\infty g(t,x)\,\mathrm{d}t. \qquad (5.7)$$

To find an analytical solution for the *[Ca^{2+}]$_c$ cumulative response*, we exploit the LSD method. This allows us to span each field by the same spatial basis functions which are eigenfunctions of the diffusion operator. We represent each function in terms of time-dependent modes $m_i(t)$ and spatial-dependent functions $\phi_i(x)$

$$e_j(t,x) \equiv \sum_{i=0}^{\infty} \phi_i(x) m_i^j(t) \quad \text{for} \quad j = \{c,e,b\}$$
$$g(t,x) \equiv \sum_{i=0}^{\infty} \phi_i(x) m_i^g(t).$$

Using the properties of the basis elements (4.1), we can calculate the time-integral of the modes associated with e_c:

$$\int_0^\infty m_i^c(t)\,\mathrm{d}t = \frac{m_i^c(0) + \gamma^{-1} m_i^e(0) - m_i^b(0) + \int_0^\infty m_i^g(t)\,\mathrm{d}t}{d\lambda_i + \alpha}.$$

Hence the *[Ca^{2+}]$_c$ cumulative response* is

$$\int_0^\infty e_c\,\mathrm{d}t = \sum_{i=0}^{\infty} \phi_i(x) \left(\frac{m_i^c(0) + \gamma^{-1} m_i^e(0) - m_i^b(0) + \int_0^\infty m_i^g(t)\,\mathrm{d}t}{d\lambda_i + \alpha} \right). \qquad (5.8)$$

In the following, we will analytically derive the *[Ca^{2+}]$_c$ cumulative response* under different scenarios. In addition we validate our results numerically by calculating the integrals in two steps: *i)* simulating the PDE set (5.4) in Matlab using the function *pdepe* and *ii)* performing a trapezoidal numerical integration via the function *trapz*.

Although the numerical integral of the simulation will yield the spatial distribution for the *[Ca^{2+}]$_c$ cumulative response*, it is difficult, if not impossible, to identify the dependence of the processes involved in the integrated response. That is to say, under different conditions for simulation, we would not be able to forecast the behaviour of *[Ca^{2+}]$_c$ cumulative response*. To overcome this difficulty, our analytical formulas for this integral will provide this missing link between the initial and boundary conditions and *[Ca^{2+}]$_c$ cumulative response*. In addition, our theoretical approach will overcome usual problems that arise from the the numerical solution of PDEs, such as accuracy errors during the simulation and numerical integration and

computational load. Foremost, for our analytical approach we do not need to have available the description of some fluxes such as the Ca^{2+} turnover due to the buffering and the Ca^{2+} cycling to/from the extracellular domain and Endoplasmic Reticulum.

In the forthcoming section, we derive analytical formulas for the *$[Ca^{2+}]_c$ cumulative response* in two different scenarios: i) localised insult of cytosolic Ca^{2+}; and ii) alterations of the membrane receptor activation, due to a perturbation of IP_3.

- **Effect of immobile Ca^{2+} buffers**

  Proteins buffer Ca^{2+} faster than the ion is sequestrated by the endoplasmatic reticulum. The former one scatters elevated Ca^{2+} along the spatial domains, whereas the later one prolong the duration of the Ca^{2+} signal in a particular location [98], resulting in what it is usually called a biphasic response. Buffering proteins are usually categorised depending on their capacity to diffuse. Here we will focus in the immobile buffers and their effect in $[Ca^{2+}]_c$ since 75% of total cytoplasmic buffers cannot diffuse [98].

  Immobile buffers, also named stationary buffers, tend to immobilise Ca^{2+} in localised areas of cells. The main purpose could be to confine Ca^{2+} and avoid triggering unwanted signalling routes [99]. In fact, the influence of this kind of buffers is particularly relevant to regulation of the redistribution of Ca^{2+} entering the cell by ion channels via diffusion [100]. We study this phenomenon by assessing the response of an initial condition of $[Ca^{2+}]_c$ representing entry of Ca^{2+} through ion channels membrane. We model this initial profile as a square pulse centred in the spatial domain, whose width is 2ε and amplitude ψ. This profile can be mathematically expressed as

$$c_c(0,x) = \bar{c}_c + \psi\left[h\left(x-\left(\tfrac{L}{2}-\varepsilon\right)\right) - h\left(x-\left(\tfrac{L}{2}+\varepsilon\right)\right)\right]. \tag{5.9}$$

  We consider the global basis

$$\lambda_i = \left[(i-1)\frac{\pi}{L}\right]^2 \tag{5.10a}$$

$$\phi_i(x) = k_i \frac{1}{\sqrt{L}} \cos\left((i-1)\frac{\pi}{L}x\right) \quad \text{where} \quad k_i = \begin{cases} 1 & \text{if } i=1 \\ \sqrt{2} & \text{if } i \neq 1 \end{cases}. \tag{5.10b}$$

Hence, the modes $m_i^c(0)$ for this initial profile, referred to the basis in (5.10), are given by

$$\begin{aligned} m_i^c(0) &= \int_{\frac{L}{2}-\varepsilon}^{\frac{L}{2}+\varepsilon} \frac{\psi k_i}{\sqrt{L}} \cos\left(\frac{i-1}{L}\pi x\right) \mathrm{d}x \\ &= 2\frac{\psi\varepsilon k_i}{\sqrt{L}} (-1)^{i-1} \operatorname{sinc}\left(2\pi(i-1)\frac{\varepsilon}{L}\right). \end{aligned}$$

Here $\operatorname{sinc}(x) := \sin(x)/x$. Moreover due to the symmetry of the initial condition, we only consider the $2(i-1)th$ elements of the basis and eigenvalues in (5.10). Hence, the *[Ca^{2+}]$_c$ cumulative response* in (5.8), due to the initial condition in (5.9) becomes

$$\int_0^\infty e_c \,\mathrm{d}t = 2\frac{\psi\varepsilon}{L} \sum_{i=1}^{\infty} (-1)^{i-1} k_i^2 \frac{\operatorname{sinc}\left(2\pi(i-1)\frac{\varepsilon}{L}\right)}{d\left(2\pi(i-1)\frac{1}{L}\right)^2 + \alpha} \cos\left(2\pi(i-1)\frac{1}{L}x\right). \quad (5.11)$$

We note that this integrated response is directly proportional to the ratio $2\psi\varepsilon/L$, which is the area under the initial condition described by (5.9) referred to the steady state $\bar{c}_c$, divided by the spatial length. This can be interpreted as the density of the administrated cytosolic Ca^{2+} to the spatial domain at time $t = 0$.

In Figure 5.5, we depict the spatio-temporal and integrated response of for all the species. The left panels **(a)** show the response in time and space of the species in the model (5.4). Whereas the right panels **(b)** show the cumulative response of all the species. Of special interest are the middle panels, which compare the numerically *[Ca^{2+}]$_c$ cumulative response* (dotted lines) with the analytical expression in (5.11) (continuous line). The difference of the *[Ca^{2+}]$_c$ cumulative response*, between the different methods of calculations, is due to the stiffness of the differential equation solved. From our computational experiments, we noted that refining the temporal mesh for solving the PDE, reduces the gap between the solution methods at the price of increasing the computational load. We note, however, that our methodology is analytical, hence avoiding the numerical errors that arise from the numerical solution.

Moreover, Figure 5.5 shows that signalling progression of Ca^{2+} is confined to a vicinity of the original location of the initiator signal. And, consequently, every physiological event triggered by this initial Ca^{2+} insult will be activated close to the original location of the initial condition. This observation supports the observation that Ca^{2+} acts locally, having multiple spatially segregated Ca^{2+} subdomains [102, Ch.2]. This approach can be used to determine the spatial extension of this Ca^{2+} insult.

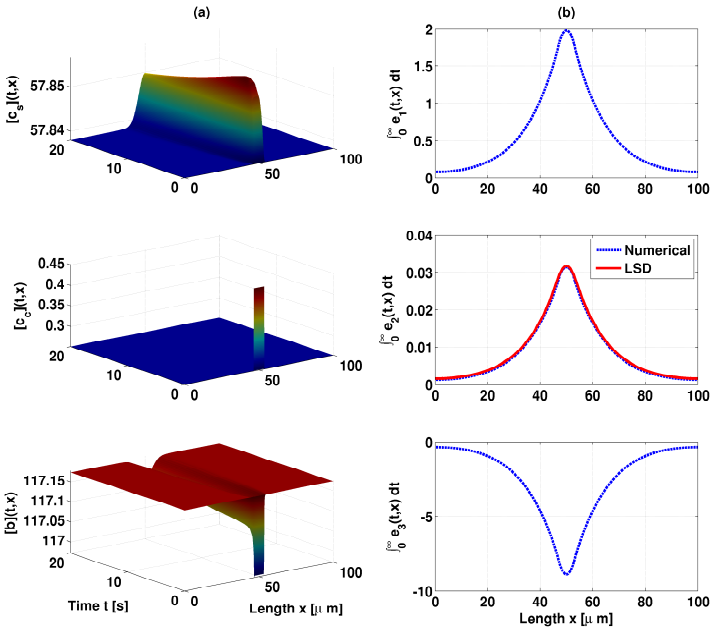

Figure 5.5: *Spatiotemporal and integrated responses in response to a localised initial $[Ca^{2+}]_c$ insult. The panels **(a)** represent, top to down, the concentrations of Ca^{2+} in store $[c_s]$, Ca^{2+} in the cytosol $[c_c]$ and buffers $[b]$. With the same organisation, the panels **(b)** show the cumulative response of the concentrations. The middle panel (b) compares the result of the numerical integration (computed for $2500[s]$) and the analytic expression for $[Ca^{2+}]_c$ cumulative response in* (5.11)*. The kinetic parameters are taken from [97]; $\{k_e, k_p\} = \{1.4953, 0.1396\}$, in addition, $d = 250[\mu m^2/s]$, $\{r, \rho, A\} = \{2[\mu m], r\pi, \pi r^2\}$, $\gamma = 0.167$ [101], $\{L, \varepsilon\} = \{100, 3.5\}[\mu m]$, $\psi = 0.2[\mu M]$ and $n = 15$.*

- **Biphasic response: IP_3 perturbations**

  In nonexcitable cells, Ca^{2+} channels mainly rely on local $[Ca^{2+}]_c$ rises in response to ligand binding and IP_3-mediated mobilisation of $[Ca^{2+}]_c$ from intracellular stores [99]. IP_3 acts as an antagonist of Ca^{2+} channels, hence leading to a momentary deactivation of these channels, both in the membrane and in the endoplasmic reticulum. We consider the activation of the Ca^{2+} channels, represented as T in (5.4) suddenly changing value at $t = \tau_1[s]$ from 0 to η and remains in this new value for $\tau_2[s]$. Thereafter, it returns to its original value $T(t) = 0$. We model the profile for $T(t)$ as a combination of step functions of the form

$$T(t) = \eta \left[h(t - \tau_1) - h(t - (\tau_1 + \tau_2)) \right], \tag{5.12}$$

  here, η is the amplitude of the pulse. This perturbation will lead to three different phases of the spatio-temporal response of the system:

1. the system will approach to its steady state with $T(t) = 0$; once reached the equilibrium,

2. the sudden change of the value of $T(t)$ shifts the systems to a new steady state concentrations. Once the perturbation has vanished,

3. the concentrations return to the original equilibrium.

These three phases are depicted in Figure 5.6(b), where, for illustration purposes, we consider an hypothetical response for $[\text{Ca}^{2+}]_c$, due to the variation for $T(t)$ proposed in (5.12), as shown in Figure 5.6.

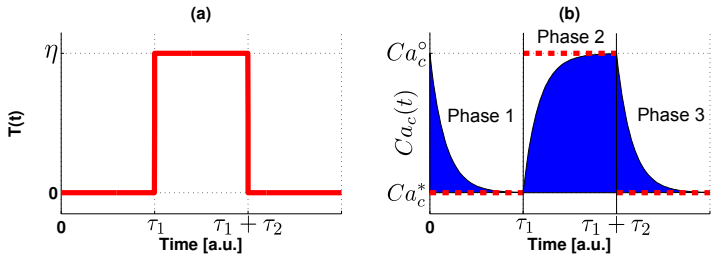

Figure 5.6: *Hypothetical response of cytosolic Ca^{2+}, due to the variation of the Ca^{2+} channels activity. Panel **(a)** depicts $T(t)$, whereas panel **(b)** shows the trajectories driven by temporal profile of $T(t)$. We distinguish three different phases of this response: **1)** A transitory response, due to the initial conditions. **2)** In the time interval $[\tau_1, \tau_1 + \tau_2)$, the equilibrium point is shifted to Ca_c°; consequently, $[Ca^{2+}]_c$ reaches this level. Finally, **3)** when $T(t)$ returns to its basal value, $[Ca^{2+}]_c$ reaches the original equilibrium point (Ca_c^*).*

We also consider that τ_1 and τ_2 are large enough, to allow the concentrations to reach the steady state in each phase. Consequently, the total *$[Ca^{2+}]_c$ cumulative response* is obtained by the addition of the areas under the surfaces for the three phases:

$$\int_0^\infty (Ca_c(t,x) - Ca_c^*)\ \mathrm{d}t = \text{Area}_1 + \text{Area}_2 + \text{Area}_3. \tag{5.13}$$

The temporal profile for $T(t)$ in (5.12) affects α and β in (5.5), which become

$$\alpha(t) = \frac{\rho}{A}\left(k_5\left(T(t) + T_0\right) + k_e\right) \tag{5.14}$$

$$\beta(t) = \frac{\rho}{A}\left(k_5\left(T(t) + T_0\right) c_{\text{out}} + k_p\right). \tag{5.15}$$

Since the equilibrium point for $[\text{Ca}^{2+}]_c$ is the ratio β/α, in each phase of the response of the system *all* the concentrations in equilibrium are modified. In the expression (5.13), we

have referred the integral to the steady state Ca_c^*, which is given by

$$Ca_c^* = \frac{k_5 T_0 c_{\text{out}} + k_p}{k_5 T_0 + k_e}. \tag{5.16}$$

However, during the Phase 2, the steady state is shifted due to the variation of parameters; in the following, we will denote the equilibrium point in Phase 2 as

$$Ca_c^\circ = \frac{k_5 \left(\eta + T_0\right) c_{\text{out}} + k_p}{k_5 \left(\eta + T_0\right) + k_e}. \tag{5.17}$$

We will avail of the expressions for the $[\text{Ca}^{2+}]_c$ steady state above, in the computation of the *cumulative response* for each one of the phases.

- Phase 1: $t \in [0, \tau_1)$. During this interval, we consider any initial condition and influx of species. Hence, the *$[Ca^{2+}]_c$ cumulative response* is given by (5.8).

- Phase 2: $t \in [\tau_1, \tau_1 + \tau_2)$. In this phase, we assume that there are no external influxes. Moreover, the initial conditions in this phase, are the steady states $\mathbf{c}^*$, referred to the equilibrium point $\mathbf{c}^\circ$. That is to say

  $$\mathbf{e}(\tau_1) = \mathbf{c}^* - \mathbf{c}^\circ, \tag{5.18}$$

  which is a vector whose coordinates are constants. By letting

  $$\varsigma = \gamma^{-1} \left(c_s^* - c_s^\circ\right) + \left(c_c^* - c_c^\circ\right) - \left(b^* - b^\circ\right), \tag{5.19}$$

  and from (5.8), the integral of $[\text{Ca}^{2+}]_c$, referred to Ca° is

  $$\int_{\tau_1}^{\tau_1+\tau_2} \left(Ca_c(t) - Ca_c^\circ\right) \mathrm{d}t = \frac{\varsigma}{\alpha(t)\sqrt{L}} \tag{5.20}$$

  Although the expression above provides the integral for the duration in time of this phase, we require to measure it from the steady state concentration Ca^*. Hence, we require to compute the complement of the area during this phase, as depicted in the Phase 2 of Figure 5.6.

  $$\text{Area}_2 = \int_{\tau_1}^{\tau_1+\tau_2} \left(Ca_c(t) - Ca_c^\circ\right) \mathrm{d}t - \tau_2 \left(Ca_c^* - Ca_c^\circ\right). \tag{5.21}$$

From the definitions in (5.16) and (5.17), we have

$$Ca_c^* - Ca_c^\circ = k_5\eta\frac{k_p - k_e c_{out}}{(k_5T_0 + k_e)\,(k_5\,(\eta + T_0) + k_e)}. \tag{5.22}$$

Thus, by substituting the expression above and (5.20) into (5.21), the *cumulative response* during this time interval is

$$\text{Area}_2 = \frac{\varsigma}{\sqrt{L}\frac{\rho}{A}\,(k_5\,(\eta + T_0) + k_e)} + \tau_2 k_5\eta\frac{k_e c_{out} - k_p}{(k_5T_0 + k_e)\,(k_5\,(\eta + T_0) + k_e)} \tag{5.23}$$

– Phase 3: $t \in [\tau_1 + \tau_2, \infty)$. Analogously to the previous phase, during this time interval, the initial condition is $\mathbf{e}\,(\tau_1 + \tau_2) = -\mathbf{e}(\tau_1)$, where $\mathbf{e}(\tau_1)$ has been defined in (5.18). Moreover, from (5.8), the integrated response is

$$\text{Area}_3 = -\frac{\varsigma}{\sqrt{L}\frac{\rho}{A}\,(k_5T_0 + k_e)}. \tag{5.24}$$

Here ς, has been defined in (5.19). Now, substituting the definition of the areas in eqns. (5.23) and (5.24) into (5.13), yields

$$\int_0^\infty e_c\,\mathrm{d}t = \text{Area}_1 + k_5\eta\frac{\sqrt{L}\frac{\rho}{A}\tau_2\,(k_e c_{\text{out}} - k_p) - \varsigma}{\sqrt{L}\frac{\rho}{A}\,(k_5T_0 + k_e)\,(k_5\,(\eta + T_0) + k_e)} \tag{5.25}$$

For simplicity, we assume that the initial conditions are those in equilibrium, therefore, $\text{Area}_1 = 0$. Hence, the *[Ca^{2+}]$_c$ cumulative response* is directly proportional to the product of the perturbation amplitude (η) and the rate of Ca^{2+} influx from the extracellular domain (k_5). In addition, the duration of the perturbation τ_2, plays a major role in the *[Ca^{2+}]$_c$ cumulative response*.

With the theoretical methodology reviewed in Chapter 4.4, we derived analytical expressions that represent the integrated response of the $[Ca^{2+}]_c$, as a response to an initial Ca^{2+} insult, and perturbation of IP_3. From this theoretical study, we conclude that

1. the downstream signalling remains localised to the original location of the Ca^{2+} insult. Therefore, this model gives spatially selective triggering of downstream phenomena.

2. Moreover, the effect of a step variation of IP_3 on the time-integral of $[Ca^{2+}]_c$ depends mainly on the duration of the perturbation.

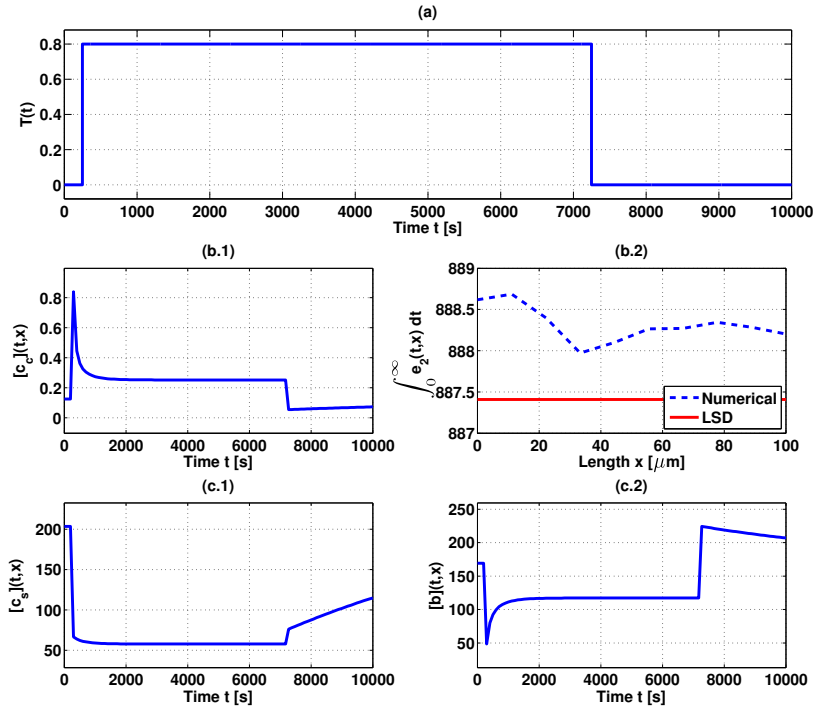

Figure 5.7: *$[Ca^{2+}]_c$ cumulative response, under the presence of IP3. Panel* ***(a)*** *shows the temporal profile for the variation of the fractional activity of Ca^{2+} channels ($T(t)$). In turn, Panel* ***(b.1)*** *shows the response in time for $[Ca^{2+}]_c$, whereas Panel* ***(b.2)*** *depicts $[Ca^{2+}]_c$ cumulative response as computed by the analytical formula in* (5.25) *and via numerical integration (computed for* $132000[s]$*). Finally, Panels* ***(c.1,2)*** *show the concentration of Ca^{2+} in store and the concentration of the buffer, respectively. The parameters for simulation are given in Figure 5.5 and $T = 0$, $\eta = 0.8$, $\{\tau_1, \tau_2\} = \{250, 7000\}[s]$.*

In addition we show in Figure 5.7 the *$[Ca^{2+}]_c$ cumulative response*, when driven by variations of extracellular IP3. With the biological interpretations of the results derived along the previous chapters, we have completed the study of the biological problems that motivated these mathematical formulations. Hence we do not only provide some new mathematical results such as *i)* the analytical derivation of the equilibrium set of the ODE that describes the concentrations of a circular protein activation; *ii)* as well as characterising its stability; *iii)* also, we identified a class of reaction networks for which their integrated response can be described analytically. Additionally we aid to shed some light in the understanding the species' interplay that compose the reaction network under study. In the following chapter, we summarise the contents derived up to now, and suggest some future work directions.

Chapter 6

Conclusions and Future Work

In this work, we presented a set of mathematical problems related to the study of the differential equations that model the dynamics of biochemical reaction (and reaction-diffusion) networks. In particular, we analysed the equilibrium set of a class of positive feedback reaction loops (Example 2.2) and characterised their local stability (Example 3.1). We extended these stability results to reaction-diffusion networks, under some conditions on the diffusion constants (Example 3.3). The results obtained in these examples were used to study the core mechanism of the apoptosis pathway in Section 5.2. These analyses together with computational results suggest that the synthesis rate of caspase-6 acts a bottleneck in the final activation of the effector casapase.

In Section 5.1, we analysed the activation of the Akt/mTOR complex under some biological scenarios, supported by the results derived in Example 3.2. Using earlier derivations of the analytical solution of the concentrations in space and time we were able to quantify several properties of the system such as the filtering of spatial fluctuations in the initial conditions. One key implication of this analysis is the suggestion that the final activation of the Akt/mTOR complex remains localised to the vicinity of the initial extracellular stimulation, for example, by insulin. Therefore, this analysis suggests that in the scenario studied, external stimulation needs to be distributed to have the desired spatially continuous promotion of skeletal muscular growth.

Lastly, we addressed the analytical computation of selected species time-integral in Section 4.4, where we identified a class of reaction-diffusion networks for which the time-integral of some of the concentrations can be obtained as a pure algebraical problem. The analytical expression we obtain is, in general, a sum of terms that typically depend on the species degradation rate along with geometric characteristics of the spatial domain. We used this approach

to study the progression of cytosolic calcium in nonexcitable cells (Section 5.3). In this case, we concluded that the integrated response of cytosolic calcium remains localised to the original location, due to the immobile calcium buffers.

We addressed all these problems with an analytical approach. This perspective allowed us to obtain formulas that describe particular characteristics of the reaction-diffusion network as a function of the systems parameters, thereby linking the processes in this reaction network with their role in the dynamics of the species concentrations. However, this analytical treatment is quickly hindered as the size of the reaction network increases. For instance, in Example 3.2 we derived analytical solutions for a reaction-diffusion system only when we derived biological-motivated scenarios that cast the nonlinear PDEs as one linear PDE. In general, to tackle these limitations, a common approach is to analyse the numerical solutions of the reaction-diffusion network. Nevertheless, form this approach, it becomes unclear which is the relationship between cause and effect, due to the nonlinear nature of these biochemical processes.

Hence, we foresee that identifying classes of biochemical reaction networks, whose underlying nonlinearities are tractable, will assist a deeper understanding of such biochemical processes. In this light, we finalise this work by suggesting some specific problems for further analysis.

6.1 Future Work

In Example 3.1, we used the Small Gain Theorem to characterise the stability of the interconnection of two dynamical systems. Although we considered only linear systems, the Small Gain Theorem can also deal with nonlinear systems, provided the nonlinear gains of the systems are available. In the forthcoming section, we pose the problem of analysing the stability of a reaction network, when is expressed as the interconnection of a linear and nonlinear systems.

6.1.1 Stability of Classes of Reaction Networks

In Chapter 2, we introduced a linear transformation of the state $\mathbf{T}$ in (2.34), to express the dynamical system that arises from a reaction network as the interconnection of a linear and nonlinear systems. Our goal there, was the computation of the equilibrium set, by a reduced number of algebraic relationships. Here, however, we will consider that the equilibrium set is already characterised, and the dynamical system is expressed in deviation coordinates, as defined

in (2.52):

$$\frac{\mathrm{d}}{\mathrm{d}t}\mathbf{e} = \mathbf{A}\mathbf{e} + \mathbf{N}_{\mathrm{NL}}\mathbf{g}(\mathbf{e}) + \mathbf{B}\mathbf{u}. \tag{6.1}$$

We focus on the ODE problem by neglecting the species diffusion. By applying the state transformation in (2.34), the model in (6.1), becomes

$$\dot{\mathbf{z}}_{\mathbf{1}} = \mathbf{A}_{\mathbf{11}}\mathbf{z}_{\mathbf{1}} + \mathbf{A}_{\mathbf{12}}\mathbf{z}_{\mathbf{2}} \tag{6.2a}$$

$$\dot{\mathbf{z}}_{\mathbf{2}} = \mathbf{A}_{\mathbf{21}}\mathbf{z}_{\mathbf{1}} + \mathbf{A}_{\mathbf{22}}\mathbf{z}_{\mathbf{2}} + {\mathbf{N}_{\mathrm{NL}}}^{T}\mathbf{N}_{\mathrm{NL}}\mathbf{g}(\mathbf{z}_{\mathbf{1}}, \mathbf{z}_{\mathbf{2}}). \tag{6.2b}$$

Where, for simplicity, we have assumed that the external input $\mathbf{u} = \mathbf{0}$, and defined:

$$\mathbf{A}_{\mathbf{11}} = {\mathbf{N}_{\mathrm{NL}}}^{\perp}\mathbf{N}_{\mathrm{L}}\mathbf{G}{\mathbf{N}_{\mathrm{NL}}}^{\perp+}, \tag{6.3a}$$

$$\mathbf{A}_{\mathbf{12}} = {\mathbf{N}_{\mathrm{NL}}}^{\perp}\mathbf{N}_{\mathrm{L}}\mathbf{G}{\mathbf{N}_{\mathrm{NL}}}^{T+}, \tag{6.3b}$$

$$\mathbf{A}_{\mathbf{21}} = {\mathbf{N}_{\mathrm{NL}}}^{T}\left(\mathbf{N}_{\mathrm{NL}}\mathbf{J}_{\mathrm{NL}} + \mathbf{N}_{\mathrm{L}}\mathbf{G}\right){\mathbf{N}_{\mathrm{NL}}}^{\perp+}, \tag{6.3c}$$

$$\mathbf{A}_{\mathbf{22}} = {\mathbf{N}_{\mathrm{NL}}}^{T}\left(\mathbf{N}_{\mathrm{NL}}\mathbf{J}_{\mathrm{NL}} + \mathbf{N}_{\mathrm{L}}\mathbf{G}\right){\mathbf{N}_{\mathrm{NL}}}^{T+}. \tag{6.3d}$$

Here, $\mathbf{J}_{\mathrm{NL}}$ and $\mathbf{G}$ denote the Jacobian of $\mathbf{v}_{\mathrm{NL}}$ and $\mathbf{v}_{\mathrm{L}}$, as defined in (2.30), evaluated in the equilibrium point. Moreover, $\mathbf{N}$ follows the order defined in (2.32).

As noted above, the dynamical system in (6.2) is the interconnection of a linear and a nonlinear system. Depending on the studied reaction network, and on the dynamical properties of each subsystem, we can exploit interconnection properties such as dissipativity, monotonicity or the Small Gain Theorem, to analyse the stability of the equilibrium point.

In this direction, *further work will be focused on the characterisation of classes of systems whose dynamical properties can be exploited, in order to conclude the stability of the equilibrium point*.

Here we have not consider any particular form of the nonlinearities in $\mathbf{g}(\mathbf{c})$. In the following section, we focus on bilinear nonlinearities.

6.1.2 Representing the Nonlinearities as Sum of Squares

In Section 2.5 we showed that the following assumptions lead to bilinear nonlinearities.

Assumption 6.1. *Let*

A1. all the nonlinear reactions have at most two reactants,

A2. all the stoichiometric coefficients for the reactants be one, and

A3. the nonlinear reactions rates $\mathbf{v_{NL}}$ *be modelled with the Mass Action Law.*

Under these assumptions, the vector $\mathbf{v_{NL}}$ is composed of bilinear terms that can be expressed as a quadratic form, i.e.,

$$v_{NLi}(\mathbf{c}) = \mathbf{c}^T \mathbf{Y}_i \mathbf{c},$$

for a suitable selection of the elements in $\mathbf{Y}_i = \mathbf{Y}_i^T \in \mathbb{R}^{n \times n}$. Hence the vector $\mathbf{v_{NL}}(\mathbf{c})$ can be expressed as

$$\mathbf{v_{NL}}(\mathbf{c}) = \left(\mathbf{I}_{m_1} \otimes \mathbf{c}^T\right) \mathbf{Y}\mathbf{c}, \tag{6.4}$$

The study of these bilinear terms is denoted in the literature as sum of squares. We suspect that a lifting of the state space, which includes the bilinear terms as part of the state vector, will provide a tractable representation of the nonlinear system. That is to say, *we will study the mathematical model of a reaction network that satisfies Assumptions 6.1 in an extended state space representation, to characterise the stability of the equilibrium set.* Moreover, this representation may be useful on the computation of the time-integral of the solution of reaction-diffusion networks, analysed in Section 4.4, and in general in handling this kind of dynamical systems. Now, we turn our attention to the positive feedback loop depicted in Figure 2.1.

6.1.3 Extending the Results of the Circular Protein Activation

In Proposition 3.3 we concluded that the stability results for the reaction network studied in Example 2.2 and Example 3.1, also guarantee the local stability of the reaction-diffusion system, when we consider that the diffusion coefficients for all the species in each subsystem are the same. Interestingly, along the derivation of the proof of Proposition 3.3 we did not use any specific definition of the reaction network, except for the interconnection topology and the fact that the product of all γ^is is less that one.

That is to say, when we have a stable circular interconnection of systems, the extension of the stability results to the spatio-temporal case, is always guaranteed, under the aforementioned conditions on the diffusion constants.

In this light, an interesting problem is to identify classes of subsystems that comprise a positive feedback loop, whose small gain γ^i *can be characterised. Further, we seek extensions*

of the stability results to the spatio-temporal set-up. A natural choice for these subsystems are systems that comply with a Integral Quadratic Constraint, for which a clear relationship between the input-output gain is available.

Although the extension to the reaction-diffusion case in Propositions 3.3 and 3.4 resulted straight-forward, we considered some assumptions on the kinetic and diffusion parameters. Thus, it remains to be analysed whether *we can derive less restrictive conditions on the diffusion coefficients and still be able to extend the ODE stability results.*

Nonetheless, we *would like to determine whether the circular protein activation studied in Example 2.2 may present diffusion-driven instability, and characterise the scenarios in which this phenomenon might appear.*

6.1.4 Calcium Homeostasis in Non-excitable Cells

Neurons are cells capable of reacting to electrical cues to propagate them and modulate specific processes. To support this progression, a group of non-excitable cells, denominated glial cells, provide a means to enhance such functions. Especially, the astrocytes play a major role in the ionic balance in the extracellular space, insulating axons, controlling blood flow and providing energy and neurotransmiters to motivate the signal transmission. Due to this importance, the astrocite-mediated synapses between neurons has been recently called "tripartite neuron." Malfunction of the regulation may be implicated on epilepsy, symptoms of schizophrenia. In addition, astrocytes may become cancerous, hence leading to gliomas or can be affected by autoimmune attacks in multiple sclerosis [103, 104].

In Section 5.3 we derived the integrated response of the spatio-temporal concentration of cytosolic calcium ions. We are currently working to link these results with their implication on astrocytes.

Appendix A

Appendix

In this section, we present three proofs required in Section to prove the local stability of the *off* and *on steady states*. Firstly, we present the proof of (3.22)

Claim A.1. *For all* $i \in [1, p]$

$$k_2^{i+1} k_{3f}^i d\left(a^{i+1}\right) = d\left(\alpha^i\right) d\left(a^i\right) + k_1^i n\left(a^{i+1}\right),$$

where α^i *has been defined in* (2.22a)*.*

Proof. The strategy of the proof is to rewrite $\mathrm{d}\left(a^{i+1}\right)$ in terms of $\mathrm{d}\left(a^i\right)$. For, we note that

$\mathrm{n}\left(\alpha^i\right) := k_2^{i+1} k_{3f}^i$ and from (2.26)

$$\begin{aligned}
\mathrm{n}\left(\alpha^i\right)\mathrm{d}\left(a^{i+1}\right) =,\\
\mathrm{n}\left(\alpha^i\right)\prod_{j=1}^{i}\mathrm{d}\left(\alpha^j\right)\sum_{k=i+1}^{p}\left(k_1^k\prod_{j=i+1}^{k-1}\mathrm{n}\left(\alpha^j\right)\prod_{j=k+1}^{p}\mathrm{d}\left(\alpha^j\right)\right)+\\
\mathrm{n}\left(\alpha^i\right)\prod_{j=i+1}^{p}\mathrm{n}\left(\alpha^j\right)\sum_{k=1}^{i}\left(k_1^k\prod_{j=1}^{k-1}\mathrm{n}\left(\alpha^j\right)\prod_{j=k+1}^{i}\mathrm{d}\left(\alpha^j\right)\right) =,\\
\prod_{j=1}^{i}\mathrm{d}\left(\alpha^j\right)\sum_{k=i+1}^{p}\left(k_1^k\prod_{j=i}^{k-1}\mathrm{n}\left(\alpha^j\right)\prod_{j=k+1}^{p}\mathrm{d}\left(\alpha^j\right)\right)+\prod_{j=i}^{p}\mathrm{n}\left(\alpha^j\right)\sum_{k=1}^{i}\left(k_1^k\prod_{j=1}^{k-1}\mathrm{n}\left(\alpha^j\right)\prod_{j=k+1}^{i}\mathrm{d}\left(\alpha^j\right)\right) =,\\
\mathrm{d}\left(\alpha^i\right)\left[\prod_{j=1}^{i-1}\mathrm{d}\left(\alpha^j\right)\sum_{k=i}^{p}\left(k_1^k\prod_{j=i}^{k-1}\mathrm{n}\left(\alpha^j\right)\prod_{j=k+1}^{p}\mathrm{d}\left(\alpha^j\right)\right)+\right.\\
\left.\prod_{j=i}^{p}\mathrm{n}\left(\alpha^j\right)\sum_{k=1}^{i-1}\left(k_1^k\prod_{j=1}^{k-1}\mathrm{n}\left(\alpha^j\right)\prod_{j=k+1}^{i-1}\mathrm{d}\left(\alpha^j\right)\right)\right]+k_1^i\left[\prod_{j=1}^{p}\mathrm{n}\left(\alpha^j\right)-\prod_{j=1}^{p}\mathrm{d}\left(\alpha^j\right)\right] =,\\
\mathrm{d}\left(\alpha^i\right)\mathrm{d}\left(a^i\right)+k_1^i\mathrm{n}\left(a^{i+1}\right).
\end{aligned}$$

□

Now, we provide the proof of Proposition 3.2, which determines the stability of the *on steady state* under the conditions on the parameters described in (3.28).

Proof. Accounting for the conditions (3.28), the solution for Ω^* in (3.25) is positive and real, for the positive sign of the square root. Let us rewrite this solution as

$$\Omega^* = -\left(k_{3f}^i\right)^2+\sqrt{\left[\left(k_{3f}^i\right)^2-\left(k_2^i\right)^2\right]\left[\left(k_{3f}^i\right)^2-\left(\mu^i\right)^2\right]} := -\left(k_{3f}^i\right)^2+\phi^i\eta^i, \tag{A.1}$$

where

$$\phi^i = \sqrt{\left(k_2^i\right)^2-\left(k_{3f}^i\right)^2}, \tag{A.2a}$$

$$\eta^i = \sqrt{\left(\mu^i\right)^2-\left(k_{3f}^i\right)^2}. \tag{A.2b}$$

Then, from (3.24), the gain of the system evaluated in the resonance frequency (A.1) is

$$\begin{aligned}
\gamma_{\text{on}}^i &= \sigma^i \sqrt{\frac{\phi^i \eta^i}{\left[-\left(k_{3f}^i\right)^2 + \phi^i\eta^i + (\mu^i)^2\right]\left[-\left(k_{3f}^i\right)^2 + \phi^i\eta^i + \left(k_2^i\right)^2\right]}} \\
&= \sigma^i \sqrt{\frac{1}{\left(\phi^i\right)^2 + 2\phi^i\eta^i + \left(\eta^i\right)^2}} \\
&= \frac{\sigma^i}{\phi^i + \eta^i} \\
&= \frac{\sigma^i}{\sqrt{\left(k_2^i\right)^2 - \left(k_{3f}^i\right)^2} + \sqrt{(\mu^i)^2 - \left(k_{3f}^i\right)^2}} \\
&= \frac{\sigma^i k_{3f}^i}{\mu^i k_2^i} \frac{k_2^i}{k_{3f}^i} \frac{\mu^i}{\sqrt{\left(k_2^i\right)^2 - \left(k_{3f}^i\right)^2} + \sqrt{(\mu^i)^2 - \left(k_{3f}^i\right)^2}} \\
\gamma_{\text{on}}^i &= \frac{k_2^{i+1} k_{3f}^i}{k_1^i k_{3b}^i} \frac{k_2^{i+1}}{k_2^i} \left[\frac{\mathrm{d}\left(a^{i+1}\right)}{\mathrm{d}\left(a^i\right)}\right]^2 \frac{1}{\frac{k_{3f}^i}{\mu^i}\sqrt{1 - \left(\frac{k_{3f}^i}{k_2^i}\right)^2} + \frac{k_{3f}^i}{k_2^i}\sqrt{1 - \left(\frac{k_{3f}^i}{\mu^i}\right)^2}}.
\end{aligned} \tag{A.3}$$

Where we have exploited the definitions in (A.2) and (3.13). Except for the last factor, the expression above resembles the gain for the *on steady state* in (3.26), analysed in Proposition 3.1. Moreover, we have just considered that for *some* i, the conditions in (3.28) are satisfied. Then the stability condition form the Small Gain Theorem can be expressed as

$$\begin{aligned}
\prod_{i=1}^{p} \frac{k_2^{i+1} k_{3f}^i}{k_1^i k_{3b}^i} \left(\nu^i\right)^{-1} &< 1 \\
\prod_{i=1}^{p} \frac{k_2^{i+1} k_{3f}^i}{k_1^i k_{3b}^i} &< \prod_{i=1}^{p} \nu^i,
\end{aligned}$$

where the definition of ν^i is given in (3.30). Although exact, the condition above might be an intricate function of the parameters. In the following, we pursue a tractable bound of γ_{on}^i. For, we note that (3.28c) implies

$$\begin{aligned}
1 - \left(\frac{k_{3f}^i}{k_2^i}\right)^2 &> \left(\frac{k_{3f}^i}{\mu^i}\right)^2 \\
1 - \left(\frac{k_{3f}^i}{\mu^i}\right)^2 &> \left(\frac{k_{3f}^i}{k_2^i}\right)^2
\end{aligned}$$

Using these two last inequalities in (A.3), we obtain the bound

$$\begin{aligned}
\gamma_{\text{on}}^i &< \frac{\sigma^i}{k_2^i \frac{k_{3f}^i}{\mu^i} + \mu^i \frac{k_{3f}^i}{k_2^i}} \\
&= \frac{k_2^i}{k_{3f}^i} \frac{\sigma^i \mu^i}{\left(k_2^i\right)^2 + \left(\mu^i\right)^2} \\
&= \frac{\sigma^i k_{3f}^i}{\mu^i k_2^i} \left(\frac{k_2^i}{k_{3f}^i}\right)^2 \frac{\left(\mu^i\right)^2}{\left(k_2^i\right)^2 + \left(\mu^i\right)^2} \\
&= \frac{k_2^{i+1} k_{3f}^i}{k_1^i k_{3b}^i} \frac{k_2^{i+1}}{k_2^i} \left[\frac{\mathrm{d}\left(a^{i+1}\right)}{\mathrm{d}\left(a^i\right)}\right]^2 \left(\frac{k_2^i}{k_{3f}^i}\right)^2 \frac{\left(\mu^i\right)^2}{\left(k_2^i\right)^2 + \left(\mu^i\right)^2} \\
\gamma_{\text{on}}^i &< \frac{k_2^{i+1} k_{3f}^i}{k_1^i k_{3b}^i} \frac{k_2^{i+1}}{k_2^i} \left[\frac{\mathrm{d}\left(a^{i+1}\right)}{\mathrm{d}\left(a^i\right)}\right]^2 \left(\frac{k_2^i}{k_{3f}^i}\right)^2 .
\end{aligned}$$

Where we have used the definitions of μ^i and σ^i in (3.13). Again, the expression above resembles the gain for the *on steady state* in (3.26), analysed in Proposition 3.1. Since the conditions in (3.28) just hold for some i, the stability of the closed loop is guaranteed if (3.31) holds.

Finally, the proof for the instability of this steady state, is equal to the one used in Proposition 3.1, since there we do not require any special relationship among the parameters. □

In order to prove the closed-form expression of the determinant of (3.6) in Proposition 3.1, we will exploit the following theorem, that presents a formula for the determinant of a block matrix.

Theorem A.1. *Let a square matrix* $\mathbf{M}$ *be defined by blocks:*

$$\mathbf{M} = \begin{pmatrix} \mathbf{M^{11}} & \mathbf{M^{12}} \\ \mathbf{M^{21}} & \mathbf{M^{22}} \end{pmatrix},$$

Provided the existence of $\left(\mathbf{M^{22}}\right)^{-1}$*, the determinant of* $\mathbf{M}$ *is given by*

$$\det\left(\mathbf{M}\right) = \det\left(\mathbf{M^{22}}\right) \det\left(\mathbf{M^{11}} - \overset{-1}{\det}\left(\mathbf{M^{22}}\right) \mathbf{M^{12}} \mathrm{Adj}^T\left(\mathbf{M^{22}}\right) \mathbf{M^{21}}\right).$$

where $\mathrm{Adj}^T\left(\mathbf{X}\right)$ *denotes the transpose of the Adjugate or Adjoint matrix of* $\mathbf{X}$*.*

We will also avail of the following theorem, which shows how to compute the determinant of a sum of matrices.

Lemma A.1 (Matrix Determinant Lemma)**.** *Let* $\mathbf{A}$ *be a non-singular square matrix and* $\mathbf{x}$*,* $\mathbf{y}$ *be column vectors of the dimension of* $\mathbf{A}$*, then*

$$\det\left(\mathbf{A}+\mathbf{x}\mathbf{y}^{\mathbf{T}}\right)=\det(\mathbf{A})+\mathbf{y}^{\mathbf{T}}\mathrm{Adj}^{T}\left(\mathbf{A}\right)\mathbf{x}.$$

The proof of the previous propositions can be found in [39], for example. Now, we use these theorems to prove the forthcoming lemma.

Lemma A.2. *The determinant of* (3.6) *is given by*

1. ***Off Steady State***

$$\det\left(\mathbf{A}_{\text{off}}\right)=\prod_{i=1}^{p}k_{2}^{i}k_{3f}^{i}-\prod_{i=1}^{p}k_{1}^{i}k_{3b}^{i}$$

2. ***On Steady State***

$$\det\left(\mathbf{A}_{\text{on}}\right)=\prod_{i=1}^{p}k_{1}^{i}k_{3b}^{i}-\prod_{i=1}^{p}k_{2}^{i}k_{3f}^{i}$$

Proof. The strategy of the proof follows a recursive application of the Theorem A.1, finalised by the application of Lemma A.1 to obtain a closed-form expression for the determinant. We note that applying $p-1$ times Theorem A.1, the determinant of (3.6) can be expressed as

$$\det\left(\mathbf{A}\right)=\prod_{i=2}^{p}\det\left(\mathbf{A}^{ii}\right)\det\left(\mathbf{A}^{1\,1}-\prod_{i=2}^{p}\overset{-1}{\det}\left(\mathbf{A}^{ii}\right)\left[\prod_{i=1}^{p-1}-\mathbf{A}^{ii+1}\mathrm{Adj}^{T}\left(\mathbf{A}^{i+1i+1}\right)\right]\mathbf{A}^{p1}\right). \tag{A.4}$$

Moreover, we note that

$$-\mathbf{A}^{p-1p}\mathrm{Adj}^{T}\left(\mathbf{A}^{pp}\right)\mathbf{A}^{p1}=-k_{1}^{p-1}\bar{c}_{1}^{p-1}\begin{pmatrix}0&-1\\0&1\end{pmatrix}\begin{pmatrix}-k_{2}^{p}&0\\k_{1}^{p}\bar{c}_{2}^{1}&-\left(k_{1}^{p}\bar{c}_{2}^{1}+k_{3f}^{p}\right)\end{pmatrix}k_{1}^{p}\bar{c}_{1}^{p}\begin{pmatrix}0&-1\\0&1\end{pmatrix}$$

$$-\mathbf{A}^{p-1p}\mathrm{Adj}^{T}\left(\mathbf{A}^{pp}\right)\mathbf{A}^{p1}=\quad k_{3f}^{p}k_{1}^{p-1}\bar{c}_{1}^{p-1}k_{1}^{p}\bar{c}_{1}^{p}\begin{pmatrix}0&-1\\0&1\end{pmatrix}.$$

Hence

$$\left[\prod_{i=1}^{p-1}-\mathbf{A}^{ii+1}\mathrm{Adj}^{T}\left(\mathbf{A}^{i+1i+1}\right)\right]\mathbf{A}^{p1}=k_{1}^{1}\bar{c}_{1}^{1}\left[\prod_{i=2}^{p}k_{3f}^{i}k_{1}^{i}\bar{c}_{1}^{i}\right]\begin{pmatrix}0&-1\\0&1\end{pmatrix}.$$

Substituting the expression above into (A.4), yields

$$\det(\mathbf{A}) = \prod_{i=2}^{p} \det\left(\mathbf{A}^{ii}\right) \det\left(\mathbf{A}^{11} + k_1^1 \bar{c}_1^1 \prod_{i=2}^{p} \overset{-1}{\det}\left(\mathbf{A}^{ii}\right) \left[\prod_{i=2}^{p} k_{3f}^i k_1^i \bar{c}_1^i\right] \begin{pmatrix} 0 & -1 \\ 0 & 1 \end{pmatrix}\right).$$

By Lemma A.1 and $\mathbf{A}^{ii}$ in (3.8a), the foregoing expression becomes

$$\begin{aligned} \det(\mathbf{A}) &= \prod_{i=2}^{p} \det\left(\mathbf{A}^{ii}\right) \left[\det\left(\mathbf{A}^{11}\right) - \prod_{i=2}^{p} \overset{-1}{\det}\left(\mathbf{A}^{ii}\right) \prod_{i=1}^{p} k_{3f}^i k_1^i \bar{c}_1^i\right], \\ \det(\mathbf{A}) &= \prod_{i=1}^{p} k_2^i \left(k_1^i \bar{c}_2^{i+1} + k_{3f}^i\right) - \prod_{i=1}^{p} k_{3f}^i k_1^i \bar{c}_1^i. \end{aligned} \tag{A.5}$$

We further consider the definition of the steady states, to conclude the proof.

1. **Off Steady State**

   By substituting the definition of this equilibrium point in (2.20), when $a^i = 0$, into (A.5), we obtain the expression

   $$\det(\mathbf{A}_{\text{off}}) = \prod_{i=1}^{p} k_2^i k_{3f}^i - \prod_{i=1}^{p} k_1^i k_{3b}^i,$$

   as desired.

2. **On Steady State**

   This equilibrium point is parametrised by a^{i+1}, defined in (2.26), via the relationships (2.20a) and (2.20b). Now, we analyse the product of the main blocks determinants in (A.5). By means of (2.20b) we can rewrite it as

   $$\begin{aligned} \det\left(\mathbf{A}_{\text{on}}^{ii}\right) &= k_2^i \frac{k_{3f}^i k_2^{i+1} \mathrm{d}\left(a^{i+1}\right) - k_1^i \mathrm{n}\left(a^{i+1}\right)}{k_2^{i+1} \mathrm{d}\left(a^{i+1}\right)} \\ \det\left(\mathbf{A}_{\text{on}}^{ii}\right) &= \mathrm{d}\left(\alpha^i\right) \frac{k_2^i \mathrm{d}\left(a^i\right)}{k_2^{i+1} \mathrm{d}\left(a^{i+1}\right)}, \end{aligned}$$

   where we availed of the expression in (3.22). From the expression above, we note

   $$\begin{aligned} \prod_{i=1}^{p} \det\left(\mathbf{A}_{\text{on}}^{ii}\right) &= \prod_{i=1}^{p} \mathrm{d}\left(\alpha^i\right) \frac{k_2^i \mathrm{d}\left(a^i\right)}{k_2^{i+1} \mathrm{d}\left(a^{i+1}\right)} \\ \prod_{i=1}^{p} \det\left(\mathbf{A}_{\text{on}}^{ii}\right) &= \prod_{i=1}^{p} k_1^i k_{3b}^i. \end{aligned} \tag{A.6}$$

Secondly, we note that, with the expressions (2.19a) and (2.20b), $\bar{c}_1^i$ may be rewritten as

$$\bar{c}_1^i = \frac{k_2^{i+1} \mathrm{d}\left(a^{i+1}\right)}{k_1^i \mathrm{d}\left(a^i\right)}.$$

Hence the later product in (A.5) becomes

$$\prod_{i=1}^{p} k_{3f}^i k_1^i \bar{c}_i^1 = \prod_{i=1}^{p} k_{3f}^i k_2^{i+1}.$$

Subtraction of (A.6) and the relationship above, yields

$$\det\left(\mathbf{A}_{\text{on}}\right) = \prod_{i=1}^{p} k_1^i k_{3b}^i - \prod_{i=1}^{p} k_{3f}^i k_2^i.$$

□

when exploiting the modularity of the product with respect to p.

Bibliography

[1] Erwin Schrödinger. *What is life? and other scientific essays*. Doubleday, Garden City, N.Y., 1944.

[2] J. D. Murray. *Mathematical Biology II*. Springer, 3rd edition, 2003.

[3] Hiroaki Kitano. *Foundations of Systems Biology*. The MIT Press, 2001.

[4] Edda Klipp, Axel Kowald, Christoph Wierling, and Hans Lehrach. *Systems Biology in Practice: Concepts, Implementation and Application*. Wiley-VCH, 2005.

[5] Frank J. Bruggeman and Hans V. Westerhoff. The nature of systems biology. *Trends in Microbiology*, 15(1):45 – 50, 2007.

[6] E. Andrianantoandro, S. Basu, D.K. Karig, and R. Weiss. Synthetic biology: New engineering rules for an emerging discipline. *Molecular Systems Biology*, 2, 2006.

[7] Filippo Menolascina, Velia Siciliano, and Diego di Bernardo. Engineering and control of biological systems: A new way to tackle complex diseases. *FEBS Letters*, 586(15):2122 – 2128, 2012.

[8] E. D. Sontag. Some new directions in control theory inspired by systems biology. *IET Systems Biology*, 1:9–18, 2004.

[9] Peter Wellstead, Eric Bullinger, Dimitrios Kalamatianos, Oliver Mason, and Mark Verwoerd. The role of control and systems theory in systems biology. *Annual Reviews in Control*, 32(1):33 – 47, 2008.

[10] B. Novák and J. J. Tyson. Design principles of biochemical oscillators. *Nature Reviews Molecular Cell Biology*, 9(12):981–991, 2008.

[11] P. Lenz and L. Søgaard-Andersen. Temporal and spatial oscillations in bacteria. *Nature Reviews Microbiology*, 9(8):565–577, 2011.

[12] J. L. Cherry and F. R. Adler. How to make a biological switch. *Journal of Theoretical Biology*, 203(2):117–133, 2000.

[13] Thomas Eissing, Holger Conzelmann, Ernst D. Gilles, Frank Allgöwer, Eric Bullinger, and Peter Scheurich. Bistability analyses of a caspase activation model for receptor-induced apoptosis. *Journal of Biological Chemistry*, 279(35):36892–36897, 2004.

[14] James Keener and James Sneyd. *Mathematical Physiology I*. Springer, 2001.

[15] Boris N. Kholodenko, John F. Hancock, and Walter Kolch. Signalling ballet in space and time. *Nature Reviews Molecular Cell Biology*, 11(6):414–426, 2010.

[16] A. M. Turing. The Chemical Basis of Morphogenesis. *Philosophical Transactions of the Royal Society B: Biological Sciences*, 237(641):37–72, 1952.

[17] Shigeru Kondo and Takashi Miura. Reaction-Diffusion Model as a Framework for Understanding Biological Pattern Formation. *Science*, 329(5999):1616–1620, 2010.

[18] Marcos Nahmad and Arthur D Lander. Spatiotemporal mechanisms of morphogen gradient interpretation. *Current Opinion in Genetics & Development*, 21(6):726 – 731, 2011.

[19] N. F. Britton. *Reaction-Diffusion Equations and their Applications to Biology*. Academic Press, 1986.

[20] Heinrich J Huber, Maike A Laussmann, Jochen HM Prehn, and Markus Rehm. Diffusion is capable of translating anisotropic apoptosis initiation into a homogeneous execution of cell death. *BMC Systems Biology*, 4(1):9, 2010.

[21] Jörg Stelling, Uwe Sauer, Zoltan Szallasi, Francis J. Doyle III, and John Doyle. Robustness of cellular functions. *Cell*, 118(6):675 – 685, 2004.

[22] F. López-Caamal, M. R. García, R. H. Middleton, and H. J. Huber. Positive feedback in the Akt/mTOR pathway and its implications for growth signal progression in skeletal muscle cells: An analytical study. *Journal of Theoretical Biology*, 301(0):15–27, 2012.

[23] F. López-Caamal, R.H. Middleton, and H.J. Huber. Equilibria and stability of a class of positive feedback loops: Mathematical analysis and its application to caspase-dependent apoptosis, **To appear**. *Journal of Mathematical Biology*, 2013.

[24] López-Caamal F., M. R. García, and R. H. Middleton. Reducing computational time via order reduction of a class of reaction-diffusion system. In *Proceedings of the American Control Conference*, 2012.

[25] F. López-Caamal, D. A. Oyarzún and, J. A. Moreno, and D. Kalamatianos. Control structure and limitations of biochemical networks. In *Proceedings of the American Control Conference*, pages 6668–6673, 2010.

[26] D. A. Oyarzún, Jo L. Bramhall, F. López-Caamal, Duncan Jodrell, and Ben-Fillippo Krippendorff. Deconvolution of growth factor signalling demonstrates linear information transmission of the EGFR, **Under review**. 2012.

[27] F López-Caamal, M. R. García, D. A. Oyarzún, and R.H. Middleton. Analytic computation of the integrated response in nonlinear reaction-diffusion systems. In *Proceedings of the 51st IEEE Conference on Decision and Control*, 2012.

[28] D. A. Oyarzún, F. López-Caamal, Míriam R. García, and R. H. Middleton. Cumulative signal transmission in nonlinear reaction-diffusion networks, **Under review**. 2013.

[29] Mukhtar Ullah and Olaf Wolkenhauer. Stochastic approaches in systems biology. *Wiley Interdisciplinary Reviews: Systems Biology and Medicine*, 2(4):385–397, 2010.

[30] B. Munsky and M. Khammash. The finite state projection approach for the analysis of stochastic noise in gene networks. *Automatic Control, IEEE Transactions on*, 53(Special Issue):201 –214, 2008.

[31] B Munsky, B Trinh, and M Khammash. Listening to the noise: random fluctuations reveal gene network parameters. *Molecular Systems Biology*, 5(5):318, 2009.

[32] V. Chellaboina, S. Bhat, W.M. Haddad, and D.S. Bernstein. Modeling and analysis of mass-action kinetics. *Control Systems, IEEE*, 29(4):60 –78, 2009.

[33] Julio Vera, Eva Balsa-Canto, Peter Wellstead, Julio R. Banga, and Olaf Wolkenhauer. Power-law models of signal transduction pathways. *Cellular Signalling*, 19(7):1531 – 1541, 2007.

[34] Christophe H. Schilling and Bernhard O. Palsson. The underlying pathway structure of biochemical reaction networks. *Proceedings of the National Academy of Sciences*, 95(8):4193–4198, 1998.

[35] Iman Famili and Bernhard O. Palsson. The convex basis of the left null space of the stoichiometric matrix leads to the definition of metabolically meaningful pools. *Biophysical Journal*, 85(1):16 – 26, 2003.

[36] Iman Famili and Bernhard O. Palsson. Systemic metabolic reactions are obtained by singular value decomposition of genome-scale stoichiometric matrices. *Journal of Theoretical Biology*, 224(1):87 – 96, 2003.

[37] Martin Feinberg. The existence and uniqueness of steady states for a class of chemical reaction networks. *Archive for Rational Mechanics and Analysis*, 132:311–370, 1995.

[38] Gheorghe Craciun, J. William Helton, and Ruth J. Williams. Homotopy methods for counting reaction network equilibria. *Mathematical Biosciences*, 216(2):140 – 149, 2008.

[39] Dennis S. Bernstein. *Matrix mathematics: theory, facts, and formulas 2nd Ed.* Princeton University Press, 2009.

[40] Andrea Weiße, Richard Middleton, and Wilhelm Huisinga. Quantifying uncertainty, variability and likelihood for ordinary differential equation models. *BMC Systems Biology*, 4(1):144, 2010.

[41] Borris N. Kholodenko. Cell-signalling dynamics in time and space. *Nature Molecular Cell Biology*, 7:165–176, 2006.

[42] Christopher P. Fall, Eric S. Marland, and John M. Wagner. *Computational Cell Biology*. Springer, Berlin, 2005.

[43] Uri Alon. *An Introduction to Systems Biology: Design Principles of Biological Circuits*. Chapman and Hall/CRC, 1 edition, 2006.

[44] Andrei D. Polyanin. *Handbook of Linear Partial Differential Equations for Engineers and Scientists*. Chapman and Hall/CRC, 1 edition, 2001.

[45] Alan J. Laub. *Matrix Analysis For Scientists And Engineers*. Society for Industrial and Applied Mathematics, Philadelphia, PA, USA, 2004.

[46] Roger A. Horn and Charles R. Johnson. *Matrix Analysis*. Cambridge University Press, 1990.

[47] Lan Ma and Pablo Iglesias. Quantifying robustness of biochemical network models. *BMC Bioinformatics*, 3(1):38+, 2002.

[48] Murat Arcak and Eduardo D. Sontag. Diagonal stability of a class of cyclic systems and its connection with the secant criterion. *Automatica*, 42:1531–1537, 2006.

[49] M.R. Jovanovic, M. Arcak, and E.D. Sontag. A passivity-based approach to stability of spatially distributed systems with a cyclic interconnection structure. *Automatic Control, IEEE Transactions on*, 53(Special Issue):75 –86, 2008.

[50] Hassan K. Khalil. *Nonlinear Systems (3rd Edition)*. Prentice Hall, 2001.

[51] Yutaka Hori, Tae-Hyoung Kim, and Shinji Hara. Existence criteria of periodic oscillations in cyclic gene regulatory networks. *Automatica*, 47(6):1203 – 1209, 2011. Special Issue on Systems Biology.

[52] Katsuhiko Ogata. *Modern Control Engineering*. Prentice Hall PTR, Upper Saddle River, NJ, USA, 4th edition, 2001.

[53] Sigurd Skogestad and Ian Postlethwaite. *Multivariable Feedback Control: Analysis and Design*. John Wiley & Sons, 1996.

[54] Steven H. Strogatz. *Nonlinear Dynamics And Chaos: With Applications To Physics, Biology, Chemistry, And Engineering (Studies in Nonlinearity)*. Studies in nonlinearity. Perseus Books Group, 1 edition, 1994.

[55] Jürgen Jost. *Partial Differential Equations*. Springer, 2nd edition, 2007.

[56] Ivar Stakgold. *Green's functions and boundary value problems*. John Wiley & Sons, 1979.

[57] Richard G. Casten and Charles J. Holland. Stability properties of solutions to systems of reaction-diffusion equations. *SIAM Journal on Applied Mathematics*, 33(2):pp. 353–364, 1977.

[58] Alexander S. Poznyak. *Advanced Mathematical Tools for Automatic Control Engineers Volume 1 Deterministic Techniques*. Elsevier, 2008.

[59] M.R. García, C. Vilas, J.R. Banga, and A.A. Alonso. Optimal field reconstruction of distributed process systems from partial measurements. *Industrial & engineering chemistry research*, 46(2):530–539, 2007.

[60] M. Rodríguez García. *Identification and real time optimisation in the food processing and biotechnology industries*. PhD thesis, Universidade de Vigo, 2008.

[61] R. Courant and D. Hilbert. *Methods of Mathematical Physics*. Wiley, 1937.

[62] A. Alonso, C. V Fernandez, and J. R Banga. Dissipative systems: from physics to robust nonlinear control. *International Journal of Robust and Nonlinear Control*, 14(2):157–179, 2004.

[63] Antonio A. Alonso and B.Erik Ydstie. Stabilization of distributed systems using irreversible thermodynamics. *Automatica*, 37(11):1739 – 1755, 2001.

[64] P.D. Christofides. *Nonlinear and robust control of PDE systems*. Birkhauser, 2001.

[65] R. Heinrich, B. G. Neel, and T. A. Rapoport. Mathematical models of protein kinase signal transduction. *Mol Cell*, 9(5):957–970, 2002.

[66] J. B. Gurdon and P. Y. Bourillot. Morphogen gradient interpretation. *Nature*, 413(6858):797–803, 2001.

[67] B. F. Krippendorff, D. A. Oyarzún, and W. Huisinga. Ligand accumulation counteracts therapeutic inhibition of receptor systems. In *Foundations of Systems Biology and Engineering*, pages 173–176, Denver, USA, 2009.

[68] Verena Becker, Marcel Schilling, Julie Bachmann, Ute Baumann, Andreas Raue, Thomas Maiwald, Jens Timmer, and Ursula Klingmüller. Covering a Broad Dynamic Range: Information Processing at the Erythropoietin Receptor. *Science*, 328(5984):1404 –1408, 2010.

[69] Eduardo D. Sontag and Madalena Chaves. Exact computation of amplification for a class of nonlinear systems arising from cellular signaling pathways. *Automatica*, 42(11):1987 – 1992, 2006.

[70] Ben-Fillippo Krippendorff. *Integrating Cell-level Kinetic Modeling into the Optimization of Cancer Therapeutics*. PhD thesis, 2009. PhD Thesis, Hamilton Institute, NUI Maynooth, Ireland.

[71] Diego A. Oyarzún. *A control-theoretic approach to dynamic optimization of metabolic networks*. PhD thesis, 2010. PhD Thesis, Hamilton Institute, NUI Maynooth, Ireland.

[72] Maximilian L. Würstle, Maike A. Laussmann, and Markus Rehm. The caspase-8 dimerization/dissociation balance is a highly potent regulator of caspase-8, -3, -6 signaling. *Journal of Biological Chemistry*, 285(43):33209–33218, 2010.

[73] Courtney A. Granville, Regan M. Memmott, Joell J. Gills, and Phillip A. Dennis. Handicapping the race to develop inhibitors of the phosphoinositide 3-Kinase/Akt/Mammalian Target of Rapamycin Pathway. *Clinical Cancer Research*, 12(3):679–689, 2006.

[74] Dos D. Sarbassov, David A. Guertin, Siraj M. Ali, and David M. Sabatini. Phosphorylation and regulation of Akt/PKB by the rictor-mtor complex. *Science*, 307(5712):1098–1101, 2005.

[75] Giorgia Pallafacchina, Elisa Calabria, Antonio L. Serrano, John M. Kalhovde, and Stefano Schiaffino. A protein kinase b-dependent and rapamycin-sensitive pathway controls skeletal muscle growth but not fiber type specification. *Proceedings of the National Academy of Sciences*, 99(14):9213 –9218, 2002.

[76] S C Bodine, T N Stitt, M Gonzalez, W O Kline, G L Stover, R Bauerlein, E Zlotchenko, A Scrimgeour, J C Lawrence, D J Glass, and G D Yancopoulos. Akt/mTOR pathway is a crucial regulator of skeletal muscle hypertrophy and can prevent muscle atrophy in vivo. *Nature Cell Biology*, 3(11):1014–1019, 2001.

[77] C Rommel, S C Bodine, B A Clarke, R Rossman, L Nunez, T N Stitt, G D Yancopoulos, and D J Glass. Mediation of IGF-1-induced skeletal myotube hypertrophy by PI(3)K/Akt/mTOR and PI(3)K/Akt/GSK3 pathways. *Nature Cell Biology*, 3(11):1009–1013, 2001.

[78] M.B Grant, T.J Wargovich, E.A Ellis, R Tarnuzzer, S Caballero, K Estes, M Rossing, P.E Spoerri, and C Pepine. Expression of IGF-I, IGF-I receptor and IGF binding proteins -1, -2, -3, -4 and -5 in human atherectomy specimens. *Regulatory Peptides*, 67(3):137–144, 1996.

[79] U. Kaiser, C. Schardt, D. Brandscheidt, E. Wollmer, and K. Havemann. Expression of insulin-like growth factor receptors I and II in normal human lung and in lung cancer. *Journal of Cancer Research and Clinical Oncology*, 119:665–668, 1993.

[80] Alastair Wilkins, Siddharthan Chandran, and Alastair Compston. A role for oligodendrocyte derived IGF1 in trophic support of cortical neurons. *Glia*, 36(1):48–57, 2001.

[81] Jr Ferrell, James E. Self-perpetuating states in signal transduction: positive feedback, double-negative feedback and bistability. *Current Opinion in Cell Biology*, 14(2):140–148, 2002. PMID: 11891111.

[82] Shinya Kuroda, Nicolas Schweighofer, and Mitsuo Kawato. Exploration of signal transduction pathways in cerebellar long-term depression by kinetic simulation. *The Journal of Neuroscience*, 21(15):5693–5702, 2001.

[83] Keiko Tanaka and George J. Augustine. A positive feedback signal transduction loop determines timing of cerebellar long-term depression. *Neuron*, 59(4):608 – 620, 2008.

[84] Inna N. Lavrik, Roland Eils, Nicolai Fricker, Carina Pforr, and Peter H. Krammer. Understanding apoptosis by systems biology approaches. *Molecular bioSystems*, 5(10):1105–1111, 2009.

[85] Richard Lockshin and Zahara Zakeri. Apoptosis, autophagy and more. *The International Journal of Biochemistry & Cell Biology*, 2004.

[86] Thomas Eissing, Madalena Chaves, and Frank Allgöwer. Live and let die – a systems biology view on cell death. *Computers & Chemical Engineering*, 33(3):583 – 589, 2009.

[87] Heiko Düßmann, Markus Rehm, Donat Kögel, and Jochen H. M. Prehn. Outer mitochondrial membrane permeabilization during apoptosis triggers caspase-independent mitochondrial and caspase-dependent plasma membrane potential depolarization: a single-cell analysis. *Journal of Cell Science*, 116(3):525–536, 2003.

[88] John G. Albeck, John M. Burke, Bree B. Aldridge, Mingsheng Zhang, Douglas A. Lauffenburger, and Peter K. Sorger. Quantitative analysis of pathways controlling extrinsic apoptosis in single cells. *Molecular Cell*, 30(1):11 – 25, 2008.

[89] M. Rehm, HJ Huber, H Dussmann, and JH Prehn. Systems analysis of effector caspase activation and its control by X-linked inhibitor of apoptosis protein. *The European Molecular Biology Organization Journal*, 2006.

[90] L. Galluzzi, O. Kepp, C. Trojel-Hansen, and G. Kroemer. Non-apoptotic functions of apoptosis-regulatory proteins. *The European Molecular Biology Organization Reports*, 13(4):322–330, 2012.

[91] V Cowling and J Downward. Caspase-6 is the direct activator of caspase-8 in the cytochrome c-induced apoptosis pathway: absolute requirement for removal of caspase-6 prodomain. *Cell Death and Differentiation*, 9(10):1046–1056, 2002.

[92] S. Inoue, G. Browne, G. Melino, and G M Cohen. Ordering of caspases in cells undergoing apoptosis by the intrinsic pathway. *Cell Death & Differentiation*, 16(7):1053–1061, 2009.

[93] M. Bentele, I. Lavrik, M. Ulrich, S Stosser, D W Heermann, H Kalthoff, P H Krammer, and R Eils. Mathematical modeling reveals threshold mechanism in CD95-induced apoptosis. *The Journal of Cell Biology*, 166(6):839–851, 2004.

[94] R. Rizzuto, P. Pinton, D. Ferrari, M. Chami, G. Szabadkai, P.J. Magalhaes, F. Di Virgilio, and T. Pozzan. Calcium and apoptosis: facts and hypotheses. *Oncogene*, 22(53):8619–8627, 2003.

[95] P. Nicotera and S. Orrenius. The role of calcium in apoptosis. *Cell Calcium*, 23(2):173–180, 1998.

[96] R. Sattler and M. Tymianski. Molecular mechanisms of calcium-dependent excitotoxicity. *J. Mol. Med.*, 78(1):3–13, 2000.

[97] A. Korngreen, V. Gold'shtein, and Z. Priel. A realistic model of biphasic calcium transients in electrically nonexcitable cells. *Biophys. J.*, 73(2):659–673, 1997.

[98] Z. Zhou and E. Neher. Mobile and immobile calcium buffers in bovine adrenal chromaffin cells. *J. Physiol.-London*, 469(1):245–273, 1993.

[99] M. Oheim, F. Kirchhoff, and W. Stühmer. Calcium microdomains in regulated exocytosis. *Cell Calcium*, 40(5-6):423–439, 2006.

[100] J. Wagner and J. Keizer. Effects of rapid buffers on ca2+ diffusion and ca2+ oscillations. *Biophys. J.*, 67(1):447, 1994.

[101] R. Thul, GD Smith, and S. Coombes. A bidomain threshold model of propagating calcium waves. *J. Math. Biol.*, 56(4):435–463, 2008.

[102] A. Verkhratsky and E.C. Toescu. *Integrative aspects of calcium signalling*. Springer, 1998.

[103] Nicola J. Allen and Ben A. Barres. Neuroscience: Glia – more than just brain glue. *Nature*, 457(7230):675–677, 2009.

[104] Tommaso Fellin, Olivier Pascual, and Philip G. Haydon. Astrocytes coordinate synaptic networks: Balanced excitation and inhibition. *Physiology*, 21(3):208–215, 2006.